IMPACT ASSESSMENT FOR THE MIT RESEARCH REACTOR LOW ENRICHMENT URANIUM FUEL FABRICATION TOLERANCES

By

Dakota Allen

B.S., Nuclear Engineering (2018) United States Naval Academy

SUBMITTED TO THE
DEPARTMENT OF NUCLEAR SCIENCE AND ENGINEERING

IN PARTIAL FULFILLMENT OF THE REQUIREMENTS FOR THE DEGREE OF
MASTER OF SCIENCE IN NUCLEAR SCIENCE AND ENGINEERING

AT THE
MASSACHUSETTS INSTITUTE OF TECHNOLOGY
MAY 2020

Signature of Author: _____
Dakota Allen
Department of Nuclear Science and Engineering
May 12, 2020

Certified by: _____
Lin-Wen Hu
NRL Director for Research and Services
Senior Research Scientist
Thesis Supervisor

Certified by: _____
Benoit Forget
Associate Department Head
and Professor of Nuclear Science and Engineering
Thesis Reader

Accepted by: _____
Ju Li
Battelle Energy Alliance Professor of Nuclear Science and Engineering
and Professor of Materials Science and Engineering
Chair, Department Committee on Graduate Students

Impact Assessment for the MIT Research Reactor Low Enrichment Uranium Fuel Fabrication Tolerances

By

Dakota Allen

Submitted to the Department of Nuclear Science and Engineering
on May 12, 2020 in Fulfillment of the Requirements for the Degree
of Master of Science in Nuclear Science and Engineering

ABSTRACT

In the framework of non-proliferation policy, the Massachusetts Institute of Technology Reactor (MITR) is planning to convert from highly enriched uranium (HEU) to low enriched uranium (LEU) fuel. A new type of high-density LEU fuel based on a monolithic U-10Mo alloy is being qualified to allow the conversion of all remaining U.S. high performance research reactors including the MITR. The purpose of this study is to understand the impact of proposed MITR LEU "FYT" fuel element fabrication tolerances on the operation and safety limits of the MITR. Therefore, the effects of fabrication specification parameters on all levels of the core, ranging from full-core alterations to individual spots on the fuel plates were analyzed. Evaluations at the design tolerances, and beyond, were conducted through neutronics and thermal hydraulics calculations. The first step was analyzing the separate effects that parameters, including enrichment, fuel mass loading, fuel plate thickness, and impurities, have on the reactor physics of the core. These analyses were used to develop curve fits to predict the effect of these parameters on the excess reactivity of fresh fuel inserted into the LEU core. These models could then be used to estimate the effect on fuel cycle length to ensure the tolerances would not cause significant changes to the operating cycle of MITR. These analyses estimated the margin to criticality present in the core and ensured that the reactivity shutdown margin (SDM) was not violated. Other parameters such as coolant channel gap and local fuel homogeneity cause primarily local impacts including the power distribution within the fuel element, and related impacts to thermal hydraulic margins. This modeling was necessary to ensure that these parameters would not cause the margin to MITR's thermal hydraulic safety limit, the onset of nucleate boiling (ONB), to be violated. The final step was a covariance analysis of the combined effects at a full-core and element level. This combined effect analysis assured that the core would maintain proper safety and operational margins with a realistic distribution of off-nominal parameters. Given the comprehensive analysis performed, the current design fabrication tolerances were determined to provide acceptable fuel cycle length and safety margins consistent with the MITR LEU preliminary safety analysis report, and a basis for updating these tolerances during planned manufacturing-scale plate fabrication demonstrations has been established.

Thesis Supervisor: Lin-Wen Hu, Ph.D., PE
Title: NRL Director for Research and Services, Senior Research Scientist

Acknowledgments

I would like to start by extending a sincere amount of gratitude to my thesis supervisor, Dr. Lin-Wen Hu. She offered me the chance to take part in this project and has been steadfast in her support of my endeavors during my time at MIT. I also owe a considerable amount of thanks to the other two members of my MITR LEU fuel conversion team: Dr. Kaichao Sun and Dr. Akshay Dave. They have served as my primary technical points for neutronics and thermal hydraulic analyses throughout my research. They have each contributed significant efforts teaching me computer codes, reviewing my work, performed independent verification as necessary for project quality assurance, and many other things. Without the tireless efforts of the entire LEU fuel conversion team, my research would have been near insurmountable.

In addition to the MIT-NRL team, I owe many thanks to the members of the Argonne National Laboratory reactor conversion team: Drs. Erik Wilson, David Jaluvka, and Son Hong Pham. They have also tirelessly assisted my research with their in-depth knowledge of high-performance research reactors' fuel development and fabrication, reviewing my work, and providing me the necessary positive criticism. In addition, I would like to extend my deep appreciation for the valuable feedback and guidance from Mr. Curt Lavender, Mr. Chad Painter, Dr. Vineet Joshi, and Dr. Christopher Clayton who graciously hosted two technical visits at Pacific Northwest National Laboratory as the lead fuel fabrication engineering team for U.S. High-Performance Research Reactor conversion.

I also thank my thesis reader, Professor Benoit Forget. I am grateful he was willing to take the time to ensure my technical approach is sound and is relevant to my degree requirements. I extend this same gratitude to all other members of the MIT-NRL and MIT-NSE community who have taken the time, whether small or large, to assist with my research and my graduate study at MIT.

Lastly, I would like to thank my friends and family who have stood by my side through it all. Whether it was late-night study sessions or the encouragement I needed, they were there to help me and ensure that I was able to complete this degree.

This research is sponsored by the U.S. Department of Energy, National Nuclear Security Administration Office of Material Management and Minimization Reactor Conversion Program under contract 2J-30101 with Argonne National Laboratory.

Table of Contents

List of Figures

List of Tables

Nomenclature

Symbol	Description	Units
$\Delta k/_k$	Reactivity, Percent change in k_{eff} between two cases	%
ΔT_{ONB}	Difference between $T_{clad,ONB}$ and T_{co}	℃
σ_B	Absorption Cross Section of Boron	barns
σ_i	Absorption Cross Section of Impurity	barns
φ	*plocsig*, uncertainty of an individual spot in STAT7	%
EBC	Equivalent Boron Content	ppm
FPD	Effective Full Power Days	1 FPD = 7 MWd
HEU	Highly Enriched Uranium	-
k_{alt}	k_{eff} for an altered case	-
k_{lim}	k_{eff} for a limiting situation	-
LEU	Low Enrichment Uranium	-
LSSS	Limited Safety System Settings	-
M_B	Atomic Mass of Boron	amu
M_i	Atomic Mass of Impurity	amu
mil	One thousandth of an inch	0.001 inch = 1 mil
ONB	Onset of Nucleate Boiling	-

ONB Power / P_{ONB}	Limiting Power at which Reactor will have a 3-σ confidence level of 99.865% that ONB will not occur at any spot within the core	MW
SDM	Reactivity Shutdown Margin	$\%^{\Delta k}/_{k}$
$T_{clad,ONB}$	Cladding Temperature at which ONB begins to occur	℃
T_{co}	Cladding Outer Temperature	℃
UNC	Coolant Channel Uncertainty in STAT7	mil

Chapter 1: Introduction

1.1 Overview of Reactor Fuel Conversion Program

The reactor fuel conversion program is part of a broader non-proliferation mission to minimize the amount of weapons-grade nuclear materials in civilian facilities around the world.

In response to the growing concerns of weapons-grade nuclear materials, the U.S. Department of Energy has established a program that includes, conversion of domestic and international civilian research reactors and isotope production facilities from HEU to LEU as a part of the Office of Material Management and Minimization (M3). Conversion serves as one of the mission pillars alongside removal and disposal of weapons-usable nuclear material [1]. U.S. organizations, including MIT NRL, work collaboratively alongside many countries worldwide to convert research and test reactors to the use of LEU fuel, continuing work that began with the Reduced Enrichment for Research and Test Reactors (RERTR) Program in 1978 [2]. There are currently five domestic HPRRs that include: MITR, the University of Missouri Research Reactor (MURR), the National Institute of Standards and Technology Reactor (NBSR), the Advanced Test Reactor (ATR) at Idaho National Laboratory, and the High Flux Isotope Reactor (HFIR) at Oak Ridge National Laboratory [3]. This program selected monolithic U-10Mo alloy as the base fuel for the LEU conversion of the first four of these reactors. This fuel contains 10 wt% molybdenum. The focus of this engineering design assessment was on the MITR's LEU fuel fabrication with possible lessons learned applied to other reactors that can conduct similar analyses specific to each reactor.

1.1.1 Research Objectives

This research focuses on the impact of the proposed fabrication tolerances for the MITR LEU fuel element. This assessment is an important step in ensuring the safety of the MITR after the LEU fuel conversion. This assessment covered a variety of parameters that affect reactor physics and the operational considerations of the core. The analyzed impact ranged in scale from the local element level to the global core level. The parameters analyzed in the full-core portion of this assessment were:

- **Enrichment**: Weight percent of U-235 in the fuel [Unit: wt%]
- **Fuel Mass Loading**: Mass of U-Mo in the core, uses fuel element spec. [Unit: kg]
- **Fuel Plate Thickness**: Thickness of fuel plate (including clad) [Unit: mil]
- **Impurities in the Fuel and Cladding/Side Plates**: Non-UMo (fuel) and non-AA6061 (cladding/plates) in their respective locations [Unit: ppm]

The parameters analyzed in the element/plate/spot aspect of this assessment were:

- **Fuel Mass Loading**: Mass of U-Mo at the plate level, uses fuel plate spec. [Unit: g]
- **Fuel Plate Thickness**: Thickness of fuel plate (including clad) [Unit: mil]
- **Coolant Channel Gap Thickness**: Thickness of coolant channels between fuel plates [Unit: mil]
- **Fuel Homogeneity**: General uncertainty associated with composition of U-Mo at "spot" level (includes density, thickness, and other small deviations from nominal) [Unit: %]

These parameters were analyzed for their separate effects on the local element level to the global core level. Their impact was evaluated by the parameter's effect on established criteria for the operation of the reactor. The margin to specific safety criteria helps define the reactor's ability to maintain criticality, have a sufficient fuel cycle length, and ensure the thermal hydraulic licensing margins are met. A combination effect analysis was performed to analyze the dependency of the various parameters.

1.2 MIT Research Reactor Background

The MIT Reactor is a 6 MW_{th} nuclear research reactor currently operated by the MIT Nuclear Reactor Laboratory (MIT-NRL). The MITR is presently the second-largest university research reactor in the US. NRL employs undergraduate students and excels in giving them real world experience in the operation of a nuclear reactor. As an important materials irradiation test facility, the MITR also offers research opportunities for undergraduate and graduate students as part of their thesis research. The MITR in its current form, the MITR-II, is moderated and cooled by light water, and has a heavy water reflector [4].

1.2.1 MITR-II HEU Core Design

The MITR consists of 27 rhomboidal fuel positions divided into three rings: A, B, and C. Three of these positions are reserved for in-core experiments during typical operation. The 24 fuel positions not devoted to in-core experiments contain identical fuel elements. The reactor uses six borated control blades and one cadmium regulating rod to control the reactor [4]. Figure 1-1 shows the axial overview of the core, including the locations of the control blades, regulating rod, and varying fuel element positions.

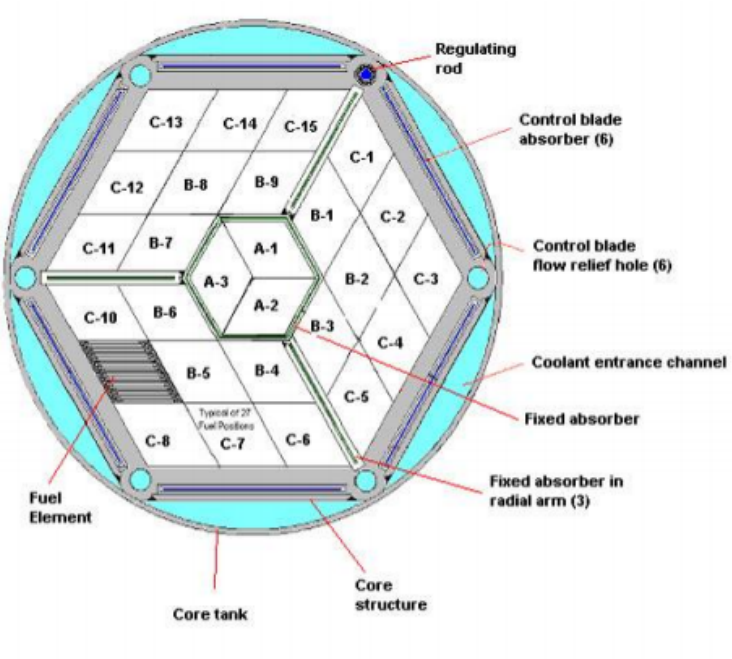

Figure 1-1: Core Map of MITR-II [5]

The current MITR-II fuel element contains 15 identical finned fuel plates. The fuel plates are 60 mil in thickness and have 10 mil deep longitudinal fins on both sides to increase heat transfer area. A cross-section view of an HEU fuel element is shown in Figure 1-2.

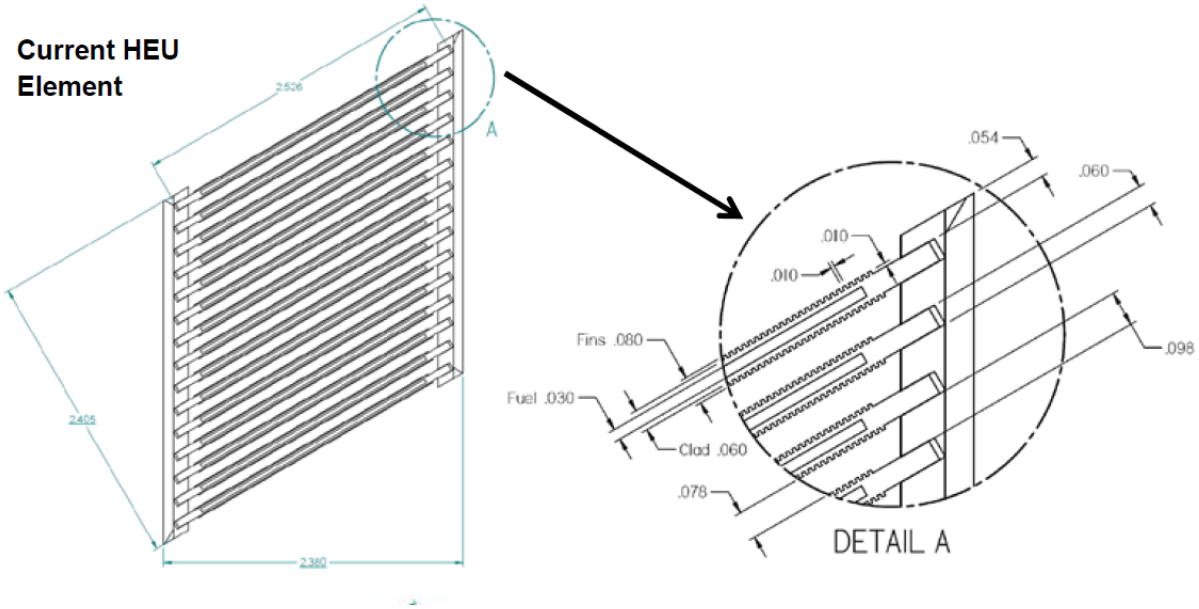

Figure 1-2: Current MITR-II HEU Fuel Element (dimensions in inch) [6]

The fuel plates used in these assemblies contain 93% enriched HEU in UAl_x and are cladded by AA6061 alloy [7]. Table 1-1 lists the specifications for these fuel plates and elements.

Table 1-1: HEU Fuel Element Parameters [8]

HEU Parameter	Value
Enrichment	93.75 wt%
Plates per Element	15
Fuel Density	1.54 gU/cc
U-235 per Element	508 g
Fuel Meat Thickness	0.76 mm / 30.0 mil
Cladding Thickness	0.38 mm / 15.0 mil
Total Fuel Plate Thickness	1.52 mm / 60.0 mil
Fin Thickness	10.0 mil

1.2.2 MITR Applications

MITR-II utilizes three test positions to perform a variety of in-core irradiation experiments. These experiments range from trace element analysis to neutron transmutation doping of silicon. MITR also utilizes one of the test positions to create the environment found within a typical commercial Light Water Reactors (LWR). This loop presents an opportunity for valuable LWR material research, such as the Accident Tolerant Fuel program. MITR is the only such U.S. research reactor on a university campus that can re-create this environment. MITR-II has also begun experiments with high-temperature molten salts such as FLiBe for molten salt reactors research and development.

1.2.3 MITR HEU Fuel Element Fabrication and Certification

An important aspect of the MITR-II quality assurance requirements, to ensure safe operation, is the fuel fabrication certification process. The certification process is completed by BWX Technologies, Inc. (BWXT), the fuel manufacturer, who issues a formal certification report after a fuel element is fabricated. This report is sent to MITR for approval before the fresh fuel elements are delivered, and the report comes in eight sections. These eight sections demonstrate that the fuel meets design specifications and acceptance requirements, and verifies the parameters lie within the pre-defined fabrication tolerances [9]. These sections are broken down as follows:

1. Certificate of Conformance
2. Fuel Element Material Identification Data Sheet
3. Fuel Plate / Element Loading Data Sheet
4. Fuel Plate Inspection Data
5. Fuel Element Measured Dimensions
6. Fuel Plate / Element Radiation Count
7. Fuel Plate D.E. Data
8. Fuel Element Pull Test Report

The TRTR-3 document, the specifications for the MITR HEU fuel elements, establishes the requirements of these certification reports [10]. The first two of these sections describe scope and relevant documents. In section III, the report identifies the U-235 enrichment, U-235 and total U loading, compact weight, Al weight, and total UAl_x in each fuel plate, along with other requirements for records, inspection methods and reports. The document also identifies the plate lot number associated with each of the plates in a given fuel element. The U-235 loading associated with the whole element is also reported and shown to lie within the established range.

In section IV, BWXT chooses three plates per plate lot at random to complete a full geometric analysis. This geometric analysis includes fuel plate width, length, thickness, and flatness to show that the analyzed plates are within specification. If any of these plates fail, the entire lot associated with the specific plate is tested. Section IV also includes analyses on the void volume within the fuel meat. Three plates per lot are chosen for this analysis, and if any fail, the entire lot must be analyzed as well. The final analysis of section IV is the inspection of the fin height, where three plates from each fuel plate lot are analyzed at 12 positions on both sides of each fuel plate [10]. While this is the only part of the fin height analysis included in the certification report, every plate is checked in three spots during the fabrication process due to the importance of fin height [10].

Section V focuses on the inspection results from various features of the fuel element. These assorted features include welds, the orientation of notches, total length, and others [9]. The most important of these fuel element inspections is coolant channel scans. These scans find the minimum, maximum, and average thickness of each side (left and right) of every coolant channel. These values are compared to the limits and marked if there are violations.

Section VI shows the alpha-beta count datasheet for all fuel plates within each lot [9]. These are found through smear tests and used to ensure they do not violate limits of either count. This analysis must include the counting period, counter, background, efficiency, and type of counters used [10].

Section VII is an inspection of the dummy fuel element required by TRTR-3. This inspection gives the thicknesses of the fuel meat and cladding at various points for one of the fuel plates [9]. The inspection validates the process of making the fuel plates for actual use.

Section VIII is the final section and gives the results of pull tests completed on three dummy sections of fuel elements [10]. These tests evaluate the strength of the swaging joints. Testing the weld strength for the attachment of a nozzle casting is also specified [10].

After MITR receives the fresh fuel, the lab performs an additional verification procedure for each fresh fuel element. This procedure ensures that the element meets selected geometric criteria set by TRTR-3. This verification includes ensuring proper position for the notch, coolant obstruction checks, checking fin height, and ensuring the radiation levels are within specification.

If there are violations of the specifications, BWXT can still send the element with an Idaho National Laboratory Change Request (ICR). This document lists the specification that is violated and by how much. These occur if BWXT believes the element may still meet safety requirements, and MITR staff reviews the document to determine if they agree. A large majority of these

documents result from off-nominal coolant channel widths. An analysis was performed based from the data from a recent ICR and is included in Appendix A. This analysis is the first-time it was formally adopted internally at MITR for HEU fuel elements to provide the technical basis as described in this report for the new LEU fuel element.

1.3 HEU and LEU Fuel Element Design Comparison

The transition from HEU to LEU included changes to the fuel element design, as well as changes to the core operation, although the overall outer geometry of the LEU fuel element remains the same. The MIT Nuclear Reactor Laboratory, in collaboration with Argonne National Laboratory, has completed the LEU fuel element design, now designated as the "FYT" fuel element [11]. Many of these design tolerances have been incorporated into the fabrication specification. The present work now expands on the number of parameters investigated beyond those required for safety analysis and evaluates impacts at, and beyond, the specified tolerances. The new fuel type/element prompted an increase in core power and coolant flow. These increases were designed to extend the fuel cycle for in-core experiments. Table 1-2 lists these changes in core power and coolant flow rate.

Advanced LEU fuels such as U-10Mo differ from UAl_x in more than just enrichment. Alterations to the fuel geometry and core operation were needed to incorporate these differences. Previous analyses had demonstrated the feasibility of converting the MITR to LEU fuel based on the FYT design, a proposed fuel element that would utilize three different types of fuel plates that differ based on the fuel thickness. Additionally, the fins are removed to simplify fuel fabrication. Figure 1-3 shows of the cross-section view of the proposed LEU-FYT element.

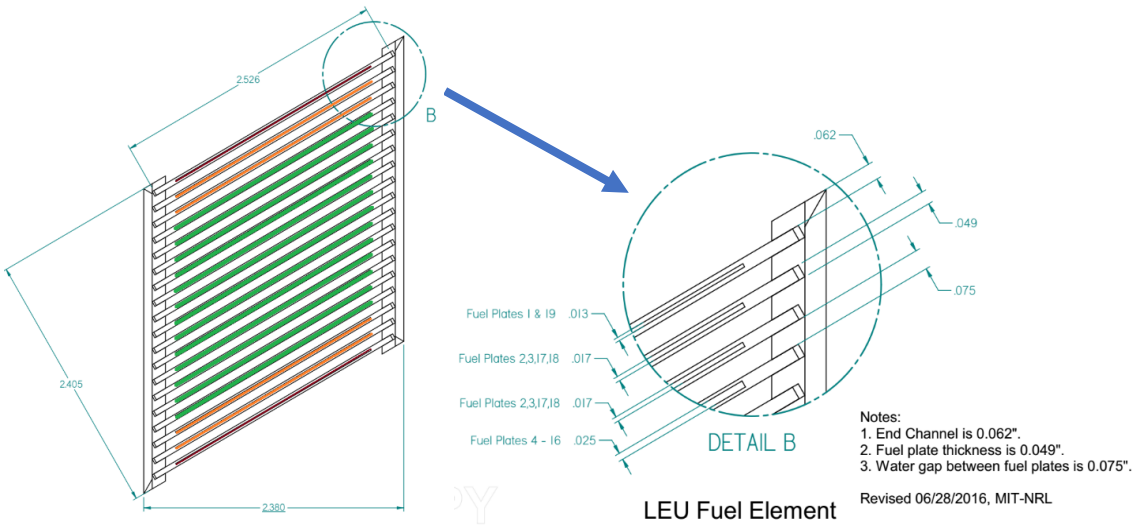

Figure 1-3: Current Proposed LEU-FYT element [12]

The T-type and Y-type plates are the outer plates of the LEU element and contain thinner fuel meats and lower amounts of fuel, as compared to the inner F-type plates. Table 1-2 is the comparison between the two fuel systems.

Table 1-2: HEU versus LEU comparison adapted from [8]

Parameter	HEU (UAl_x)	LEU-FYT (U-10Mo)
Enrichment	93.15 wt%	19.75 wt%
Operating Power	6 MW	7 MW
Nominal Flow Rate	2000 gpm	2400 gpm
Plates per Element	15	19
Uranium Density	1.54 gU/cm^3	15.3 gU/cm^3
U-235 per element	508 g	968 g
Fuel Thickness	0.76 mm / 30.0 mil	0.64 mm / 25.0 mil (F-Type) 0.43 mm / 17.0 mil (Y-Type) 0.33 mm / 13.0 mil (T-Type)
AA6061 Cladding Thickness	0.38 mm / 15.0 mil	0.28 mm / 11.0 mil (F-Type) 0.38 mm / 15.0 mil (Y-Type) 0.43 mm / 17.0 mil (T-Type)
Zr Interlayer Thickness	-	0.03 mm / 1.0 mil
Plate Thickness	1.52 mm / 60.0 mil	1.24 mm / 49.0 mil

Important takeaways from this table lie in the uranium density. To accommodate the lower percentage of U-235 within the core for an LEU fuel, the replacement fuel needed to have a much higher uranium density. U-10Mo has a uranium density that is approximately one order of magnitude higher than UAl_x, allowing for overall more U-235 in the reactor core due to neutron absorption of U-238. This higher uranium density, higher power density, and removal of fins are the important considerations for the FYT fuel assembly design to minimize the power peaking in the outer plates. Additionally, the LEU fuel design increased the number of fuel plates and decreased the size of the coolant channel. These alterations to the fuel element design necessitated more analyses to better understand the impact of fabrication tolerances on not just the neutronics effects, but also the margin to thermal hydraulic safety limits.

1.3.1 HEU to LEU Transition

The current LEU transition plan for the MITR begins with a 22 fresh fuel element core [12]. This 22-element fresh core is the configuration used for a large majority of the analyses in this assessment. Figure 1-4 displays this 22 fresh element core, referred to as LEU Core 1 for the remainder of this report. The unfueled positions are represented in orange and modeled as aluminum canisters filled with water in the MCNP file. As seen in the figure, the two additional

empty fuel positions are in the B-ring. This decision provides some peaking in position A-2, but vastly lowers the amount of fissile material within the core at the beginning of life.

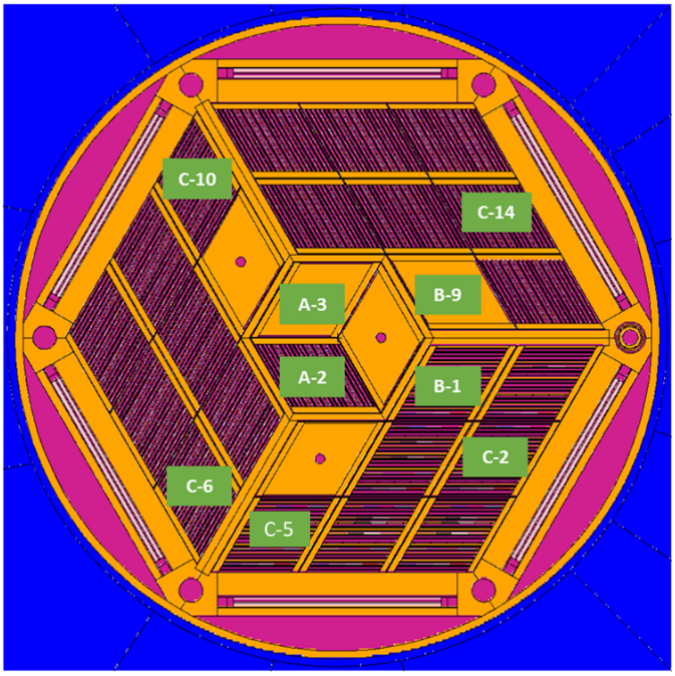

Figure 1-4: Axial View of LEU Core 1 (Fresh Core) [13]

Previous analyses completed have mapped out the path to equilibrium, beginning with LEU Core 1. The following figures summarize this process by mapping the nuclear material mass within the core and the height of the control blades over the course of 14 cycles, each fuel cycle lasts for 10 weeks.

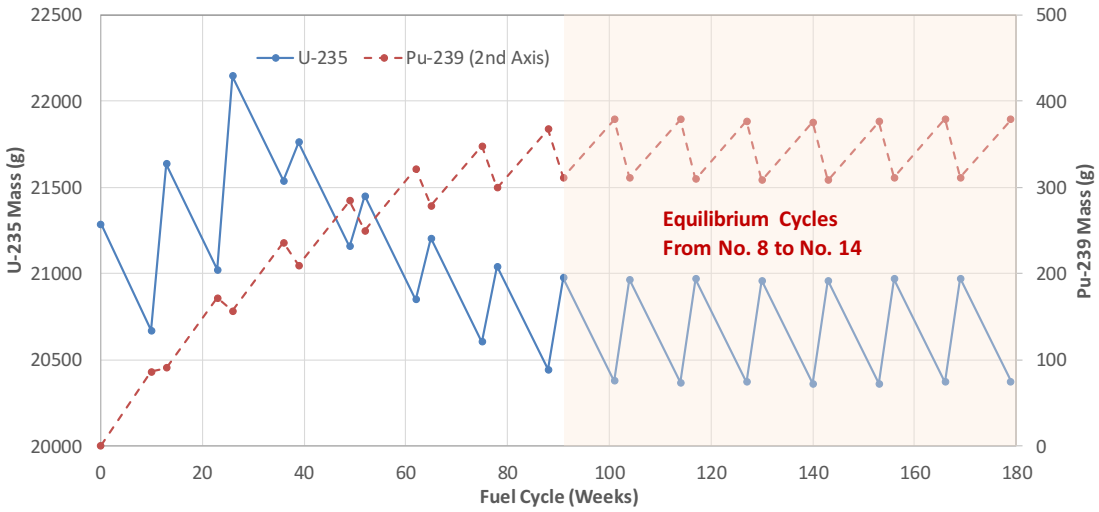

Figure 1-5: Mass of U-235 and Pu-239 within MITR during transition and equilibrium cycles [5]

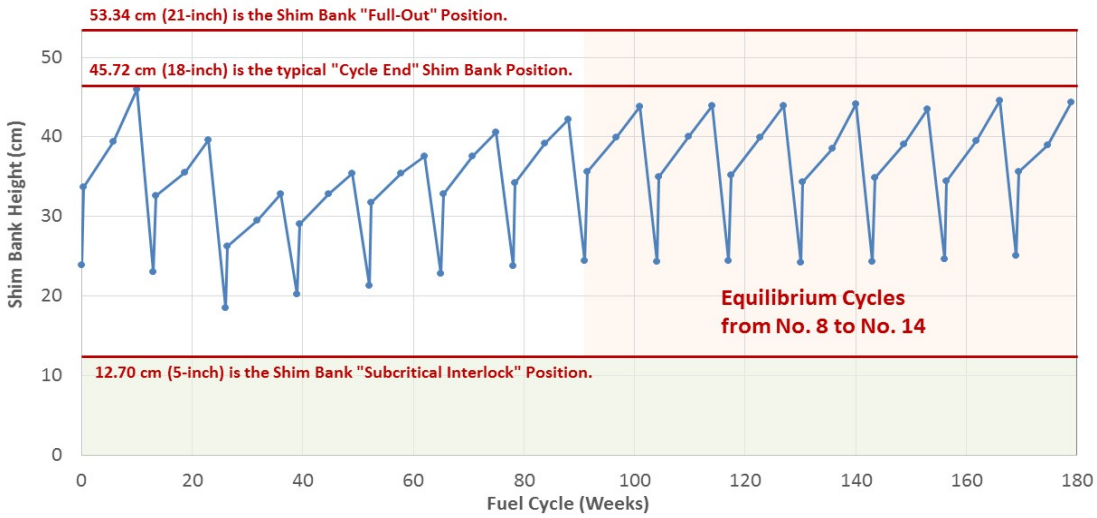

Figure 1-6: Shim bank movement during transition and equilibrium fuel cycles [5]

These figures show that an LEU core, starting with 22 fresh LEU fuel elements at nominal specifications, can achieve a stable amount of U-235 and Pu-239 after ~90 weeks. This condition defined an equilibrium core. Note that mixed HEU-LEU transition cores are being analyzed as a potential transition path for conversion to LEU fuel; however, that is outside the scope of this assessment.

1.4 Safety Criteria

The impact of all fabrication tolerances analyzed in this assessment were based on the limits determined as part of the safety analysis report, currently being reviewed by Nuclear Regulatory Commission (NRC), to ensure safe operation of the MITR. There are two different types of criteria, depending on the type of analysis: neutronics or thermal hydraulics.

1.4.1 Neutronics Evaluation Criteria

The primary neutronics criterion used by MITR is shutdown margin (SDM). The NRC defines SDM as the "instantaneous amount of reactivity by which a reactor is subcritical or would be subcritical from its present condition assuming all full-length rod cluster assemblies (shutdown and control) are fully inserted except for the single rod cluster assembly of highest reactivity worth that is assumed to be fully withdrawn" [14]. This value is essential to understand as it represents the margin to criticality that the reactor can achieve if an accident were to occur. The requirement for SDM is such that a given core configuration can be safely brought to subcritical when accounting for any possible reactivity additions during accident scenarios. The SDM is calculated using (1-1.

$$SDM\left[\%\ {\Delta k}/{k}\right] = \frac{1.000 - k_{lim}}{k_{lim}} * 100\% \quad (1\text{-}1)$$

where k_{lim} is the k_{eff} for a condition in which all of the control elements are fully inserted except for the one with highest reactivity worth.

The limiting condition for MITR is all control blades fully inserted except for the most limiting blade and the regulating rod fully drawn out. The minimum SDM is not a value mandated by the NRC and is instead up to the reactor to choose a value. The reactor must then show that this value is sufficient for any possible reactivity additions. The minimum SDM established by MITR as a neutronics safety criterion is 1% ${\Delta k}/{k}$, meaning the k_{eff} of any evaluated case must be <0.99 when the previously described limiting condition is applied.

1.4.2 Thermal Hydraulic Evaluation Criteria

The thermal hydraulic impact of alterations to the reactor is evaluated using criteria based on the reactor's steady-state operating limit, Onset of Nucleate Boiling (ONB). When power or heat flux increases, ONB is the first two-phase phenomenon to occur. ONB is followed by Onset of Significant Voiding (OSV), where bubbles grow and detach into the bulk coolant. Thus, OSV may lead to the premature Onset of Flow Instability (OFI) or Departure from Nucleate Boiling (DNB), and ultimately critical heat flux. Therefore, to preclude OFI or DNB during steady-state MITR operation, ONB is adopted as the basis of the Limiting Safety System Settings (LSSS) criterion. LSSS is a set of operational criteria identified where automatic scram occurs if limits are violated [14]. Table 1-3 lists the operating parameters for the nominal condition and LSSS. All thermal hydraulic analyses completed during this assessment use the LSSS condition.

Table 1-3: Nominal and LSSS Design Parameters [7]

Design Parameter	Normal Operation	LSSS
Power [MW]	7.00	8.68
Coolant Outlet Temperature [°C]	55	60
Mass Flow Rate[1] [kg/s]	150.5	138.0

Note 1: kg/s are calculated using a water density at 60 °C

The first criterion is ONB, the margin to this state is measured using uncertainty propagation to find the power where ONB will not occur at any spot in the core on a 3-σ confidence level (99.865%). This criterion is adopted to ensure that automatic protective systems activate before ONB occurs in MITR. This report refers to this criterion as limiting reactor power or ONB Power (P_{ONB}). The second thermal hydraulic criterion is the ONB temperature margin as defined in equation (1-2.

$$\Delta T_{ONB}[\text{°C}] = T_{clad,ONB}[\text{°C}] - T_{co}[\text{°C}] \,, \tag{1-2}$$

where $T_{clad,ONB}$ is the cladding temperature at which ONB occurs (determined by the Bergles-Rohsenow correlation) and T_{co} is the calculated cladding outer temperature using nominal input parameters.

Chapter 2: Computer Codes Utilized

2.1 MCNP5

The neutronics analyses of this assessment utilized MCNP5 and ENDF-VII.0 cross section library to evaluate parameters that directly impact the core physics. This combination of solver and library is what the MITR-II model is currently validated on and used to complete the LEU conversion. MCNP is a general-purpose Monte-Carlo code that can be used for particle transport calculations [15]. For this assessment, MCNP was used to find two outputs for each case: k_{eff} and a power distribution. The k_{eff} was found through a Monte-Carlo process and is used to estimate the effect the alteration had on the stability of MITR. A power distribution is found using f7 tallies, which record the fission heat generated in the fuel throughout the core. These tallies are broken into a 4 by 16 grid for each fuel plate, 4 lateral and 16 axial, totaling to 64 tallies per plate. These tallies create the 4 "stripes" used by STAT7 to find the thermal hydraulic effects.

2.2 STAT7

2.2.1 Bergles-Rohsenow Correlation

The temperature at which ONB occurs on a heated surface is determined by the Bergles-Rohsenow correlation [16],

$$T_{clad,ONB} = T_{sat} + 0.556\left[\frac{q''}{1082p^{1.156}}\right]^{0.463p^{0.0234}} \quad (2\text{-}1)$$

where $T_{clad,ONB}$ is the temperature at which ONB occurs at the outer cladding surface [°C], T_{sat} is the saturation temperature of the bulk coolant [°C], q'' is the wall heat flux [W/cm^2], and p is the pressure [bar].

2.2.2 STAT7 Methodology

The statistical thermal hydraulic analyses associated with this assessment were performed using STAT7. STAT7 is a steady-state thermal hydraulic code used to determine the temperature profile of a fuel element. The inputs include the number of plates, fuel plate and coolant channel thicknesses, coolant flow rate, power distributions, and a variety of other parameters. The STAT7 input file uses a power profile generated from MCNP5 for the studied element. STAT7 models the

power in the core by discretizing each plate into 16 axial nodes, and 4 lateral nodes ("stripes"). Each of the four stripes is then normalized for the input file [16]. Figure 2-1 shows a part of the geometry of an element modeled in STAT7 with four stripes.

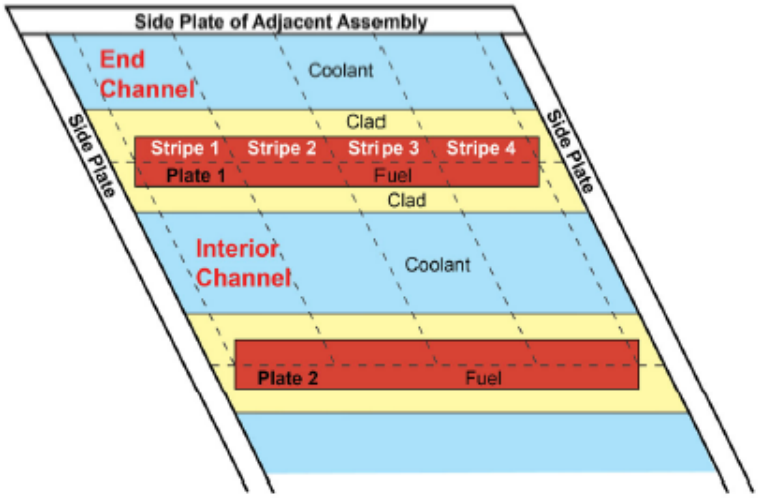

Figure 2-1: Base Geometry unit and Coolant Channels [5]

Three specific outputs from STAT7 are used in this assessment: $T_{clad,ONB}$, T_{co}, and the limiting reactor power or ONB Power (P_{ONB}). As multiple values exist at each axial location and fuel stripe, the reported ΔT_{ONB} for each case is the minima found. However, the lowest ONB temperature margin may not be the most significant percent decrease in the ONB temperature margin (the criteria for MITR safety analyses). Thus, the value reported is the percent change of the lowest ONB temperature margin from an element with all nominal parameters. An arbitrary limit of a 10% decrease in the ONB temperature margin was selected for evaluation of the parameters.

The P_{ONB} is determined through an iterative process. In the initial step, the probability of ONB occurring is found for the initial power (provided by the user, usually input as the LSSS power). STAT7 provides a probability based on random sampling from the probability density functions for various parameters. These distributions are modeled as Gaussian. Figure 2-2 displays a probability density function for the thickness of an inner coolant channel taken from the LEU fuel drawings.

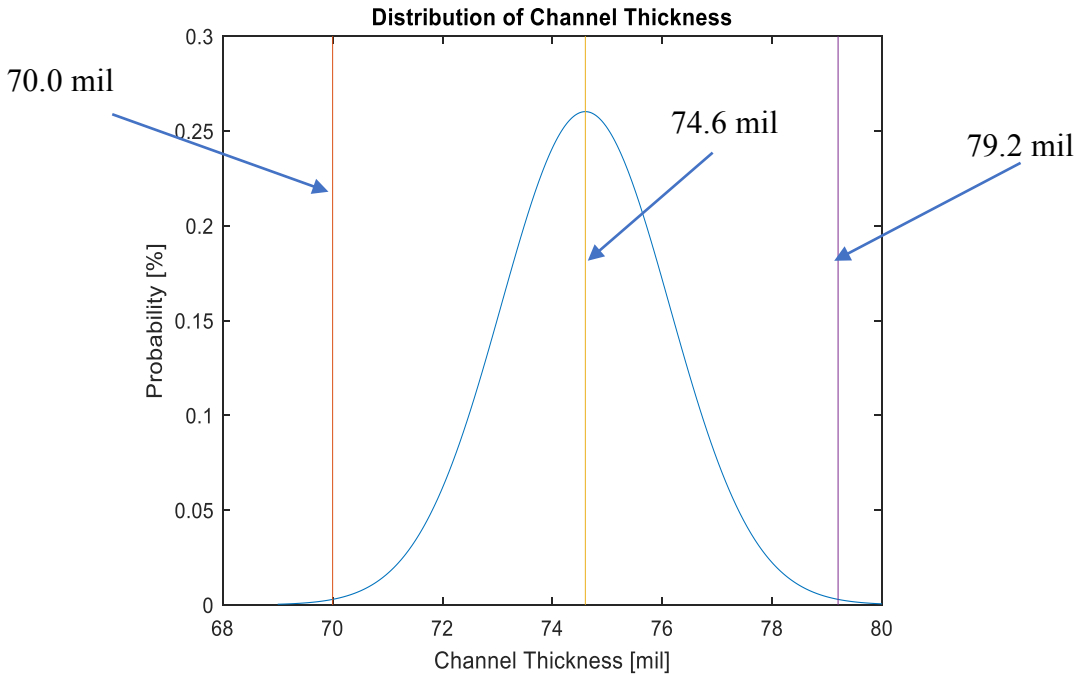

Figure 2-2: Gaussian Distribution of Channel Thickness

Gaussian distributions are defined by the mean (μ) and the standard deviation (σ). In this case, the nominal channel thickness (74.6 mil) is the mean. The standard deviation is provided based on a 1-σ percent (e.g., a 3-σ uncertainty of 5% is inputted as 0.01667). The user defines the sample size and the number of batches. For the analyses in this assessment, there are 25 batches with 4000 samples each, giving 100,000 histories. STAT7 creates a temperature profile for each of these histories. If at any one or more axial spots (total of 64 on each surface of each plate) $T_{co} > T_{clad,ONB}$ (i.e., the surface temperature is higher than the temperature at which ONB would occur) the history is recorded as a 1. If there are no instances of a surface temperature higher than the temperature at which ONB would occur in the core, the history is recorded as 0. These values are used by the code to determine the probability at which ONB will occur for a set of parameters. This probability is then assigned to the given power. If the probability is less than a specified criterion, then power is increased, and all 100,000 histories are repeated.

This iteration process continues until the ONB probability falls within the interval established by the convergence criterion. The converged power is recorded as P_{ONB} for that case. The criterion used in this analysis is 0.135%, with a convergence tolerance of 1% (0.134-0.136%). If the iteration process cannot achieve the 1% tolerance, then the number of histories is increased, and the process is repeated. The criterion value represents the power at which there is a 3-σ confidence level of 99.865% that ONB does not occur within the element. To illustrate this, Figure 2-3 shows a cumulative distribution function of a Gaussian. Three powers are annotated on this figure and represent the powers at which the probability of ONB occurring is 0.135% (3-σ below mean), 50% (mean), and 99.865% (3-σ above mean) for a nominal LEU core. Table 2-1 includes an example of this iteration process completed for an element with all nominal channels.

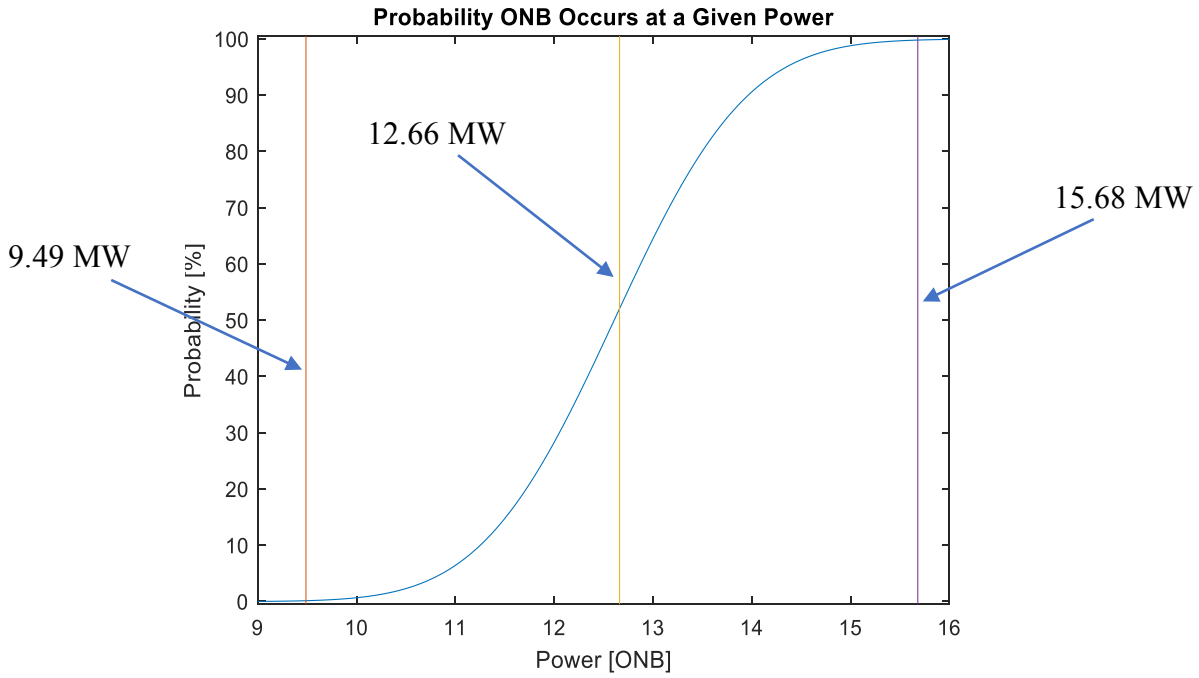

Figure 2-3: Probability ONB occurs at Given Power

Table 2-1: Power Iteration of Nominal Case to find P_{ONB}

Iteration	Power [MW]	ONB Probability
1	8.6800	6.000E-05
2	9.6800	2.670E-03
3	9.5003	1.420E-03
4	9.4872	1.340E-03

2.2.3 Verification of STAT7

STAT7 is a code developed by Argonne National Laboratory to assist with the thermal hydraulic calculations for plate-type reactors. Argonne National Laboratory verified the accuracy of the code, first without statistical sampling, using hand calculations. These verifications were completed for all of the code's capabilities and showed exceptional correlation with the hand calculations for all capabilities [17]. Additional research verified STAT7's use for MITR using RELAP5 mod 3.3. Table 2-2 shows this comparison for all cycles at the beginning of cycle (BOC). BOC was chosen as the focus due to zero xenon accumulation, making it the most limiting part of the cycle.

Table 2-2: Comparison of ONB temperature margin between STAT7 and RELAP5 for Beginning of Cycle (BOC) states [5]

Cycle	BOC					
			RELAP5		STAT7	
	Loc	Str	Plt	ΔT_{ONB}	Plt	ΔT_{ONB}
1	A2	4	16	17.69	16	17.72
2	A2	4	16	16.75	16	16.73
3	A2	4	16	14.84	16	14.76
4	A2	4	16	16.02	16	15.94
5	A2	4	16	14.70	16	14.60
6	B7	1	4	15.45	4	15.30
7	A2	4	15	15.28	16	15.19
8	A2	4	16	16.00	16	15.92
9	A2	4	16	14.97	16	14.89
10	A2	4	16	16.28	16	16.19
11	A2	4	16	15.44	16	15.34
12	B7	1	5	15.67	4	15.8
13	A2	4	16	15.00	16	14.93
14	A2	4	16	15.83	16	15.75

Table 2-2 shows "a comparison of ONB temperature margin (ΔT_{ONB} [°C]) for operation at LSSS between RELAP5 and STAT7. The hot stripe element location ("Loc") and stripe number ("Str") is determined by the evaluation of all core stripes using STAT7. For each code, the plate at which the minimum margin occurs ("Plt") is listed" [5]. If identified plates are not equivalent, the STAT7 plate and margin are identified and highlighted. STAT7 identified the same plate as limiting within the precision of the codes and calculated the ONB temperature margin to be at most a 1% difference from RELAP5. Hence, it is concluded that STAT7 provides an accurate prediction of the minimum ONB temperature margin [5].

Chapter 3: LEU Fuel Element Coolant Channel Analysis

3.1 Objectives

The first analysis completed was not to answer the neutronics question, but rather to investigate the effect of the coolant channel gap tolerance on thermal hydraulic safety margins. This tolerance became an early focus of the project due to the overall decrease in size of the coolant channel compared to the HEU design and the increase in thermal power produced by MITR. The procedure for this analysis was derived from a similar analysis (ICR assessment referenced in the Introduction) completed for the current HEU reactor that can be found in Appendix A. This analysis was completed on an equilibrium cycle as opposed to a fresh fuel core. A fresh fuel core will presumably operate at lower power than typical operating power due to the significant amount of fissile material and lack of fission product poisons. Later fuel cycles need to operate at the desired higher powers to complete the in-core experiments, with this analysis having the goal of proving this ability. Cycle 13 represents the equilibrium cycles as it exhibited the lowest ONB Power (P_{ONB}) amongst them [6].

This chapter focuses on the statistical propagation of uncertainties in fuel element manufacturing and its effects on thermal hydraulic safety margin, with a focus on the coolant channel gap thickness. The objective of this chapter of the assessment is to determine the effect of varying channel gap thicknesses and uncertainties on the MITR safety margin, achieved through the following tasks:

1. Quantify the impact of tolerances on the reactor power operating margin
2. Quantify the change in ΔT_{ONB} at varying thicknesses of the most limiting channel
3. Quantify the change in ΔT_{ONB} at varying thicknesses of all channels

This analysis does not incorporate the neutronic effects of altering the coolant channels. This change in thickness would add or subtract moderation to the fuel plates and thus have an effect on the power distribution within the element. This analysis instead focused on the separate thermal hydraulic impact of having the smaller or larger channels and the effect this would have on the margin to ONB. Later analyses address the combined neutronics and thermal hydraulics impact of off-nominal channel thicknesses.

3.2 Coolant Channel Analysis Methodology

3.2.1 Coolant Channel Thickness Analysis

The first part of this analysis was to understand the effects of alterations to individual channels. A variety of thicknesses for each type of channel were incorporated to see their effect on the operating margin for power and temperature. These thicknesses represented the current upper and lower bounds of the fabrication tolerance, and two values higher and lower than the bounds. The thicknesses differ between inner and end channels due to the tolerance for the end channel being significantly higher than the tolerance for the inner channel, 12.0 mil versus 4.6 mil.

The thicknesses chosen are included in Table 3-1 below and are inputs for STAT7 in this analysis. All uncertainties listed are 3-σ confidence level. The table contains the nominal specifications and tolerances used to represent every channel other than the altered one. The altered channel rows give the list of thicknesses evaluated for each type of channel and the uncertainty input for the altered channel. In addition to altering the channel thickness, the uncertainty was changed to an estimate of the current BWXT measurement uncertainty of ±1.0 mil. The lower uncertainty allows for the P_{ONB} results not to be skewed by minimum channels being allowed to decrease further. Channels significantly outside the evaluated thicknesses are beyond reasonable expectations and could make the element unable to fit within the current position size.

Table 3-1: Thicknesses and Uncertainty associated with the Channel Thickness Analysis

		Thicknesses to be Evaluated [mil]	Uncertainty[1]
Nominal Channel	Inner Channel	74.6 mil	±4.6 mil
	End Channel	65.6 mil	±17.0 mil[2]
Altered Channel	Inner Channel	70.0 mil & 79.0 mil (min/max) 68.0 mil & 81.0 mil (±2.0 mil) 66.0 mil & 83.0 mil (±4.0 mil)	±1.0 mil
	End Channel	54.0 mil & 78.0 mil (min/max) 48.0 mil & 84.0 mil (±6.0 mil) 42.0 mil & 90.0 mil (±12.0 mil)	±6.0 mil[2]

Note 1: All uncertainties are 3-σ confidence level
Note 2: The actual fabrication tolerance is ±12.0 mil for nominal end channels and ±1.0 for out-of-spec end channels, however, each of these include the additional 5.0 mil due to space between core structures

The P_{ONB} and percent change in ONB temperature margin were recorded for each of these analyses. The lowest of these values represents the most limiting channel and determines if the current tolerances fall within the established thermal hydraulic criteria. The criterion on the P_{ONB} is that it cannot be lower than the LSSS power of 8.68 MW. The criterion for percent change in ONB temperature margin is that it cannot decrease by more than 10%. If the percent decrease in ONB temperature margin is greater than 10%, it requires further analyses.

3.2.2 Coolant Channel Uncertainty Analysis

This section of the analysis focused on the changes to the uncertainties instead of the thicknesses themselves. This change in focus identifies how large the fabrication tolerances can be, in the event the tolerances need to be relaxed. During this analysis, the uncertainties were scaled with a multiplier using the following equations.

$$UNC_{end} = (X * 12.0) + 5 \tag{3-1}$$

$$UNC_{inner} = X * 4.6 \tag{3-2}$$

The difference in these equations exists due to the change in the tolerance and the unscaled 5.0 mil for core spacing. The multipliers used in these cases, along with the uncertainties associated with each, are shown in Table 3-2.

Table 3-2: Thicknesses associated with Multiplier X

Channel	Thicknesses associated with Multiplier (X) [mil]									
	x0.00	x1.00	x2.00	x2.25	x2.50	x2.75	x2.85	x2.90	x2.95	x3.00
Inner	±0.0	±4.6	±9.2	±10.4	±11.5	±12.7	±13.1	±13.3	±13.6	±13.8
End	±5.0	±17.0	±29.0	±32.0	±36.0	±38.0	±39.2	±39.8	±40.4	±41.0

This analysis was further broken down into 3 test cases:

- Test Case A:
  - All channel tolerances were scaled by a factor X
- Test Case B:
  - Similar to test case A, but channel 16 is reduced to the minimum of the range and held without uncertainty
- Test Case C:
  - Similar to test case B, but with no channel gap tolerances, to understand better the effect of a minimum thickness channel 16

Test case A is the ideal case to understand the effect of the fabrication tolerances, but test case B is also essential due to the most limiting channel having a more substantial effect on the P_{ONB} than other channels. As stated, test case C is an attempt to understand better the effect of the most limiting channel being at a minimum. This case takes away the effect other channels have on the P_{ONB}. For these test cases, P_{ONB} is the only result recorded. Limiting alteration to uncertainties alone does not affect the primary reported ONB temperature margin.

3.3 Coolant Channel Thickness Analysis Results

The results of this assessment are split into three different sections: the effects on the P_{ONB}, effects on the most limiting channel (channel 16), and effects on the local channel (altered channel). All margins presented are at the most limiting axial location.

3.3.1 Effects on ONB Power (P_{ONB})

The first part of this assessment focused on the change in P_{ONB} associated with the off-nominal thickness. The limit for the LSSS power is 8.68 MW. The P_{ONB} in the nominal core for this cycle is 9.49 MW. Figure 3-1 displays the P_{ONB} associated with off-nominal thicknesses for all channels. Each block in the figure represents the P_{ONB} associated with changing that specific channel to the associated thickness.

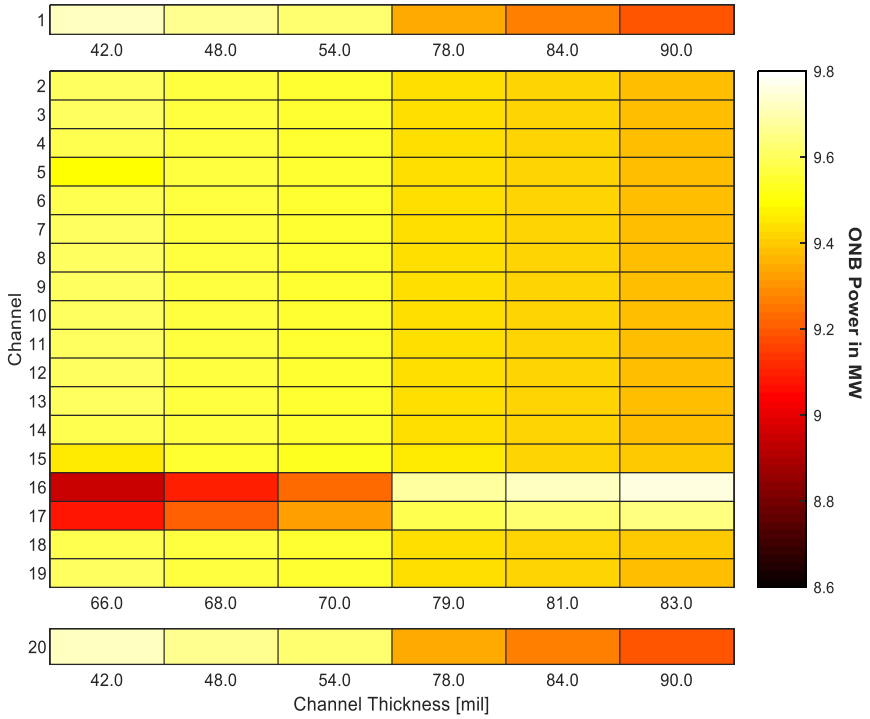

Figure 3-1: P_{ONB} [MW] of Off-Nominal Channels

This figure shows that the P_{ONB} is primarily affected by the most limiting channel's geometry and channels near it. This effect is observed in the vast decreases in P_{ONB} seen in channels 16 and 17. Other channels affect the P_{ONB} in an inverse way: increasing channel thicknesses, appropriating flow from the limiting channels, and thus decreasing P_{ONB}. In no cases modeled did the P_{ONB} decrease below the LSSS power. The lowest P_{ONB} observed was 8.95 MW when channel 16 was held at 66.0 mil thickness.

3.3.2 Effects on the Most Limiting Channel

The other thermal hydraulic criterion is the effect on the percent change in ONB temperature margin. This criterion needs to be addressed in two ways: the percent change for the most limiting channel and the percent change for the altered channel, the "local" channel. This research considers both values due to the effect the most limiting channel has on core safety. Channel 16, in almost all cases, has the lowest ONB temperature margin in the reactor. Thus, the change of this margin must be observed.

The most limiting channel has a nominal margin of 15.76 °C at the most limiting axial position. Figure 3-2 shows the percent change in the ONB temperature margin of the most limiting channel as a function of each altered channel at varying thicknesses. Since ONB occurs on the surface of a plate, each channel has two values associated with the respective plate numbers listed on the right side of the figure. These plate numbers are accompanied by an L and R to distinguish sides of the plate, with the left side of the element signified by plate 1. In this figure, every value reported is associated with either 15R (right side of plate 15) or 16L (left side of plate 16) as these are the plates that surround the most limiting channel.

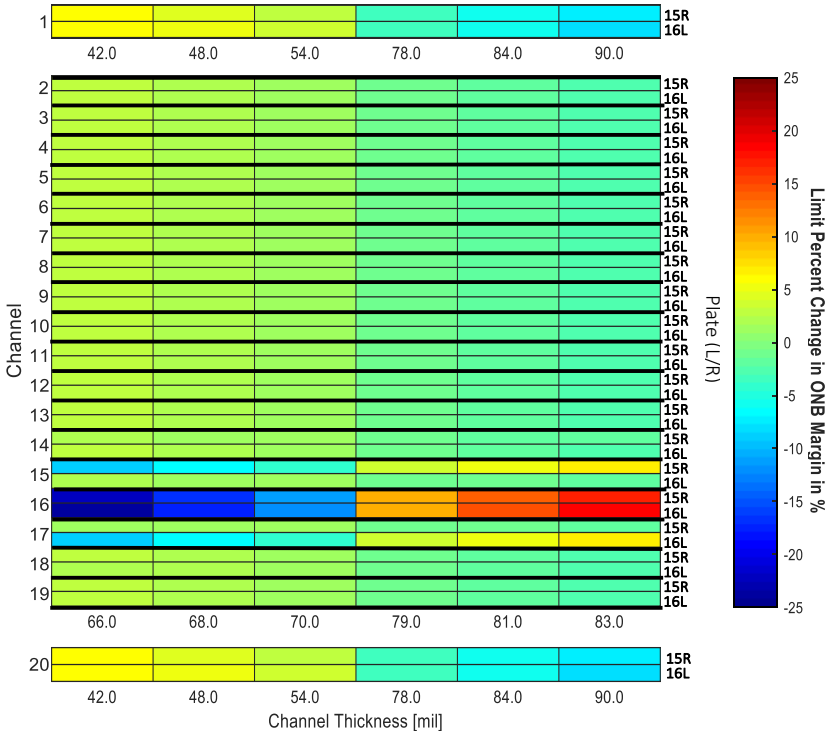

Figure 3-2: Percent Change in ONB Temperature Margin for Most Limiting Channel associated with Off-Nominal Channels

Figure 3-2 shows that off-nominal channels alter the flow to other channels evenly due to the constant pressure boundary conditions. A lower than nominal channel thickness in any channel other than the most limiting channel (adjacent to the most limiting plate) causes an increase in the

ONB temperature margin. The exceptions to this observation are the channels adjacent to the most limiting channel (i.e., Channels 15 and 17). Decreased flow in these channels affects the fuel plates adjacent to Ch. 16 and causes the margin to decrease.

When the most limiting channel (Channel 16) is the off-nominal channel, there are significant decreases in the ONB temperature margin. Due to this, the lower bound (70.0 mil) experiences a slightly higher than 10% decrease in ONB temperature margin (decreases to 13.89 °C). An element that has a greater than 10% decrease in the ONB temperature margin requires additional studies and restrictions on its location in the reactor.

3.3.3 Effects on Local Channel

This section discusses the effect of channels having an off-nominal thickness on the ONB temperature margin of local fuel plates. This consideration is necessary as the local ONB temperature margin may be lower than the most limiting channel's margin. Figure 3-3 shows the effect on the ONB temperature margin for the altered channel. The figure also lists the plates associated with the altered channel on the right side. Of note, the end channels (1 and 20) are on the outside of either T-plate and only have 1 plate associated with them.

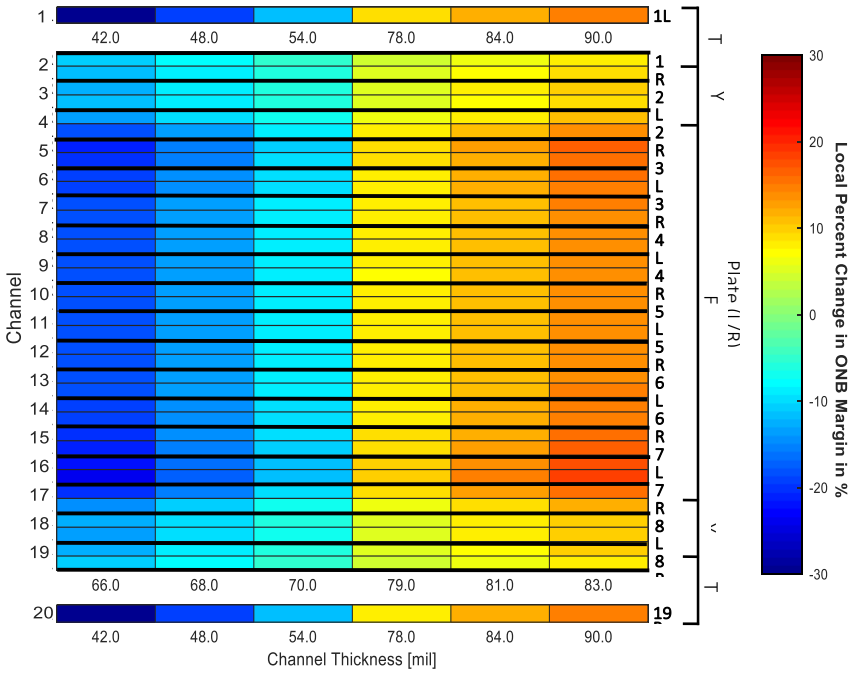

Figure 3-3: Local Percent Change in ONB Temperature Margin of Off-Nominal Inner Channels

Figure 3-3 shows that local effects can still be significant, and in some instances, cause the local channel to have a smaller ONB temperature margin than the most limiting channel. However, only

a few cases within the current manufacturing uncertainties (70.0-79.0 mil for inner and 54.0-78.0 mil for outer) cause a local channel, other than the most limiting channel, to have a larger than 10% decrease. These are channels 5, 15, and 17, which each have slightly higher than 10% decreases in ONB temperature margin (decreasing to 15.34 °C, 15.07 °C, and 14.95 °C, respectively).

While this section focused on the percent change in ONB temperature margin, it is still essential to understand the actual ONB temperature margin that occurs due to altered channels. Table 3-3 shows the location of the lowest ONB temperature margin due to each off-nominal thickness. In most cases, it is channel 16; however, there are a few channels that, at current allowable thicknesses, have the lowest ONB temperature margin. These channels line up with the channels that see a larger than 10% decrease in ONB temperature margin: 5, 15, and 17. This table also shows how unlikely it is for ONB to occur in specific channels, where drastic changes in thickness would need to occur for these channels to have the lowest ONB temperature margin.

Table 3-3: Most Limiting Channel for each Off-Nominal Thickness

Off-Nominal End Channel						
Th. [mil]	42.0	48.0	54.0	78.0	84.0	90.0
Ch. 1	16	16	16	16	16	16
Ch. 20	16	16	16	16	16	16
Off-Nominal Interior Channel						
Th. [mil]	66.0	68.0	70.0	79.0	81.0	83.0
Ch. 2	16	16	16	16	16	16
Ch. 3	16	16	16	16	16	16
Ch. 4	4	4	16	16	16	16
Ch. 5	5	5	5	16	16	16
Ch. 6	6	6	16	16	16	16
Ch. 7	7	16	16	16	16	16
Ch. 8	8	16	16	16	16	16
Ch. 9	9	16	16	16	16	16
Ch. 10	10	16	16	16	16	16
Ch. 11	11	16	16	16	16	16
Ch. 12	12	16	16	16	16	16
Ch. 13	13	16	16	16	16	16
Ch. 14	14	14	16	16	16	16
Ch. 15	15	15	15	16	16	16
Ch. 16	16	16	16	16	16	16
Ch. 17	17	17	17	16	16	16
Ch. 18	16	16	16	16	16	16
Ch. 19	16	16	16	16	16	16

3.4 Coolant Channel Uncertainty Analysis Results

This section compiles the results from the coolant channel uncertainty analysis. Only the P_{ONB} was recorded from each of these analyses, as altering the uncertainty has no effect on the temperature profile reported for nominal input parameters. The following plot displays the P_{ONB} of each analysis and the associated multiplier. The results of each test case are shown together in Figure 3-4. The dashed line represents the LSSS power of 8.68 MW, the criterion used for this assessment. A zero-uncertainty point is included for each test case to understand the full shape of the effect better.

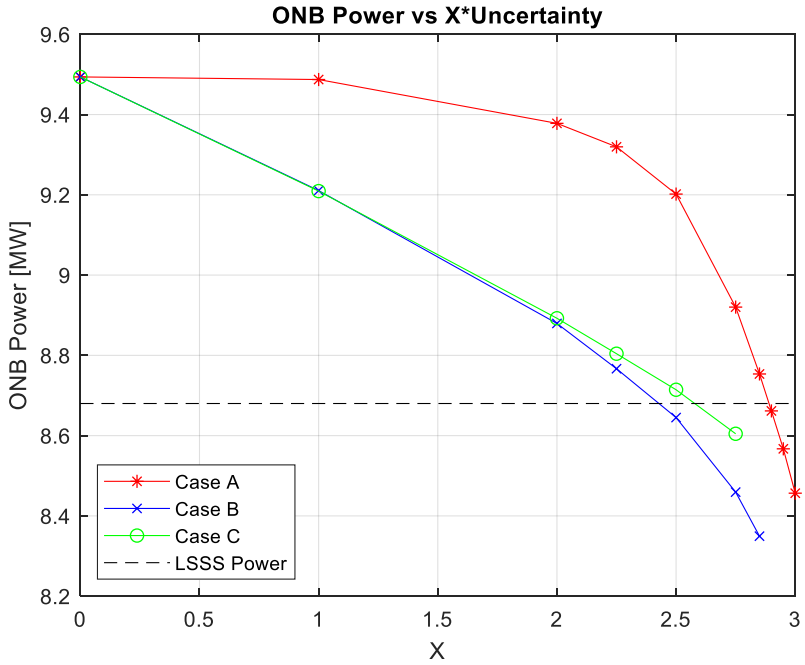

Figure 3-4: Results for all Test Cases of Channel Uncertainty Analysis

These results show that the fabrication tolerances can increase by 185% before a violation of the P_{ONB} criterion occurs. Test case A shows a decreasing logarithmic relationship between the uncertainty and the P_{ONB}. The only caveat to this, found in test cases B and C, would be if channel 16 is the minimum channel. A minimum channel 16 causes it to resemble a more linear relationship due to the limiting aspect of channel 16. Even with the most limiting channel held to a lower value, tolerances can increase by ~150%. In either case, assuming other fabrication specifications are met, there is still plenty of margin to the LSSS Power if the tolerances of the coolant channel need to increase.

3.5 LEU Coolant Channel Analysis Conclusions

The first section of this chapter aims to quantify the impact of off-nominal coolant channel thicknesses on thermal hydraulic safety parameters for an MITR LEU fuel element. In no cases modeled did the ONB Power (P_{ONB}) decrease below the LSSS power. A majority of the channels pass the safety analyses. Only channels 5, 15, 16, and 17 at the lower bound thickness (70.0 mil) have a larger than 10% decrease in ONB temperature margin, due to the proximity of these channels to the first F-type fuel plate on each side (plates 4 and 16). These channels have a large decrease in the ONB temperature margin due to the varying fuel thickness of the LEU element. The neutron flux changes as the fuel thickness decreases towards the ends of the fuel element. The flux gradient causes an increase in thermal backscattering, which increases the rate of fissions occurring in the full plates, leading to higher heat flux and lower ONB temperature margin.

The second section of this chapter aims to evaluate the margin to LSSS power if the fabrication tolerances need to increase. For this analysis, the limiting ONB Power (P_{ONB}) was the only result. Results indicated that if other technical specifications are met, the tolerances of coolant channel uncertainty could increase by over 150% in all cases, even with the most limiting channel held at a minimum. This margin is an important aspect to understand as the project moves forward, allowing for necessary expansion of tolerances if needed.

After completing these analyses, it is concluded that the proposed coolant channel thickness tolerances are sufficient. This specification can reach either bound on any channel without violating the LSSS power of 8.68 MW. A few channels can reach a higher than 10% decrease in ONB temperature margin, but this does not constitute declaring the tolerances insufficient. These elements can still be used in the reactor and not placed in the most limiting positions. While this analysis focused on the separate effect and did not incorporate the additional neutronics impact, it was a necessary step in understanding the impact of the coolant channel tolerances. The results of this analysis indicate that the coolant channel gap tolerances may be further increased.

Chapter 4: Fresh Core Analysis

4.1 Objectives

This chapter focuses on a full analysis of a 22-element fresh core, LEU Core 1. The parameters included in this section have a significant effect on the reactor physics and power distribution of the core. These parameters have a variety of impacts on the core, depending on the level at which they are off-nominal. This variety necessitates two approaches to this parametric analysis: the impact on the reactivity effect on fuel cycle length and SDM, as well as the impact of these tolerances on the local power density. The parameters that have an impact on reactor physics are:

- U-235 Enrichment
- Fuel Mass Loading
- Impurities (Equivalent boron content) in fuel and cladding/side plates
- Fuel Plate Thickness

The reactor physics analyses relied on full-core alterations to the above parameters, which can lead to significant reactivity insertions. Understanding these effects is necessary for ensuring the control of the reactor. The second section of the LEU Core 1 analysis focused on altering the parameters at a plate or element level, as this affects the local power density. The parameters included are:

- Fuel Mass Loading
- Fuel Plate Thickness

The local power density analysis incorporated these parameters for different reasons. Fuel mass loading has a broader tolerance at the plate level, while a majority of the above parameters keep a consistent tolerance at every level. Altering the fuel mass loading at a plate level does not have a significant effect on the reactor physics, but can have a more substantial effect on the power distribution in the element. Fuel plate thickness necessitated both approaches due to the conservative nature of a full-core alteration. The full-core analysis was important to understand, but very conservative and unlikely to occur. The element level alteration addresses the impact of this tolerance at a more reasonable level of alteration. The thermal hydraulics effect became the focus of an element level analysis due to the minimal effect on neutronics these smaller alterations would have. This change in focus required the margin to ONB criteria as the proper method of analysis.

4.2 Fresh Core Analyses

4.2.1 Equivalent Boron Content Factors

The ideal fabrication process keeps the fuel and other materials as pure as possible. However, creating materials that have perfect chemical composition is difficult and expensive. Many of these impurities act as neutron poisons for the reactor and add negative reactivity to the core. Impurities modeling helps evaluate what the limit should be for these trace elements to ensure they do not significantly impact the fuel cycle length. To more easily model and predict the negative reactivity added by varying levels of different impurities, all impurities are modeled as natural boron. This practice, referred to as Equivalent Boron Content (EBC), is used as it allows for a more efficient statistical analysis. Without the practice of EBC, there would need to be a sufficient number of analyses completed to model how differing amounts of each impurity interacted. This practice would be computationally expensive, while the practice of EBC limits the number of runs necessary.

The industrial practice of using EBC is outlined in ASTM C1233-15 and uses equations (4-1 & (4-2 to create a multiplier, the EBC factor. This factor determines the amount of natural boron needed to model a specific impurity [18].

$$EBC\ Factor = \frac{M_B * \sigma_i}{M_i * \sigma_B} \tag{4-1}$$

$$EBC\ [ppm] = EBC\ Factor * impurity[ppm] \tag{4-2}$$

where M_B is the atomic mass of boron, M_i is the atomic mass of the individual impurity, σ_B is the absorption cross section of natural boron, and σ_i is the absorption cross section of the individual impurity.

Table 4-1 displays the EBC factors of the 7 strongest impurities used in this analysis. Other impurities, while present, are significantly weaker and have a lower effect on the neutron population.

Table 4-1: EBC ASTM Factors [18]

Impurity	Atomic Mass	Cross Section at 0.0253eV [barns]	ASTM EBC Factors
Boron	10.801	764	1.0000
Cadmium	122.419	2520	0.3172
Dysprosium	162.5691	940	0.0818
Europium	152.0438	4565	0.4250
Gadolinium	157.3281	48890	4.3991
Lithium	6.9241	70.6	0.1439
Samarium	150.4481	5670	0.5336

This approach has a limitation in that the cross sections used in the above equation are for neutrons at 0.0253 eV. This energy level does not accurately reflect the neutron population within the core, where ~30% of the fissions occur outside of the thermal range. A method was developed to evaluate the neutron absorption of these impurities over the entire spectrum of the reactor. This method involved creating a tally within MCNP that contains the fuel within the core and counts the neutron fluence in the fuel. A tally multiplier then modeled the absorption rate by each of the individual impurities over the whole of the reactor's spectrum. This total absorption rate for each energy bin was then divided by the atomic density to find a total "cross section". This value is not solely the cross section but includes values that divide out when ratioed to other impurities. The impurities modeled with this method are the same impurities listed in Table 4-1. Each of these impurities were modeled at natural isotopic composition since impurities imbued during fabrication do not favor any specific isotope.

After completion of the MCNP file, the cross sections found were used in equation (4-1 to find the EBC factor for the whole of MITR's spectrum. Table 4-2 shows the comparison between these reactor specific EBC factors and the factors given by the ASTM standard [18].

Table 4-2: ASTM EBC Factors versus MITR Specific Factors [18]

Impurity	ASTM Standard EBC Factor	MITR Specific EBC Factor	Percent Difference
Boron	1.0000	1.0000	--
Cadmium	0.3172	0.5408	+70.4%
Dysprosium	0.0818	0.1249	+52.7%
Europium	0.4250	0.4948	+16.4%
Gadolinium	4.3991	1.8802	-57.3%
Lithium	0.1439	0.1475	+2.5%
Samarium	0.5336	0.8583	+60.8%

The majority of the impurities see an increase in absorption compared to boron. This increase is due to many of the impurities having resonances or higher cross sections just after the thermal point. The following plots display these facts, showing the cross section of all the impurities compared to boron. These plots include the spectrum of the reactor as well to visualize the lower amount of thermal neutrons. These cross sections are for natural concentration and were found by weighing the individual impurity cross sections using the atom ratios. The first plot shows the three impurities, which increased the most: samarium, cadmium, and dysprosium.

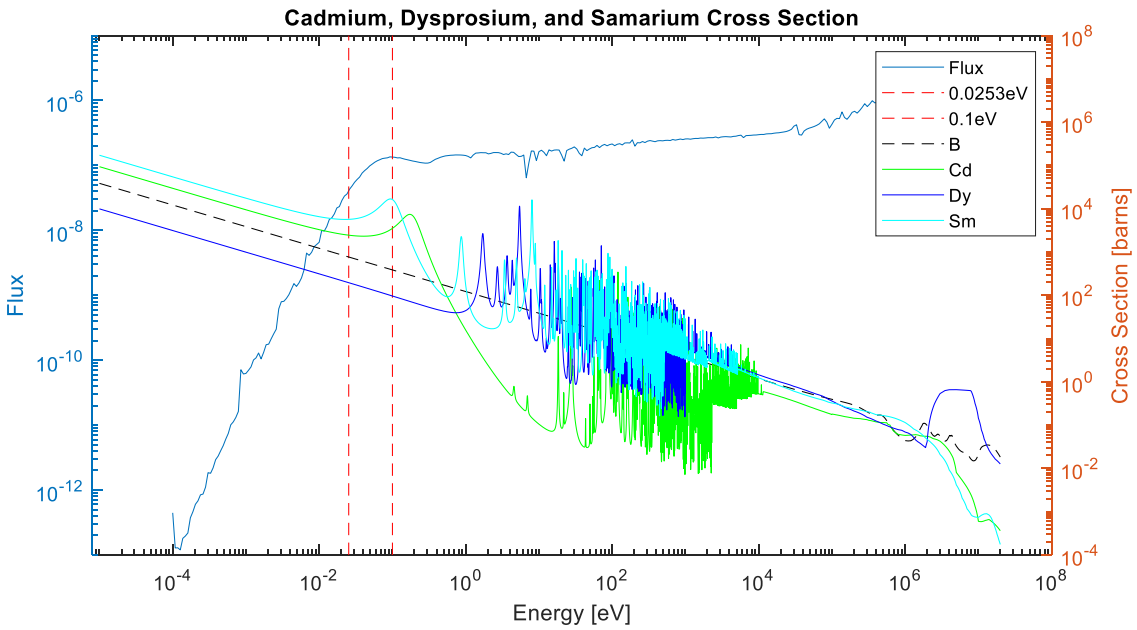

Figure 4-1: Comparison of Cadmium, Dysprosium, and Samarium Cross Section to Boron [19]

Figure 4-1 shows cadmium, dysprosium, and samarium absorption cross sections compared to boron, overlapping the spectrum of the reactor. The two red dashed lines represent the thermal neutron level and 0.1eV, which is the energy where a majority of the neutron absorption occurs. The black dashed line is the cross section of boron. The first two takeaways from this plot are that both samarium and cadmium have a resonance near 0.1eV, which significantly increases their absorption at that point. This resonance explains why each of them exhibits increases in their EBC factor compared to the ASTM method, which calculates the factor only at 0.0253eV. Dysprosium also exhibits a similar percentage increase in its EBC factor but does not have a resonance near the 0.1eV level. The reason behind this increase is presumably two-fold. First, the ASTM EBC factor is already much smaller than other factors, which means it does not take a lot of increase in cross section to change how much it absorbs. The second cause of this change is presumably due to the resonance region for dysprosium, which boron lacks. The resonance region increases the number of neutrons absorbed by the impurity. These two combined allow for an increase of ~50% to be observed while not necessarily having the same effect that cadmium and samarium exhibit.

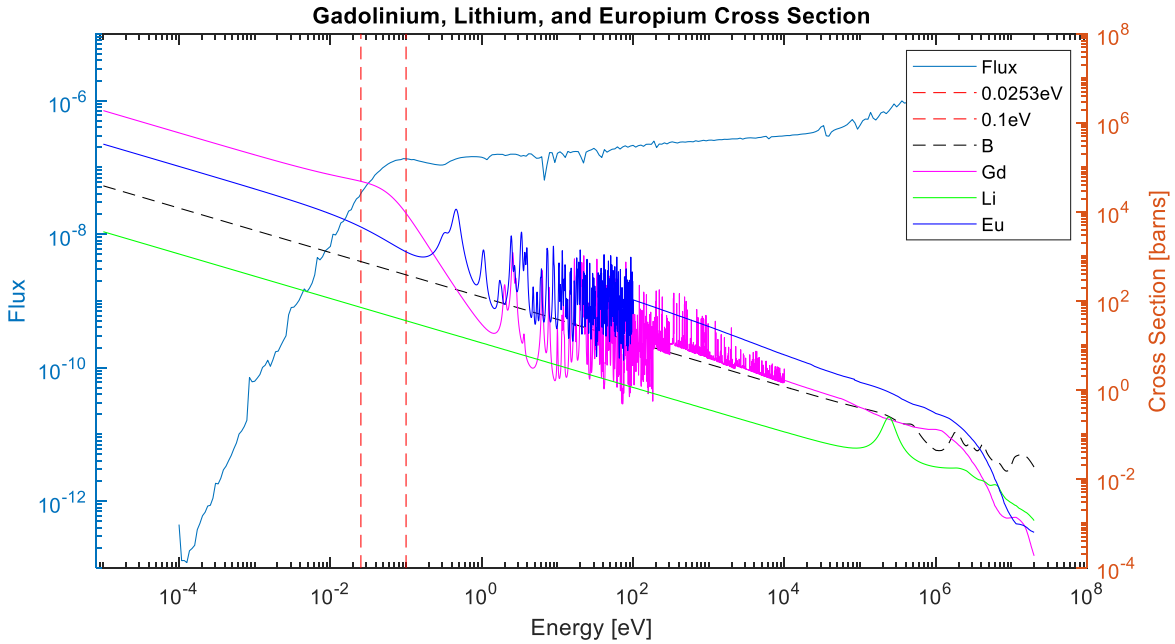

Figure 4-2: Comparison of Gadolinium, Lithium, and Europium Cross Section to Boron [19]

Figure 4-2 is similar to the previous figure but shows the cross sections of gadolinium, lithium, and europium compared to boron. Europium is similar to dysprosium and exhibits a slightly lower percent change in the EBC factor while increasing more. This increase in absorption is presumably due to a similar reason as dysprosium, the presence of a resonance region. Lithium increases only slightly due in part to the small resonances in the higher energy range. Gadolinium is the only impurity that sees a decrease in its EBC factor. This decrease is due to the sudden drop in the absorption cross section from the thermal range to the 0.1eV level.

While the cross sections showed reasonable explanations for all of the changes in the reactor specific EBC factors, verification was still needed. To do this, an additional MCNP run calculated reaction rates for different energy levels, specifically isolating an energy bin around 0.0253eV (0.0252-0.0254eV). The previously-described method used this reaction rate to find EBC factors at the thermal energy level that ASTM uses as their basis. A comparison between these values and the ASTM factors show the accuracy of the method. In addition to comparing their EBC factor, the ratio of thermal to 0.1eV cross sections was also recorded. Table 4-3 shows these comparisons.

Table 4-3: Verification of Reactor-Specific EBC Calculation Method

Impurity	ASTM Factor	MITR Factor	EBC Factor % Diff.	ASTM Cross Section Ratio	MITR Cross Section Ratio	Cross Section % Diff.
Boron	1.0000	1.0000	--	1.0000	1.0000	--
Cadmium	0.3172	0.3185	0.40%	3.2984	3.3143	0.48%
Dysprosium	0.0818	0.0819	0.11%	1.2304	1.2325	0.17%
Europium	0.4250	0.4229	-0.48%	5.9751	5.9536	-0.36%
Gadolinium	4.3991	4.3716	-0.62%	63.9921	63.6776	-0.49%
Lithium	0.1439	0.1479	2.77%	0.0924	0.0948	2.60%
Samarium	0.5336	0.5324	-0.23%	7.4215	7.4158	-0.08%

Results in Table 4-3 show that the reactor specific method develops EBC factors very close to the EBC factor calculated using the ASTM method. The only exception is lithium, which exhibited a 2 percent difference. In this case, there is a similar percent difference in the cross section ratio, which indicates the ASTM standard adopts slightly different cross sections to those included in ENDF-VII.0 used by MCNP5.

4.2.2 Full-Core Parameter Evaluations

As stated previously, the current LEU transition plan for the MITR begins with a 22 fresh fuel element core, LEU Core 1 [12]. During this initial 10-week cycle, the core is more sensitive to any off-nominal parameters due to the lack of fission product poisons typically present in the partially burned fuel elements. Even though the reactor is not in its nominal operating configuration, meeting criteria is still necessary to provide proper safety margins for the core. This necessity means that the reactivity shutdown margin must still be higher than 1% $\Delta k/_k$, ensuring the reactor can still shut down. All of the previously discussed parameters were evaluated at varying degrees to measure the impact of the current fabrication tolerances and the limit to which these parameters can be off-nominal.

Table 4-4 includes the parameters' nominal values and ranges chosen for testing.

Table 4-4: Neutronics Parameters and Tolerances

<table>
<tr><th colspan="3" rowspan="2">Parameter</th><th rowspan="2">Nom. Value [20]</th><th rowspan="2">Current Fabrication Tolerance [20]</th><th rowspan="2">Tested Values</th></tr>
<tr></tr>
<tr><td colspan="3">Enrichment [wt%]</td><td>19.75</td><td>±0.20</td><td>±0.20
±0.25
±0.30
+0.75 (20.50)</td></tr>
<tr><td colspan="2" rowspan="2">Impurities (EBC) [ppm]</td><td>Fuel</td><td>≤5.0</td><td>N/A</td><td>5.0, 11.6</td></tr>
<tr><td>Cladding[1]</td><td>≤67.0</td><td>N/A</td><td>67.0, 150.0</td></tr>
<tr><td colspan="3">Fresh Core U-235 Mass Loading[2] [kg]</td><td>21.296</td><td>±0.2156</td><td>±1.0%
±3.0%</td></tr>
<tr><td rowspan="6">Fuel Plate Thickness [mil]</td><td rowspan="3">Cladding Thickness</td><td>F-Type</td><td>11.0</td><td rowspan="6">Total Fuel Plate Tolerance: ±3.0</td><td rowspan="6">±1.5 Fuel
±1.5 Cladding
±0.75 Cladding & Fuel
±3.0 Fuel
±3.0 Cladding
±1.5 Cladding & Fuel</td></tr>
<tr><td>Y-Type</td><td>15.0</td></tr>
<tr><td>T-Type</td><td>17.0</td></tr>
<tr><td rowspan="3">Plate Thickness</td><td>F-Type</td><td>25.0</td></tr>
<tr><td>Y-Type</td><td>17.0</td></tr>
<tr><td>T-Type</td><td>13.0</td></tr>
</table>

Note 1: Impurities in Cladding includes impurities within the side plates of the element as well
Note 2: The specification displayed was taken from the specification for element fuel mass loading: 968±9.8 g. These values were multiplied by 22 to represent the 22-element fresh core. There is not a full-core fuel mass loading specification.

The tested values for enrichment represent the upper and lower boundaries of the current fabrication tolerances, in addition to two values outside these boundaries. The extra values completed help to identify better the relationship between enrichment and its effect on reactivity. The extra value of 20.50 wt% tested the range to which a linear relationship existed. The reactor would not accept an enrichment this high.

The values tested for impurities within the fuel and cladding, arise from the impurities currently allowed for within the proposed tolerances. Appendix B contains extensive details on these impurities. The impurities limit differs based on the location of the impurities due to their difference in expected strength. The limit of 5.0 ppm of EBC is the proposed tolerance and maximum for impurities within the fuel. However, this value does not account for the possibility of all impurities currently allowed for by the specification [20]. The analysis includes the value of 11.6 ppm as well, as this value represents the total EBC if all individual impurities were at their maximum allowed amount. The values decided upon for the cladding are contrived as there is no proposed tolerance for EBC within the cladding. There is a limit for impurities within the cladding and side plates, also listed in Appendix B, that identifies limits for various elements [21]. The value of 67.0 ppm would be the EBC of the given limits if all elements were at their maximum

concentration. The value of 150.0 ppm is a value chosen outside of the current range to examine the height to which these impurities could exist.

The values for fuel mass loading are ±1.0%, as that is the proposed tolerance on an element level (968 ± 9.8g) [20]. Individual plates have more substantial tolerances that were the subject of the local fuel mass loading analysis. The ±3.0% values served as additional points to establish a better curve fit.

Although there are separate tolerances for fuel overloading, the proposed tolerance for fuel plate thickness may arise from variations in the U-10Mo fuel, the AA6061 cladding, and to a lesser extent the thin zirconium interlayer (and so is not varied in this assessment). Therefore, to ensure there are no safety violations for either case, this tolerance was analyzed with 4 plate thickness cases: +3.0 mil, -3.0 mil, +1.5 mil, and -1.5 mil to total plate thickness. These cases were then each split into three separate cases where each alteration was done entirely to the fuel, done entirely to the cladding, and split into the fuel and cladding. Figure 4-3 illustrates the approach behind this analysis.

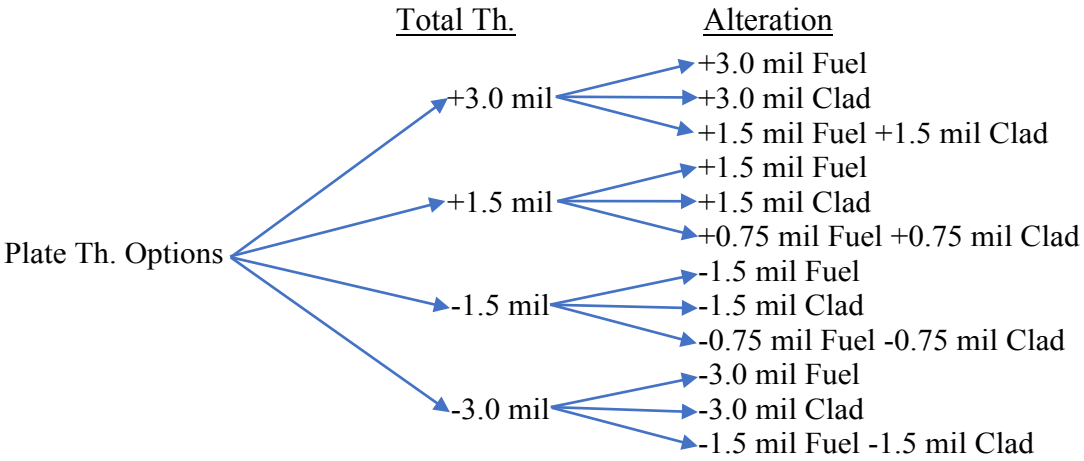

Figure 4-3: Off-Nominal Plate Thickness Analysis Approach

For this analysis, the mass of the material in the element was kept consistent by changing the density. In this way, the fuel plate thickness alteration only influences the amount of moderator within the core. For each of the proposed alterations, all evaluated plates change in the same way (e.g., all plates have fuel increase by 3.0 mil for +3.0 mil Fuel).

4.2.3 Full-Core Parameter Test Methodology

Each of these alterations was modeled in MCNP to find the k_{eff} and power distribution. To better compare the off-nominal parameters, each k_{eff} was used to find the $\Delta k/k$ using equation (4-3). The $\Delta k/k$ demonstrates the effect of an altered parameter on the core physics by quantifying the amount of positive or negative reactivity added.

$$\Delta k/_k\,[\%] = \frac{k_{alt} - k_{nom}}{k_{alt} * k_{nom}} * 100\% \quad (4\text{-}3)$$

where k_{alt} represents the k_{eff} of the altered case and k_{nom} represents the k_{eff} of the nominal case

This method of evaluation is useful for finding the effect the altered parameter has on the amount of excess reactivity within the fuel. This effect on excess reactivity means the $\Delta k/_k$ can be used to estimate the impact on the fuel cycle length of the element. This estimate is done by relating the $\Delta k/_k$ value to Effective Full Power Days (FPD) as any negative value of $\Delta k/_k$ indicates lower excess reactivity in the fuel, a loss of ~1 FPD is equivalent to -0.0151% $\Delta k/_k$ [1]. MITR fuel elements have enough excess reactivity for ~70 FPD. There is not an official criterion on the limit to this decrease and is instead used solely for estimating the impact on fuel cycle length, something not accomplished by the primary neutronics criterion.

The primary neutronics criterion used by MITR is the previously described SDM, a measure of how much the reactor is subcritical with the most reactive shim blade and regulating rod withdrawn [14]. Table 4-5 lists the SDM for a nominal case with each blade serving as the withdrawn blade.

Table 4-5: SDM associated with each blade in nominal LEU Core #1

Blade	SDM [% $\Delta k/_k$]
1	3.618
2	3.550
3	3.527
4	3.636
5	3.696
6	3.685

Blades 2 and 3 are the most limiting blades as they have the lowest SDM in the nominal case. Due to this, these two blades were the ones tested for each SDM analysis. The assessment included analyses of both blades serving as the withdrawn blade, in case an off-nominal parameter changed the location of the most limiting blade. The assessment focused on cases that involved the addition of positive reactivity to the core. The nominal case has shown a sufficient SDM, and that margin would only increase in cases involving the addition of negative reactivity to the core.

The $\Delta k/_k$ and reactivity shutdown margin are each recorded to understand the worth associated with each parameter, as well as if the reactor maintains adequate safety during operation.

[1] The value of 1FPD = 0.0151% $\Delta k/_k$ was developed through personal communication with Dr. Kaichao Sun

4.2.4 Local Parameter Test Methodology

This section of the fresh core analysis transitions away from full-core alterations and the effect on reactor physics. In this analysis, the focus shifts to local power density and the overall power distribution of individual elements. The first step in this analysis was to find the most limiting position within the core. An MCNP file with f7 tallies calculated the fission energy generated for each element, values then used to develop element-wise peaking factors for each position in the core. Table 4-6 displays these peaking factors, ratios of the power generated in that position versus an average position in the core, for each of the fuel positions of LEU Core 1**Error! Reference source not found.**.

Table 4-6: Element-Wise Peaking Factors

Position	Peak Factor	Position	Peak Factor	Position	Peak Factor
A-2	1.2535	C-2	0.9203	C-10	0.9955
B-1	1.1022	C-3	0.9704	C-11	0.9459
B-2	1.0482	C-4	0.9572	C-12	0.9087
B-4	1.1094	C-5	1.0093	C-13	0.9403
B-5	1.0623	C-6	0.9788	C-14	0.9178
B-7	1.1063	C-7	0.9465	C-15	0.9492
B-8	1.0314	C-8	0.9825		
C-1	0.9115	C-9	0.9528		

From this data, position A-2 is the hottest element in the core, due to it being the only position within the central ring that isn't a test position. Additionally, position C-5 represents the hottest element in the C-ring. The C-ring is next to the heavy water reflector and contains locations of possible peaking within the core. Since these two positions represent areas of possible concern, the local parameter analysis focused on each position for the fresh core studies.

The first parameter to be evaluated is the fuel mass loading. A majority of the parameters discussed in the previous section maintain a consistent fabrication tolerance at any level of the core. As stated previously, fuel mass loading has larger tolerances for an individual plate as compared to the element or core. This section discusses the test methodology for analyzing fuel mass loading at higher levels for the individual plates. Table 4-7 includes the fabrication tolerances for fuel mass loading associated with the specific plate types.

Table 4-7: U-235 Loading Tolerance at Plate Level [21]

Fuel Plate Type	U-235 Loading [g]	Fabrication Tolerance [g]
F-Type	57.74	±2.02
Y-Type	39.26	±1.37
T-Type	30.02	±1.05

Altering the fuel mass loading at a plate level affects the power distribution of the element. This change impacts the reactor power operating margin and the percent change in ONB temperature margin.

With positions A-2 and C-5 chosen as the focus of these studies, F, Y, and T-type plates from each side of both elements became the test plates to model the fuel mass loading alterations. Only the density of the fuel was changed in this analysis to isolate the effects of fuel mass loading. This isolation was necessary as changes in thickness would also alter the amount of moderator in the elements. The densities chosen for evaluation were approximately 1, 3, 6, and 9% greater and lesser than the nominal value. These values encompass the plate level tolerances and extend greatly beyond them to better develop a relationship. Table 4-8 displays the U-235 loading for each type of plate at the tested loadings. The table displays the difference between the nominal loading (density of 17.02 g/cc) for each type of plate at every loading as well.

Table 4-8: Altered U-235 Loading for Element and Plate

Density [g/cc]	Plate (±) [g]		
	F-Type	Y-Type	T-type
15.5	52.58 (-5.16)	35.75 (-3.51)	27.34 (-2.68)
16.0	54.28(-3.46)	36.91 (-2.35)	28.22 (-1.80)
16.5	55.98 (-1.76)	38.06 (-1.20)	29.10 (-0.92)
16.85	57.16 (-0.58)	38.87 (-0.39)	29.72 (-0.30)
17.02 (Nom.)	57.74	39.26	30.02
17.19	58.32 (+0.58)	39.65 (+0.39)	30.32 (+0.30)
17.5	59.37 (+1.63)	40.37 (+1.11)	30.87 (+0.85)
18.0	61.06(+3.32)	41.52 (+2.26)	31.75 (+1.73)
18.5	62.76 (+5.02)	42.67 (+3.41)	32.63 (+2.61)

Plates 1/19 (T-type), 3/17 (Y-type), and 4/16 (F-type) were the plates selected for this analysis. The location of these plates can be seen in Figure 1-3 in the Introduction section. The analysis involved each of these plates altered to the densities listed in Table 4-8. The resulting MCNP files included f7 tallies made for each spot of every fuel plate, split up into 16 axial nodes and 4 lateral nodes ("stripes"). These tallies created a tally file that lists all of the fission energy generated for each spot. This data created a profile of the percent change in power of each plate in the altered elements. In addition to plate power, STAT7 files modeled each similar stripe of all plates within the two positions in question (i.e., all stripes on the left side of the plates, all stripes on the right side of the plates). Each of these files calculated the power at which ONB would not occur at a 3-σ confidence level; the lowest power amongst the stripes represented the given plate loading alteration. While P_{ONB} was the focus of this analysis, the additional criterion required the percent change in ONB temperature margin found for each plate loading as well.

4.3 Fresh Core Neutronics Results

The first part of the results of this assessment includes the effects from each of the full-core parameters: enrichment, full-core fuel mass loading, EBC, and fuel plate thickness alterations (full-core and position A-2). These results display the reactivity change associated with each alteration and what effect that has on the SDM.

4.3.1 Neutronic Effects of Enrichment

The first parameter analyzed was enrichment. Enrichment was a vital parameter to understand due to the change from HEU to LEU. The ratio of U-235 to U-238 would be much smaller for LEU, which would presumably lead to more absorption by U-238 and, thus, a lower resonance escape probability. Due to this, the initial expectation was that any reduction in enrichment would have a significant effect on the ability to achieve criticality. However, the analysis showed that even with substantial changes in enrichment, the reactivity added or subtracted would be minimal. The most significant decrease in reactivity within current bounds is -0.1103% $^{\Delta k}/_{k}$ which leads to a loss of ~7 FPD. Table 4-9 displays the rest of these results.

Table 4-9: Reactivity Effects from Alterations to the Enrichment

Enrichment [wt%]	k_{eff}	Standard Dev. (σ)	$^{\Delta k}/_{k}$ [%]	FPD[2]
19.45	0.99749	0.00006	-0.1746	-12
19.50	0.99775	0.00006	-0.1484	-10
19.55	0.99813	0.00006	-0.1103	-7
19.75	0.99923	0.00002[1]	--	--
19.95	1.00044	0.00006	+0.1210	+8
20.00	1.00086	0.00006	+0.1630	+11
20.05	1.00112	0.00006	+0.1889	+13
20.50	1.00366	0.00006	+0.4417	+29

Note 1: The standard deviation for the nominal case of 19.75 wt% is lower than others as it was run with higher clarity due to be using in all cases

Note 2: All values of FPD are estimations using 1 FPD = 0.0151 $\%^{\Delta k}/_{k}$

The data showed a linear relationship between the change in reactivity and the percent change in enrichment. Figure 4-4 displays this relationship, along with the associated curve fit. This fit can predict the effects of alterations in the currently evaluated range not included in the current test matrix. The figure also shows a 95% confidence interval to indicate how well the linear relationship fits the data shown. This confidence interval was developed using the *polyfit* and *polyval* functions on MATLAB. These functions utilize the Vandermonde matrix of the data set, the triangular decomposition of that matrix, and its norm residual to develop the standard error associated with the function [22]. An essential aspect of every Monte-Carlo analysis is accounting

for the given uncertainty. This analysis incorporated these uncertainties and used them to develop uncertainties in the calculated slope of the linear relationship. This process involved finding the maximum slope allowed, accomplished by decreasing all values below nominal by 3-σ and increasing all values above nominal by 3-σ. The minimum slope uses the opposite approach. These values were equally distant from the nominal slope and included below the function.

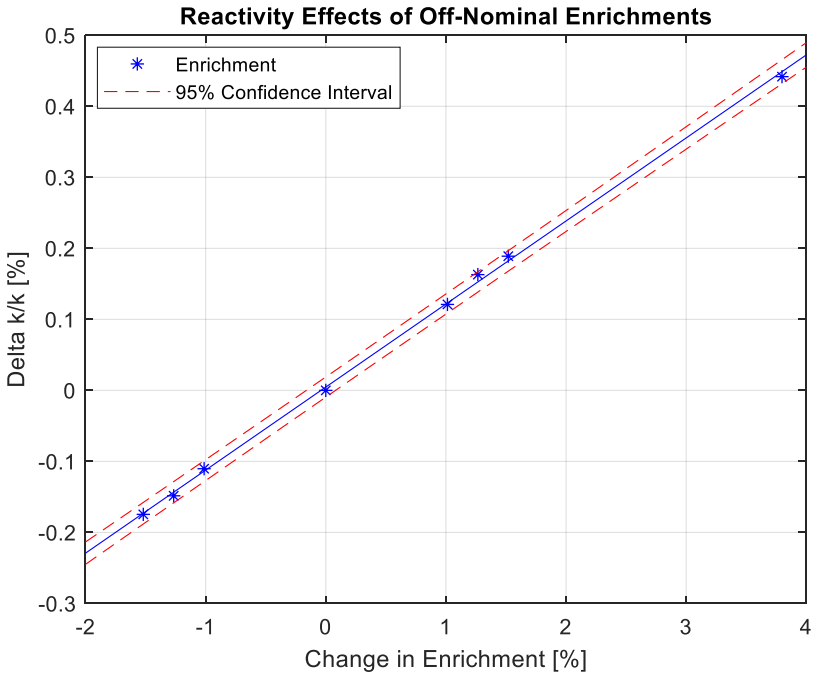

Figure 4-4: Reactivity Effects of Off-Nominal Enrichment

$$\Delta k/_{k_{enr}}\,[\%] = 0.1169(\%enr) + 0.0047 \qquad (4\text{-}4)$$

Slope Uncertainty: ± 0.0087

This relationship, equation 4-4, is helpful to understand the effects of non-evaluated enrichments and the slope is a useful way to compare the parameter's impact to the effect of other parameters.

After completing the initial analysis on enrichment, the next step was to ensure the tolerance would not violate the SDM criterion. Table 4-10 lists the SDM's calculated for every enrichment value that added positive reactivity to the core.

Table 4-10: SDM Enrichment Values

Enrichment [wt%]	SDM $[\%\,\Delta k/_k]$	
	Blade 2	Blade 3
19.95	3.4212	3.4222
20.00	3.3880	3.3773
20.05	3.3592	3.3378

20.50	3.0747	3.0790

The results show that none of the analyzed enrichments cause a SDM margin to be less than 1% $\Delta k/k$.

This analysis shows that the current tolerances and enrichment values outside the bounds do not cause any violations of the neutronics criterion or cause significant decreases in fuel cycle lifetime.

4.3.2 Neutronic Effects of Full-Core Fuel Mass Loading

In addition to enrichment, the other parameter that affects the amount of fissile material in the core is the fuel mass loading. Enrichment changes the ratio of U-235 vs. U-238 while keeping approximately the same mass of U-Mo in the core. Fuel mass loading keeps a consistent ratio while changing the amount of U-Mo. This process involved altering the density of the fuel rather than the size of the fuel plates. This approach allowed the amount of moderator (i.e., the coolant) or potential absorber (i.e., the cladding) to be constant.

This part of the fuel mass loading analysis focused on the neutronics effect of a full-core alteration.

Table 4-4: Neutronics Parameters and TolerancesTable 4-11 lists the densities and fuel mass loading of each case of the full-core analysis. The change in reactivity was recorded for each and included below. The most significant decrease in reactivity currently within bounds is -0.048% $\Delta k/k$ which would lead to a loss of ~3 FPD.

Table 4-11: Reactivity Effects of Altered Uranium Loading

Fuel Mass Loading		k_{eff}	Standard Dev. (σ)	$\Delta k/k$ [%]	FPD[1]
Density [g/cc]	Mass (±) [kg]				
16.5	20.636 (-0.66)	0.99758	0.00006	-0.1651	-11
16.85	21.076 (-0.22)	0.99875	0.00006	-0.0480	-3
17.02	21.296	0.99923	0.00002	--	--
17.19	21.516 (+0.22)	0.99990	0.00006	0.0671	+4
17.5	21.890 (+0.594)	1.00080	0.00006	0.1571	+10

Note 1: All values of FPD are estimations using 1 FPD = 0.0151 $\%\Delta k/k$

Similar to the enrichment analysis, the data showed a relationship between percent change in reactivity and percent change in density (fuel mass loading). This relationship was also linear and included below the plot. As with the enrichment analysis, the plot includes a 95% confidence interval, and the uncertainty in the calculated slope is below the function.

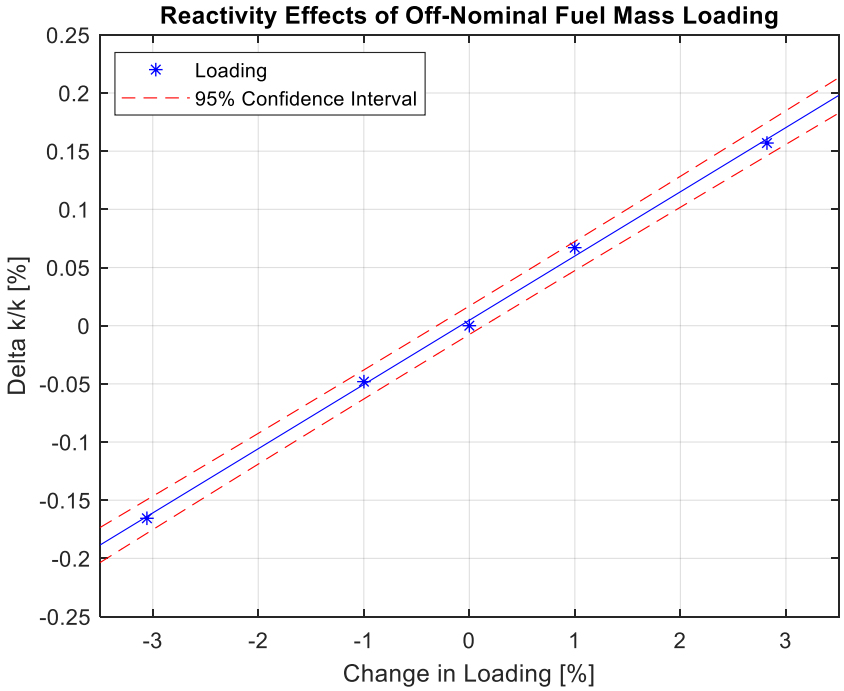

Figure 4-5: Percent Relationship between Full-Core Mass Loading and Reactivity

$$\Delta k/_{k_{den}} = 0.0552(\%den) + 0.0048 \qquad (4\text{-}5)$$

Slope Uncertainty: ± 0.0074

The linear relationship developed for fuel mass loading shows that it has a much lower effect than enrichment. Equation 4-5 shows this curve fit. The slope for fuel mass loading is 52% lower, which means that enrichment has approximately twice the impact of fuel mass loading. This large difference is because increasing fuel mass loading also increases the amount of U-238, which in turn increases the amount of poison within the fuel and lowers the resonance escape probability.

Similar to the enrichment analysis, the SDM portion of this analysis includes all fuel mass loadings that added positive reactivity. Table 4-12 lists these SDM values with blades 2 and 3 individually serving as the most limiting blade of each case.

Table 4-12: SDM Fuel Mass Loading Values

Fuel Mass Loading [kg]	SDM [$\%\ \Delta k/_k$]	
	Blade 2	Blade 3

21.516	3.4832	3.4779
21.890	3.3549	3.3496

As with the analysis completed for enrichment, none of the fuel mass loading values cause a violation of the SDM criterion of 1.0% $\Delta k/k$.

This analysis shows that the current tolerances and fuel mass loading values outside the bounds do not cause any violations of the neutronics criterion or cause significant decreases in fuel cycle lifetime.

4.3.3 Neutronic Effects of Impurities in Fuel and Cladding/Side Plates

This section addresses the significant poison effect of the proposed tolerances of impurities, modeled in the previously described amounts of natural boron. The first step of this analysis was modeling the EBC in the fuel. This process involved altering the fuel material card in MCNP to contain 5.0 and 11.6 ppm of natural boron. After finding the k_{eff} for each of these cases, the next step was to model the additional impurities in the cladding and side plates. This step involved creating an additional AA6061 material card for the cladding and side plates, that contained 67.0 or 150.0 ppm of EBC and calculating the associated k_{eff}. Table 4-13 includes the values of every k_{eff} calculated during this section of the research.

Table 4-13: Neutronics Effects of Impurities in Fuel and Cladding/Side Plates

EBC [ppm]		k_{eff}	Standard Dev. (σ)	$\Delta k/k$ [%]	FPD[1]
Ideal Case (Fuel: 0 Cladding/Side Plates: 135)		0.99923	0.00002	--	--
Fuel	Ideal + 5.0	0.99874	0.00006	-0.0490	-3
	Ideal + 11.6	0.99789	0.00006	-0.1341	-9
Cladding /Side Plates	Ideal + 67.0	0.99428	0.00006	-0.4954	-33
	Ideal + 150.0	0.98811	0.00006	-1.1129	-74

Note 1: All values of FPD are estimations using 1 FPD = 0.0151 $\%\Delta k/k$

The first of each of these analyses, 5.0 EBC for fuel and 67.0 EBC for cladding and side plates, are the proposed limits for the LEU specification and are used to estimate the effect impurities have on fuel cycle length. The limit for the fuel causes a $\Delta k/k$ of -0.0490% that causes a decrease of ~3 FPD. The limit for the cladding and side plates causes a $\Delta k/k$ of -0.4954% that causes a decrease of ~33 FPD or nearly 50% of the expected fuel cycle length. Figure 4-6 shows the values from the table plotted to find a relationship concerning the impact of the impurities. Due to the significant difference in effect, the reactivity effect of the fuel follows the left y-axis, and the reactivity effect of the cladding and side plates follows the right y-axis. These plots do not include

confidence intervals due to the lack of data points. The uncertainties associated with the slope of each line are included below the plot. These uncertainties were calculated by increasing each value 3-σ or decreasing each value 3-σ and finding the slope for each case.

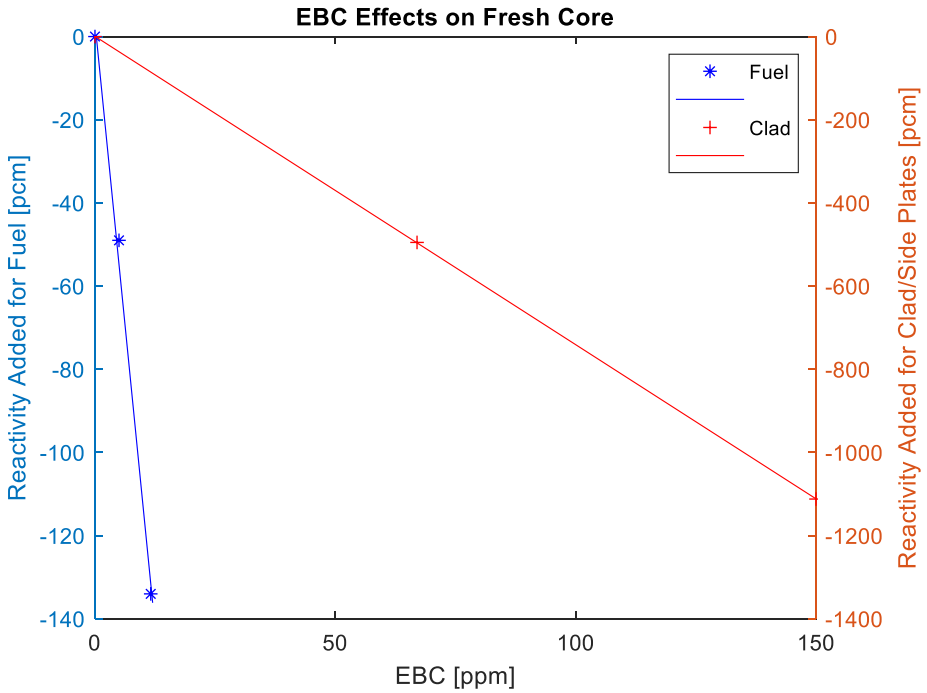

Figure 4-6: Reactivity Effects of Impurities in Fuel and Cladding/Side Plates

This figure shows that the effect of impurities is a linear relationship with different slopes. These slopes are an estimator of reactivity added. The values for each location are:

$$\text{Fuel} \rightarrow -11.6 \pm 1.5 \ \frac{pcm}{ppm}$$

$$\text{Cladding/Side Plates} \rightarrow -7.4 \pm 0.1 \ \frac{pcm}{ppm}$$

These slopes compared to the previously seen effects on fuel cycle length show two things about the effect impurities have on the core. The first of these effects is that, as expected, impurities within the fuel have a stronger effect than impurities in the cladding and side plates. A comparison of the slopes shows that 1 ppm in the fuel leads to an addition of 62% more negative reactivity than 1 ppm in the cladding and side plates. However, even though the impurities within the fuel are stronger than impurities in the cladding and side plates, they are significantly more regulated, with the limit being 5 ppm of EBC. The impurities in the cladding and side plates are currently allowed to reach 67.0 ppm of EBC. Due to this fact, the proposed tolerance is not sufficient, as the impurities in the cladding and side plates can decrease the fuel cycle length by nearly 50%. There will be further work done to lower the tolerances associated with the cladding and side plates.

The SDM was not calculated for this parameter as impurities add negative reactivity to the core and do not lower the SDM from nominal.

4.3.4 Neutronics Effects of Fuel Plate Thickness Alterations

As mentioned in the objectives section of this chapter, off-nominal plate thickness was tested in two different ways: evaluating this tolerance at a full-core level and evaluating the tolerance on an individual element. For the first part of this analysis, each fuel plate in the core is off-nominal in the same way. However, it is extremely conservative to assume every plate within the core would change in the same way. The other part of this analysis was to look at the tolerance on a single position level. Table 4-14 shows the results of each of these analyses. All of the k_{eff}'s for the altered cases have the same standard deviation of 0.00006 as with previous studies.

Table 4-14: Neutronics Effect of Fuel Plate Thickness Alterations

Alteration [mil]	Full-Core			Position A-2		
	k_{eff}	$\Delta k/k$	FPD[1]	k_{eff}	$\Delta k/k$	FPD[1]
+3.0 Cladding	0.98531	-1.393%	-92	0.99855	-0.068%	-5
+1.5 Fuel +1.5 Cladding	0.98572	-1.352%	-90	0.99852	-0.071%	-5
+3.0 Fuel	0.98615	-1.309%	-87	0.99851	-0.072%	-5
+1.5 Cladding	0.99231	-0.693%	-46	0.99885	-0.038%	-3
+0.75 Fuel +0.75 Cladding	0.99256	-0.668%	-44	0.99896	-0.027%	-2
+1.5 Fuel	0.99282	-0.641%	-42	0.99897	-0.026%	-2
Nominal	0.99923	--	--	0.99923	--	--
-1.5 Cladding	1.00630	+0.708%	+47	0.99972	+0.049%	+3
-0.75 Fuel -0.75 Cladding	1.00600	+0.678%	+45	0.99975	+0.052%	+3
-1.5 Fuel	1.00576	+0.654%	+43	0.99971	+0.048%	+3
-3.0 Cladding	1.01316	+1.394%	+92	1.00014	+0.091%	+6
-1.5 Fuel -1.5 Cladding	1.01246	+1.324%	+88	1.00023	+0.100%	+7
-3.0 Fuel	1.01204	+1.282%	+85	1.00007	+0.084%	+6

Note 2: All values of FPD are estimations using 1 FPD = 0.0151 $\%\Delta k/k$

The first observation from these results is that full-core fuel plate thickness alterations have a significant effect on reactivity. This impact is due to the large increases or decreases of moderator within the core associated with those changes. Increasing or decreasing 3.0 mil to all fuel plates, therefore doing the same to all channels, leads to a ~4% change in total moderation. This change in moderation leads to significant reactivity changes, both positive and negative. The most substantial reactivity effect currently modeled in the full-core occurs when the cladding is increased by 3.0 mil, where the alteration causes -1.393% $\Delta k/k$. This reactivity effect would lead to an estimated cycle length decrease of ~92 FPD. As mentioned above, this result is obtained with an unrealistic and extremely conservative assumption that all plates within the core would change in the same way. For the position A-2 analysis, the most substantial reactivity effect modeled occurs when the fuel in position A-2 is increased by 3.0 mil, where the alteration causes -0.072%

$\Delta k/_k$. This alteration leads to an estimated decrease of ~5 FPD, which is allowable for the MITR LEU conversion. Similar to previous neutronic analyses, the data shows a linear relationship for both cases. The figures below display these relationships with a 95% confidence interval.

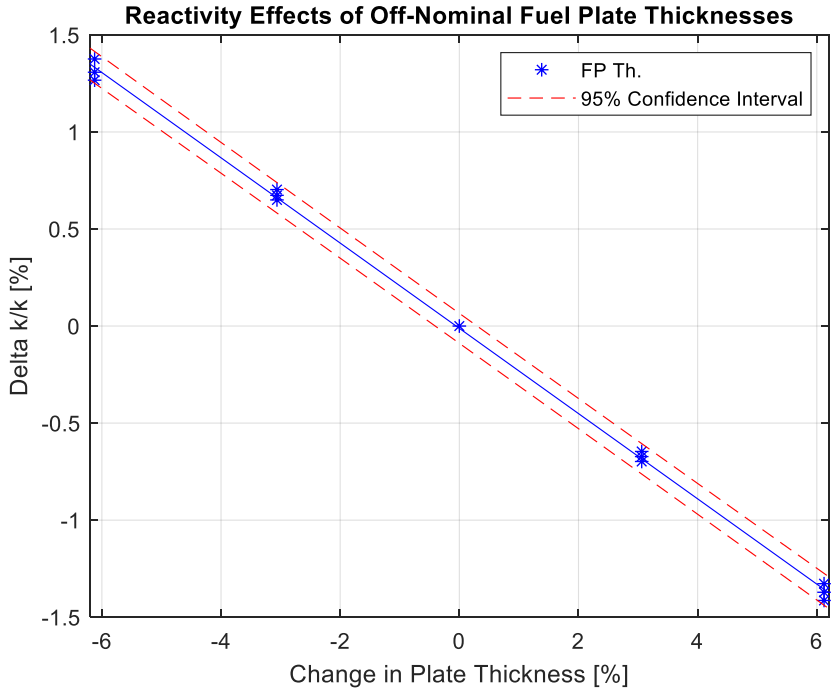

Figure 4-7: Reactivity Effects of Full-Core Fuel Plate Thickness Alterations

$$\Delta k/_{k_{Fuel\ Pl.\ Th.}} = -0.2196\left(\%plate\ th._{full\ core}\right) - 0.0117 \quad \text{(4-6)}$$

Slope Uncertainty: ± 0.0035

Figure 4-7 shows the drastic effects of a full-core fuel plate thickness alteration. As discussed in the previous section, the current decrease in reactivity allowed by current tolerances would be too significant to allow. Equation 4-6 is the curve fit of this function and shows that the parameter has approximately double the impact of enrichment at a full-core level. Figure 4-8 shows the relationship associated with altering a single position.

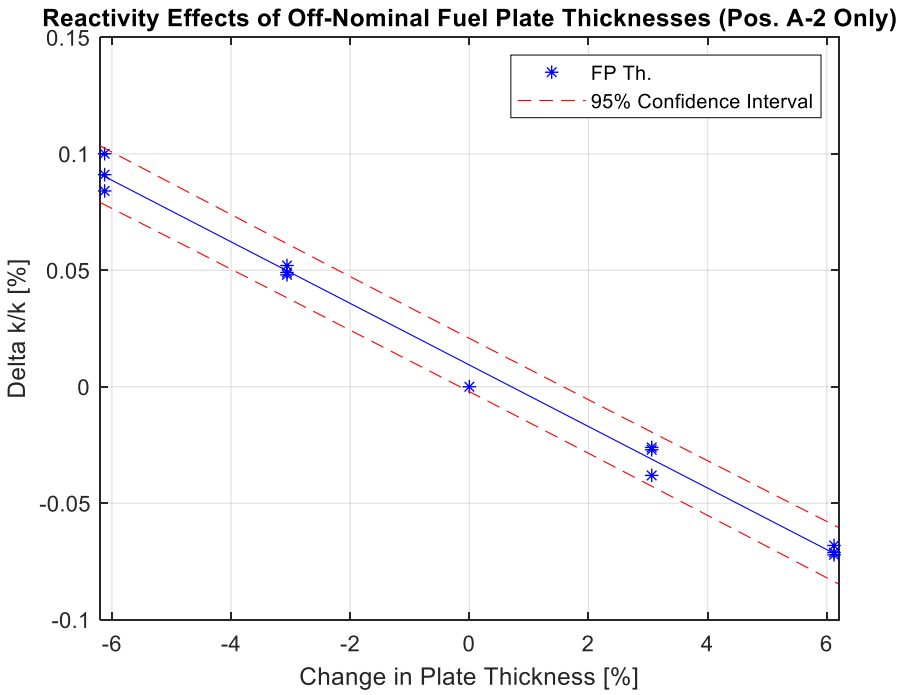

Figure 4-8: Reactivity Effects of Position A-2 Fuel Plate Thickness Alterations

$$\Delta k/_{k_{Fuel\ Pl.\ Th.}} = -0.0132(\%ratio_{Pos.\ A-2}) + 0.0094 \quad (4\text{-}7)$$

Slope Uncertainty: ± 0.0035

This figure shows that while a full-core alteration would have dramatic effects, changing only position A-2 would have a much lower effect on fuel cycle length. Equation 4-7 shows the associated slope with this parameter at the position A-2 level. Comparing the slopes from equations 4-6 and 4-7 show that the estimated effects on cycle length are ~20 times lower for a single position. The uncertainty in the slope for position A-2 is also rather high due to the magnitude of the effects compared to the MCNP statistical uncertainty. The local alterations have a greater effect on the thermal hydraulic aspects of the core, an analysis discussed in a later section.

The final aspect of the full-core neutronics analyses was to complete the SDM analysis for the fuel plate thickness. The SDM analysis incorporated only the full-core assessment since it was significantly more limiting than solely changing position A-2. Table 4-15 displays the SDM's calculated.

Table 4-15: SDM Fuel Plate Thickness Values

Full-Core Fuel Plate Thickness Change	SDM $[\% \Delta k/_k]$	
	Blade 2	Blade 3
Decrease Cladding 3.0 mil	1.9046	1.8994
Decrease Cladding and Fuel 1.5 mil	2.0002	1.9185
Decrease Fuel 3.0 mil	2.0648	2.0648
Decrease Cladding 1.5 mil	2.7179	2.7084
Decrease Cladding and Fuel 0.75 mil	2.7644	2.7422
Decrease Fuel 1.5 mil	2.7887	2.7813

This data shows that none of the cases violate the SDM criterion of 1.0% $\Delta k/_k$.

This analysis shows that the current tolerances for fuel plate thickness do not violate any of the neutronics criteria set by MITR. If altered on a full-core level, the tolerances have a significant effect on the fuel cycle length, but this alteration is too conservative. The tolerance at a single position level occurs to a much lower magnitude and is expected not to violate the criteria or have a significant effect on fuel cycle length.

4.4 Fresh Core Thermal Hydraulic Results

The second part of the results are from the local fuel mass loading assessment, starting with the neutronics effects, and then the effects on the margin to ONB. The last part of the results is the effects of element-level fuel plate thickness alterations on the margin to ONB.

4.4.1 Effects of Local Alterations in Fuel Mass Loading in Position A-2

This section of the fuel mass loading analysis focuses on the local thermal hydraulic effects due to alterations in position A-2, the hottest position in the core. The first part of this analysis is to understand the effects on plate power. Similar to creating the element-wise peaking factors, f7 tallies generated fission power distributions of every fuel mass loading alteration completed. The data created by these power distributions showed the percent change from nominal for all alterations completed. This data showed that all plates exhibited the same changes in plate power for each loading alteration (e.g., plate 4 at 16.85 g/cc exhibited the same percent change from nominal in plate power as plate 1 at 16.85 g/cc). Figure 4-9 shows an example of the effect on plate power, specifically the effect on plate 4's power. In the figure, the percent change in plate power is displayed for plates 1-10 when plate 4 is altered to the given densities. Only plates 1-10

are displayed to show more detail. The plates not shown, 11-19, exhibit very minimal effects due to their distance from the altered plate.

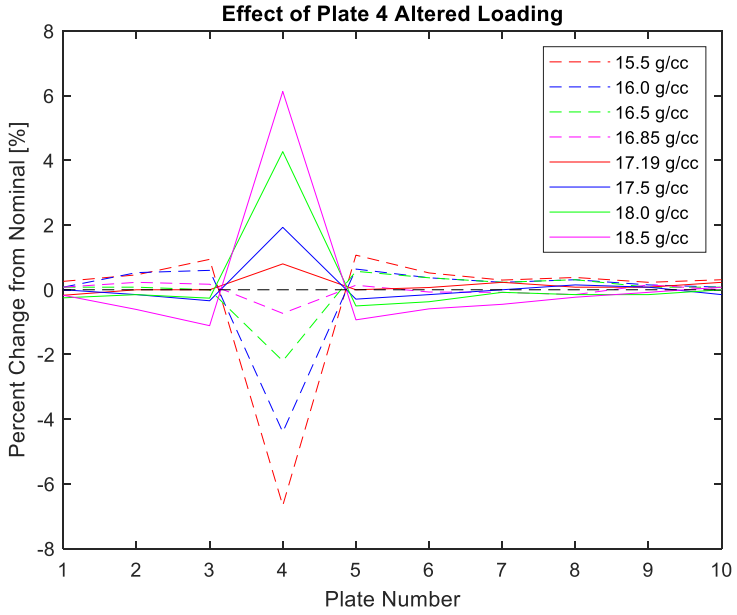

Figure 4-9: Percent Change in plate power for Plate 4 Altered Loading in Position A-2

The next step was to find a relationship between the percent change in density and percent change in plate power. Figure 4-10 shows this relationship, which is also linear. The function describing the relationship is similar amongst all plates and can be used to find the plate power for further thermal hydraulic analyses. Table 4-16 includes the functions for each altered plate.

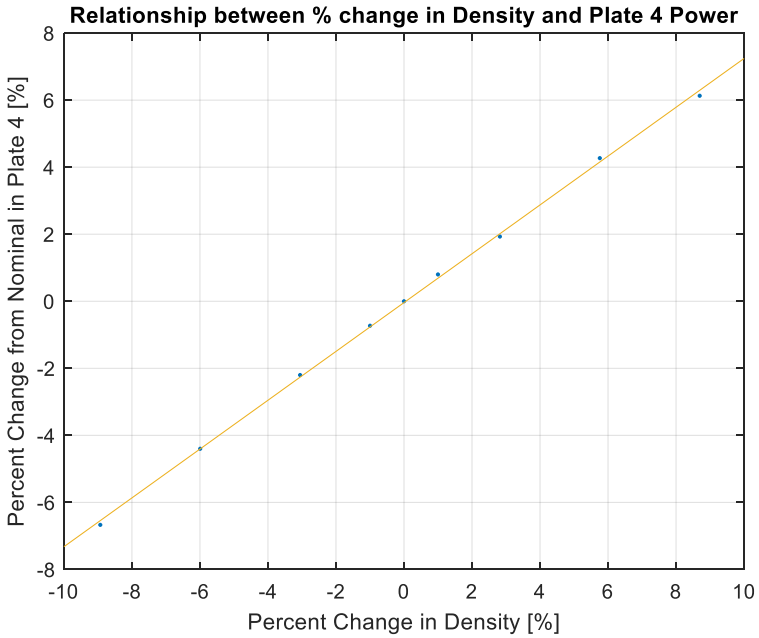

Figure 4-10: Relationship between % change in Density and Plate 4 Power for Position A-2

Table 4-16: Linear Relationships for all Position A-2 Altered Plates

Plate Number	Slope	Intercept
1	0.7704	-0.0785
3	0.7658	+0.0222
4	0.7283	-0.0396
16	0.7254	-0.1110
17	0.7622	-0.1003
19	0.7477	-0.0514

Note: As discussed previously, the functions all follow a very similar relationship, and each has an R^2 of ~0.999.

After examining the changes in plate power, the next step was to create STAT7 files that represented all of the stripes in each loading alteration. These STAT7 files calculated the P_{ONB}, with the lowest P_{ONB} being the most limiting stripe and the value assigned to that plate and loading combination. These results were compiled to find the most limiting plate and are displayed in Figure 4-11.

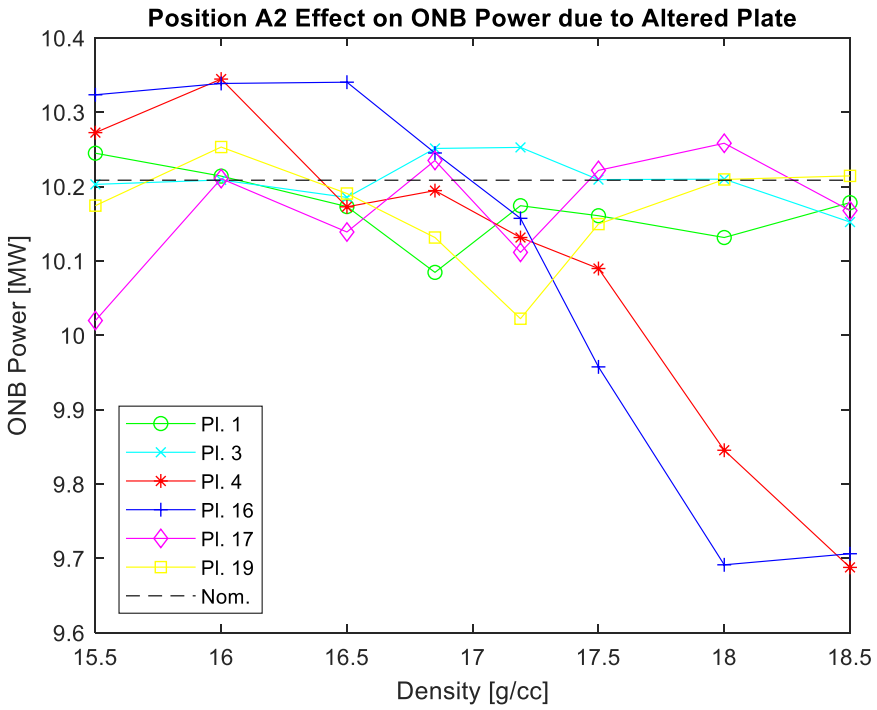

Figure 4-11: Effect on P_{ONB} due to Altered Plate Loadings in Position A-2

These results show that plates 4 and 16 are the most limiting plates, as they each exhibited the lowest modeled P_{ONB}'s. All other plate alterations lead to a P_{ONB} deviating only slightly from the nominal power. Even as the most limiting plates, plates 4 and 16 do not violate the P_{ONB} criterion of 8.68 MW. Plates 4 and 16 are the limiting plates due to their position being the outermost F-type plate on either side of the element. This location allows them to see a higher neutron flux than any of the other F-type plates.

For the majority of these analyses, plate 16 is the location of ONB. However, the location of ONB can change to plate 4 in two main situations: plate 4 increases loading by ~6.0% or plate 16 decreases loading by ~3.0%. Each of those situations is dependent on all other plates held at nominal loading. Additionally, there are two situations in which the location of ONB changed to plate 4 (Plate 1 at 16.0 g/cc and Plate 3 at 17.5 g/cc). These are lone circumstances that occur due to plates 4 and 16 being close in power level. Table 4-17 gives a full list of ONB locations for every alteration.

Table 4-17: Plate Location of ONB for Various Plate Loading values

Density	Plate 1	Plate 3	Plate 4	Plate 16	Plate 17	Plate 19
15.5 g/cc	16	16	16	4	16	16
16.0 g/cc	4	16	16	4	16	16
16.5 g/cc	16	16	16	4	16	16
16.85 g/cc	16	16	16	16	16	16
17.19 g/cc	16	16	16	16	16	16
17.5 g/cc	16	4	16	16	16	16
18.0 g/cc	16	16	4	16	16	16
18.5 g/cc	16	16	4	16	16	16

The other thermal hydraulic measurement needed is the percent change in ONB temperature margin. The criterion for this value is a 10% decrease in ONB temperature margin. Violating this does not disqualify an element, but if it were to occur, it would require further evaluations to ensure no safety violations for the specific case. The percent change in ONB temperature margin is measured between the most limiting for each of the altered cases and the matching stripe in the nominal case. Comparing similar stripes is necessary as a comparison between the most limiting stripe in the altered and nominal cases could inflate the values reported if the alteration causes the most limiting plate to change. Plate 16's most limiting stripe is stripe 4, while plate 4's most limiting stripe is stripe 1. **Error! Reference source not found.** only shows increases in fuel mass loading to illustrate the results better. These are the only cases that see decreases in ONB temperature margin.

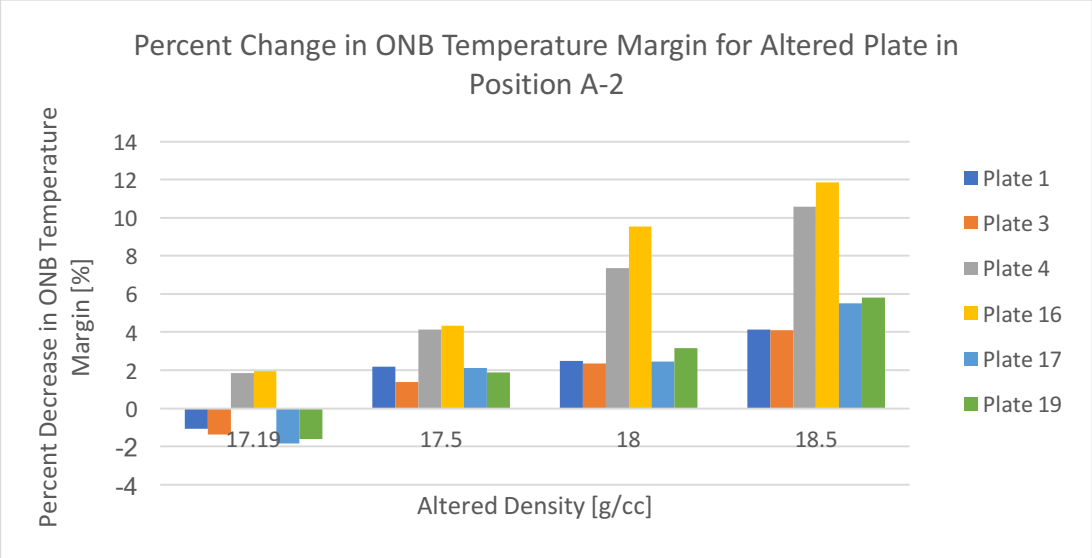

Figure 4-12: Percent Change in ONB Temperature Margin for Altered Plate in Position A-2

The above figure shows that only plates 4 and 16 can exhibit a decrease in the ONB temperature margin greater than 10%. This decrease occurs when each plate has a loading ~9% higher than nominal, which is significantly outside of the current tolerances.

4.4.2 Effects of Local Alterations in Fuel Mass Loading in Position C-5

This section repeats the analyses of the previous section for position C-5. This position was necessary as well to evaluate the local effects in a position near the heavy water reflector. This location in the core can lead to power peaking within the element, and the effects of increased loading on this edge need to be understood.

Similar to the previous analysis, the first step was to find the relationship in plate power change. This analysis found the relationship to be the same as observed in position A-2 for all plates. Table 4-18 includes the descriptions for all of the linear relationships for position C-5.

Table 4-18: Linear Relationships for all Position C-5 Altered Plates

Plate Number	Slope	Intercept
1	0.7704	-0.0785
3	0.7658	+0.0222
4	0.7283	-0.0396
16	0.7254	-0.1110
17	0.7622	-0.1003
19	0.7477	-0.0514

The results began to differ once the thermal hydraulic analyses began. Unlike position A-2, the most limiting plates within C-5 are not the first F-type plates on either side. Instead, the most limiting plate in position C-5 is plate 1. Figure 4-13 shows the P_{ONB} associated with each alteration completed during this analysis.

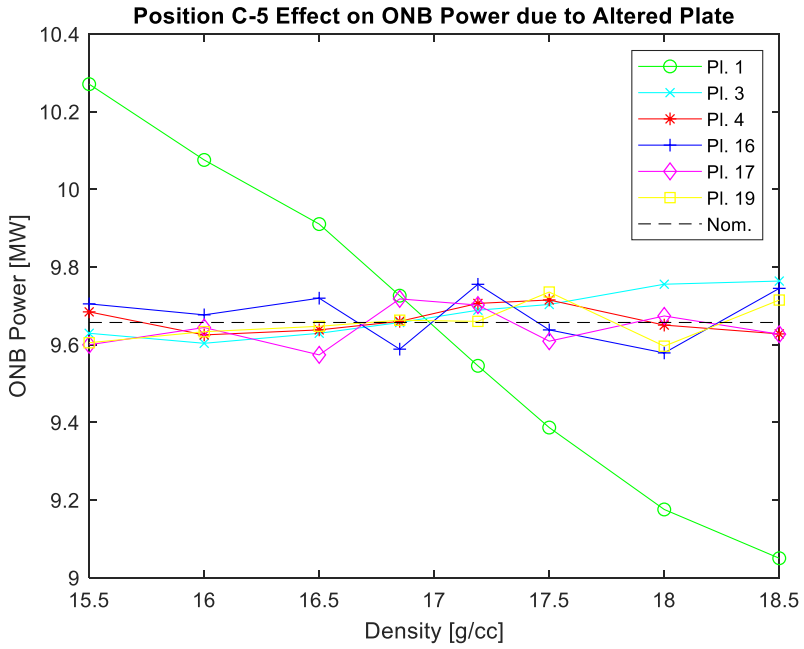

Figure 4-13: Effect on P_{ONB} due to Altered Plate Loadings in Position C-5

This figure shows that plate 1 is the only plate that has a significant effect on P_{ONB}, while all other plates cause small deviations. This effect occurs even though plate 1 is a T-type plate that has a ~50% lower nominal loading than an F-type plate. This deviation from the previous outcome is due to the proximity of plate 1 to the heavy water reflector.

In addition to the effect on P_{ONB}, the analysis found the percent change in ONB temperature margin for each case. Figure 4-14 displays the results for this analysis. Similar to position A-2, the figure only shows cases that have an increase in loading.

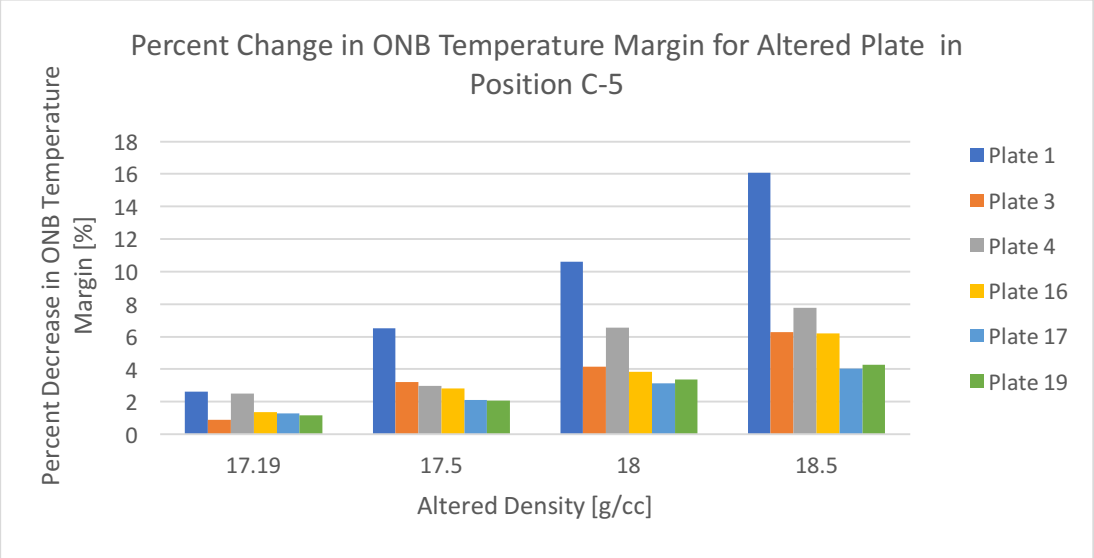

Figure 4-14: ONB Temperature Margin Effect of Plate 16 Altered Loading in Position C-5

As seen in the above figure, plate 1 is the only plate that has a significant effect on the ONB temperature margin. Similar to the effects on P_{ONB} in position C-5, all other plates only have minor deviations and do not cause any violations of the 10% decrease criterion.

4.4.3 Effects of Fuel Plate Thickness Alterations in Position A-2

This section revisits the fuel plate thickness alterations completed for position A-2. Each of the cases in that assessment included fission energy tallies used to create STAT7 files to model all of the position A-2 fuel plate thickness cases. This effect was considered for only the position A-2 analysis as the full-core analysis was shown to violate the neutronics criterion and cannot be allowed on that basis. The position A-2 analysis passes the neutronics criteria but needed further analyses to understand better the impact this tolerance has on the margin to LSSS power and the effect on the ONB temperature margin.

These STAT7 files were created similar to the local fuel mass loading analyses. The most limiting of the four stripes were chosen based off of the P_{ONB} exhibited by each case. Figure 4-15 below shows the P_{ONB} results of this analysis.

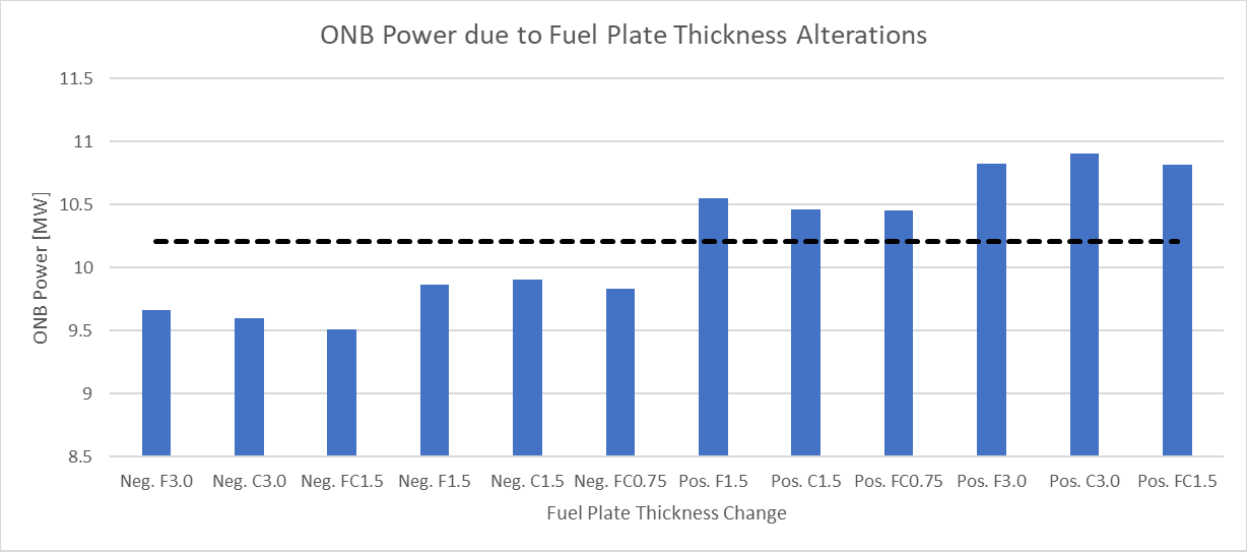

Figure 4-15: Effects of Fuel Plate Thickness Alterations on P_{ONB}

Neg. F3.0	→	Decrease fuel thickness by 3.0 mil
Neg. C3.0	→	Decrease cladding thickness by 3.0 mil
Neg. FC1.5	→	Decrease fuel and cladding thickness by 1.5 mil
Neg. F1.5	→	Decrease fuel thickness by 1.5 mil
Neg. C1.5	→	Decrease cladding thickness by 1.5 mil
Neg. FC0.75	→	Decrease fuel and cladding thickness by 0.75 mil
Pos. F3.0	→	Increase fuel thickness by 3.0 mil
Pos. C3.0	→	Increase cladding thickness by 3.0 mil
Pos. FC1.5	→	Increase fuel and cladding thickness by 1.5 mil
Pos. F1.5	→	Increase fuel thickness by 1.5 mil
Pos. C1.5	→	Increase cladding thickness by 1.5 mil
Pos. FC0.75	→	Increase fuel and cladding thickness by 0.75 mil

This figure shows that all decreases in plate thickness lead to decreases in P_{ONB} from nominal (shown as a black dashed line). This effect occurs even though there is more cooling. In any case where the plate was increased (decreasing the moderator), the lack of cooling still did not prevent the P_{ONB} from increasing from the nominal case. These results show that the change in moderating capability is more significant than that of cooling capability.

The second part of this analysis was to evaluate the effect these changes had on the ONB temperature margin. Figure 4-16 shows the results of this analysis. Of note, the figure only displays cases where the plate was decreased as they are the only cases that saw decreases in the ONB temperature margin.

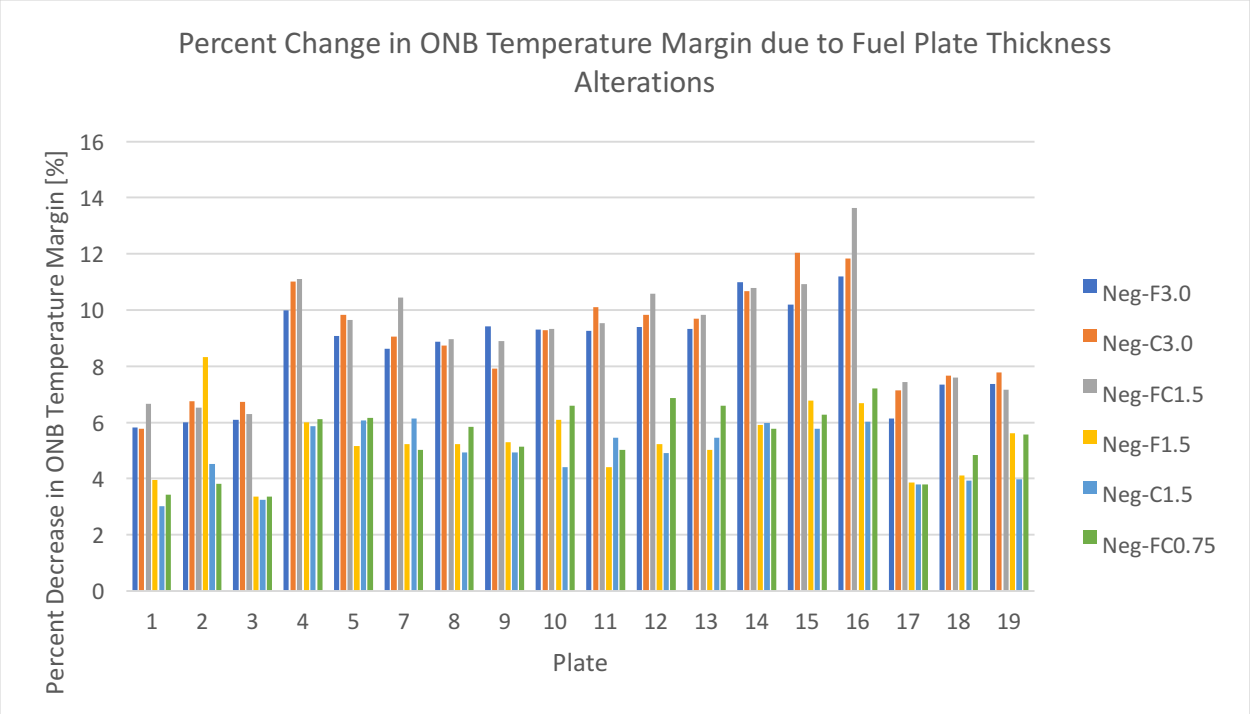

Figure 4-16: Percent Change in ONB Temperature Margin due to Fuel Plate Thickness Alterations

This figure shows that there are a few cases in which some of the F-type plates exhibit decreases in the ONB temperature margin greater than 10 percent. If these cases were to happen, then these assemblies will be disqualified from the most limiting position. The shape of this curve is indicative of the flux profile associated with the element.

4.5 Fresh Core Analysis Conclusions

The fresh core analysis accounted for a significant part of this research due to the limiting nature, as compared to an equilibrium core. The fuel elements in a fresh core maintain a higher average power density due to the lower number of elements in the core while maintaining the same power level. In addition to the higher power density, the elements removed from the B-ring promote further peaking in other positions, like A-2. This analysis was done in two parts: a full-core evaluation of neutronics parameters and local element-level evaluation of margins to ONB. The full-core neutronics analysis focused on four main parameters:

- Enrichment
- Fuel Mass Loading
- Fuel Plate Thickness
- Impurities in Fuel and Cladding/Side Plates

The neutronics analyses was evaluated based on any parameters expected effect on the excess reactivity, used to estimate the impact on fuel cycle length. The data found was used to develop a slope for each parameter that can estimate the effects of specific values not tested during the analysis. These slopes can also compare the "weight" of each parameter. A large slope indicates that the parameter in question has a more significant impact on the fuel cycle length than a different parameter with a smaller slope. These slopes use percent change in each parameter to better compare the alterations, except for impurities where the slope represents the strength per ppm. Impurities were completed differently due to the nominal value being a range rather than a specific value that can be under or over specification. Table 4-19 includes the slopes of every parameter tested during the full-core neutronics analyses. In addition to the slope, every parameter includes the most significant effect on fuel cycle length associated with each parameter that the specification allows (e.g., specification currently allows enrichment to decrease at a max of 1.0%, which leads to a decrease in ~7 FPD).

Table 4-19: Summary of Full-Core Neutronics Impact

Parameter	Case	Slope	Current Maximum Decrease (Nom. Length: ~70 FPD)
Enrichment	1.0% dec.	$0.1169 \pm 0.0087 \frac{\%\Delta k/k}{\%enr}$	~7 FPD
Fuel Mass Loading	1.0% dec.	$0.0552 \pm 0.0074 \frac{\%\Delta k/k}{\%load}$	~3 FPD
Full-Core Fuel Plate Thickness	3.0 mil dec.	$-0.2196 \pm 0.0035 \frac{\%\Delta k/k}{\%pl.th._{full\ core}}$	~92 FPD
Position A-2 Fuel Plate Thickness	3.0 mil dec.	$-0.0132 \pm 0.0035 \frac{\%\Delta k/k}{\%pl.th._{Pos.A-2}}$	~4.5 FPD
Impurities in Fuel	5.0 ppm	$-11.6 \pm 1.47\ {}^{pcm}/_{ppm_{U-10Mo}}$	~3 FPD
Impurities in Cladding/Side Plates	67.0 ppm	$-7.4 \pm 0.12\ {}^{pcm}/_{ppm_{AA6061}}$	~33 FPD

The table compares the impact of different parameters using the calculated slopes and current maximum decrease in fuel cycle length. The first two parameters analyzed, enrichment and fuel mass loading, directly affect the amount of fissile material in the core. The data shows that enrichment has a more substantial impact than fuel mass loading because of the latter adding U-238 to the core. These parameters, however, have an insignificant impact on the fuel cycle length. In terms of global impact, the data shows that full-core fuel plate thickness has the greatest impact on reactivity added. This effect means that while enrichment and fuel mass loading directly impact the amount of fissile material, the amount of moderation has a more significant impact on the core. Slope alone does not determine viability and must incorporate the proposed tolerances. The worst-case scenarios allowed by the proposed tolerances show that in most cases, the effect on fuel cycle

length can be allowed. However, a 3.0 mil decrease in fuel plate thickness in the cladding leads to significant impacts on the fuel cycle length, ~92 FPD. While this scenario is excessive and allowable within the proposed tolerances, it does represent an extremely conservative case assuming all of the fuel plates in the core were off-nominal in the same extreme fashion. This conservativeness prompted the additional analysis on position A-2 to show the effect of a single element, which was approximately 20 times lower.

The impurities involved a slightly different approach as it was not the plan to compare or weight their effects on the reactor to the other parameters. Instead, the slopes calculated allow the reactor to estimate the negative reactivity added based on the impurities. This value can be added to any other negative reactivity in the core and will not have any combined effects with other parameters. The impurities analysis did show that, as expected, impurities within the fuel exhibit a stronger effect due to the higher fluxes within the fuel. However, the specification is very tight for reactor fuel and is much broader for impurities in the cladding and side plates. The larger tolerances lead to the current maximum of impurities in the cladding and side plates allowing for a decrease of ~33 FPD in fuel cycle length. This impact was deemed too detrimental, but further research has been undertaken into the actual amounts of impurities present in the cladding and side plates. These values could be outdated, and the current manufacturing abilities could limit the impurities much more. Other options to address this that have been started involve researching the burnup of these poisons to get a better understanding of the actual effect on fuel cycle length. Another option to address this issue is using reactor-grade aluminum in the production of the AA6061. The reactor fuel can have lower amounts of impurities due to regulation in place that vastly limits the amount of impurities in the uranium and molybdenum stock used. A similar process can be used for the aluminum if the impurities are deemed too excessive, and the tolerances cannot be eased with the current grade of aluminum. A recommendation has been made to complete this further research, as it is believed this will solve the apparent problem brought up by these findings.

This research puts a priority on evaluating each parameter's effect on the fuel cycle length, but the only established MITR criterion for neutronics is SDM. SDM is a $\Delta k/_k$ calculated between a k_{eff} of 1.0 (critical condition) and a limiting condition that is reactor specific. In the case of MITR, this condition is all control blades fully inserted except for the blade with the highest worth and the regulating rod completely removed. The SDM criterion for the MITR is 1.0%, in that all cases must have a SDM >1.0% $\Delta k/_k$. All cases that involved the addition of positive reactivity to the core were incorporated in this analysis. The cases that involve the addition of negative reactivity were not tested since the nominal core has a sufficient SDM; this includes all calculations done during the impurities analyses. The two most limiting blades from the nominal case, blades 2 and 3, were each used as the most limiting blade for every case in the instance that the off-nominal parameter changed the location of the most limiting blade. Table 4-20 includes the lowest SDM for each of the neutronics parameters and the case during which they occur. This table contains SDM for any analysis that was completed and is not limited to within proposed tolerances.

Table 4-20: Worst Case SDM for Fresh Core Evaluated Parameters

Parameter	Case	SDM $[\% \Delta k/k]$	
		Blade 2	Blade 3
Enrichment	20.50 wt%	3.0747	3.0790
Fuel Mass Loading	21.890 kg	3.3549	3.3496
Full-Core Fuel Plate Thickness	Dec. Cladding 3.0 mil	1.9046	1.8994
Combined Parameters	21.516 kg Dec. Plate 3.0 mil	2.1450	2.1294

This table shows that even the worst-case scenarios do not cause a violation of the neutronics criterion for MITR. Decreasing the cladding by 3.0 mil on a full-core level represents the most significant possible reactivity addition, and the data shows that it does not violate the SDM criterion.

After calculating all of the SDM and finding no violations of the criterion, it was determined that the proposed tolerances for neutronics parameters are acceptable. While there are two cases of significant fuel cycle length effects, these cases are deemed either too conservative or may require further research to confirm.

The second aspect of the fresh core analysis focused on the thermal hydraulic criteria of ONB Power (P_{ONB}) and percent change in ONB temperature margin. This analysis focused on fuel mass loading, which has a larger tolerance at the plate level, and fuel plate thickness, which had full-core alterations deemed too conservative. The fuel mass loading analysis incorporated two positions: position A-2, the hottest element in the core, and position C-5, the hottest element in the C-ring. The analysis involved looking at a wide range of loadings, increases/decreases of 1-9%, and evaluating the ONB Power (P_{ONB}) and percent change in ONB temperature margin for each. Position A-2 was completed first and showed that the first full thickness (F-type) plate on either side of the element was the most limiting plate within the position. In addition to these plates, a Y-type and T-type from each side of the element were analyzed as well. Position C-5 was different than position A-2 due to its proximity to the heavy water reflector. This change in position altered the location of the most limiting plate to be the outermost plate, plate 1. The fuel plate thickness section of this analysis was an extension of the neutronics analysis already completed. This analysis evaluated the tolerances at an element level due to the minimal neutronics impact of a less than full-core alteration. Table 4-21 includes the most limiting ONB Power (P_{ONB}) of any of the evaluated cases.

Table 4-21: Effects on P_{ONB} in Fresh Core

Fresh Core Parameter	Position	Case	P_{ONB} [MW]
Fuel Mass Loading	A-2	Pl. 4 @ 18.5 g/cc	9.6878
	C-5	Pl. 1 @ 18.5 g/cc	9.05
Fuel Plate Thickness	A-2	Dec. Fuel & Cladding by 1.5 mil	9.52

This table shows that none of the parameters exhibit any violations of the LSSS criterion of 8.68 MW. One of the interesting takeaways is that while position A-2 is the hottest element in the core and produces the most power, position C-5 has the lowest ONB Power (P_{ONB}) due to the peaking caused by the heavy water reflector. Table 4-22 includes the cases that exhibit a larger than 10% decrease in ONB temperature margin.

Table 4-22: Effects on Fresh Core ONB Temperature Margin

Fresh Core Parameter	Position	Cases that Exhibit >10% Dec. in ONB temperature margin
Fuel Mass Loading	A-2	Plate 4 @ +9% Loading Plate 16 @ +9% Loading
	C-5	Plate 1 @ +6% and +9% Loading
Fuel Plate Thickness	A-2	Decrease Position A-2 Plates by 3.0 mil (Occurs on Plates 4, 7, 11, 12, 14, 15, 16, 17)

As stated previously, this criterion is not used to fail an element. Any failures of this criterion prompt further studies into what positions the element can go to without causing any violations of safety margins. In the fresh core, only fuel plate thickness has values within the tolerances that necessitate these studies.

After reviewing the data from these thermal hydraulic analyses, the current tolerances do not violate the safety margins established by MITR. The current tolerances do not allow for a P_{ONB} below LSSS power. The FYT design allows for the margins to be maintained, even with the lack of fins. The FYT utilizes the gradient of fuel thicknesses to even out the power profile of the element, preventing harmful peaking. Certain parameter tolerances (fuel plate thickness and coolant channel gap) cause violations of the ONB temperature margin criterion, but this criterion acts as an advisory for the fuel manager of the reactor rather than a reason to fail the element.

Chapter 5: Local Fuel Homogeneity Analysis

5.1 Objectives

The previous chapters addressed the impact of some of the primary fabrication tolerances at the full-core, element, and plate level. Some of these tolerances do increase as the area of observation grows smaller. An example of this is the fuel mass loading tolerance growing from ±1.0% at the element level to ±3.5% at a plate level. This chapter shifts focus to an even smaller area: the individual "spot". A "spot" is one of the 64 individual locations for each fuel plate that are necessary to accurately model the power distribution over the entirety of the fuel plate. This chapter reviews the impact of the statistical propagation of uncertainties in local fuel homogeneity at the "spot" level. The proposed tolerance for this is ±10% in fuel homogeneity and can refer to small changes in thickness, density, and other changes to the fuel plate. Due to the localized aspect of this uncertainty, this analysis focuses on the thermal hydraulic effects associated with this small change.

5.2 Local Fuel Homogeneity Methodology

5.2.1 STAT7 Combined Uncertainty

As previously described, STAT7 accounts for a multitude of uncertainties and uses them to estimate the P_{ONB} associated with each of the analyzed cases. For each of the cases previously completed in this assessment, one uncertainty input was constant, *plocsig* (φ). This uncertainty is the local power uncertainty and is used by STAT7 to affect the power produced by a "spot" during calculations for P_{ONB}. Since there is only one input for this value, the uncertainty is a combination of two different uncertainties: power distribution and fuel homogeneity. The value is calculated using equation (5-1.

$$Tot.Unc = \sqrt{(Power\ Dist.\ [\%])^2 + (Fuel\ Homog.\ [\%])^2} \tag{5-1}$$

This process is referred to as "combined standard uncertainty" and is a generally accepted process for combining multiple uncertainties.

The uncertainty associated with power distribution is vital to understand, as it represents the inability to measure power throughout the core precisely. The uncertainty can also represent the uncertainty in the f7 tallies used in MCNP5 to create the STAT7 files. The nominal uncertainty values for each of these are 10%, which combines to a total uncertainty of 14.14% [20]. This

uncertainty is a 3-σ level uncertainty with a 1-σ input value of 4.71%. This uncertainty is present in all STAT7 analyses and has remained unaltered before this evaluation.

5.2.2 Local Fuel Homogeneity Test Methodology

This analysis focused on the fuel homogeneity uncertainty and altered the value within φ to find a relationship between the uncertainty and P_{ONB}. The following table shows the values chosen for this analysis.

Table 5-1: Total Uncertainty Values Associated with Altered Fuel Homogeneity Uncertainties

Uncertainty (3-σ)		Combined Uncertainty	φ
Power Distribution	Fuel Homogeneity	3- σ	1- σ
10%	5%	11.18%	3.73%
10%	10%	14.14%	4.71%
10%	12.5%	16.01%	5.34%
10%	15%	18.03%	6.01%
10%	17.5%	20.16%	6.72%
10%	20%	22.36%	7.45%
10%	22.5%	24.62%	8.21%
10%	25%	26.93%	8.98%

These values represent the nominal as well as values above and below the current tolerance. A variety of values was essential in creating an effective relationship that could evaluate uncertainties not explicitly tested.

This analysis focuses solely on the effect this uncertainty has on the P_{ONB} of the system. As stated previously, alterations to uncertainties alone do not affect the nominal temperature profile reported by STAT7 and thus do not change the ONB temperature margin.

5.3 Local Fuel Homogeneity Results

The results of this assessment include the P_{ONB}'s associated with each of the above cases. These values were then used to create a curve fit between the fuel homogeneity uncertainty and P_{ONB}. The first step was to use a linear fit to create this relationship, as done in previous analyses. Figure 5-1 displays this linear fit.

This figure includes the 3-σ confidence interval associated with how well the data fit a linear relationship. This confidence interval was especially crucial for this analysis due to the differences from the neutronics analyses in chapter 4, which all showed linear relationships. This analysis was

more akin to the coolant channel uncertainty analysis previously completed. That analysis showed a non-linear relationship and prompted the decision to evaluate how effectively the data fit a linear relationship.

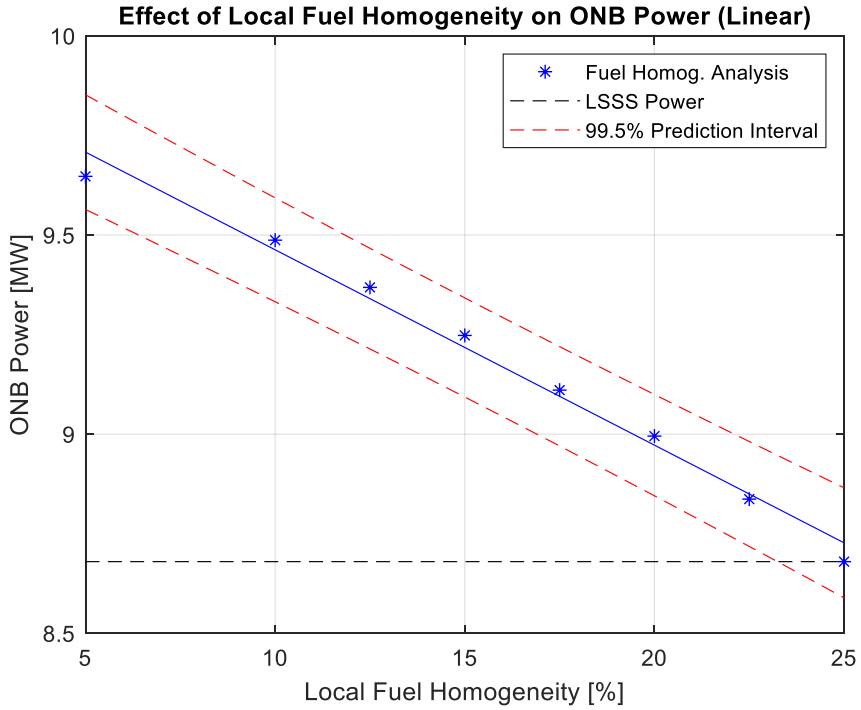

Figure 5-1: Effect of Local Fuel Homogeneity on P_{ONB} (Linear)

$$P_{ONB}\ [MW] = -0.049(\%homog) + 9.535 \tag{5-2}$$

As expected, the data does not necessarily fit a linear relationship (equation 5-2), and a higher-order fit would be more appropriate to display the data. This change was even more critical as the actual analysis found that the LSSS criterion of 8.68 MW would occur at a fuel homogeneity uncertainty of 25%. This calculation contradicts equation 5-2, which estimated that the criterion would occur at 26%. An overestimation in limiting uncertainty was deemed unacceptable and further prompted a higher-order fit. A quadratic fit was selected and created. Figure 5-2 displays this quadratic fit.

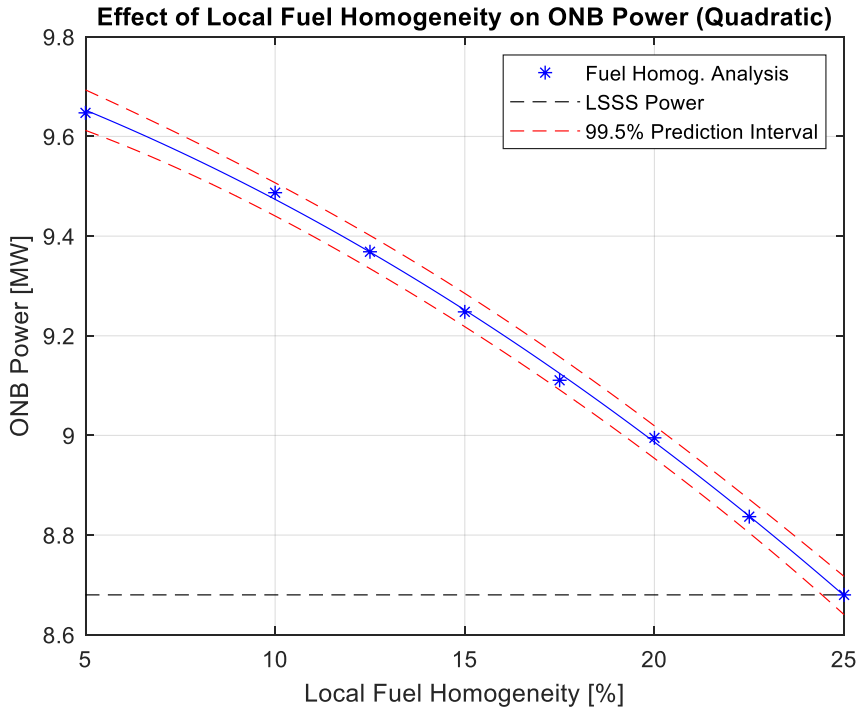

Figure 5-2: Effect of Local Fuel Homogeneity on P_{ONB} (Quadratic)

$$P_{ONB}\,[MW] = -0.0009(\%homog)^2 - 0.0229(\%homog) + 9.789 \quad (5\text{-}3)$$

The first observation in comparing these curve fits is that the quadratic fit has a much smaller 3-σ confidence interval for the overall fit of the data. The quadratic relationship, displayed as equation 5-3, also estimates the local fuel homogeneity uncertainty that would cause LSSS power to be almost exactly 25%. This value matches the modeled value shown in the analysis. Another approach to compare these expected fits was to compare the average residual associated with each. The residuals are the differences between the exact data points and what value the fitted relationship estimates for that point. A lower average residual means that the function fits the data points more precisely. In these cases, the average residual for the quadratic fit was much lower at 0.02 MW as compared to 0.10 MW for the linear fit.

5.4 Local Fuel Homogeneity Conclusions

This analysis focused on the effect of uncertainty in local fuel homogeneity on the ONB Power (P_{ONB}) of the reactor. From these analyses, the reactor does not violate the LSSS criterion of 8.68 MW until the local fuel homogeneity uncertainty increases to ~25%. This value shows that there is a significant margin to this criterion (>100% increase before any violations occur). The effect of any uncertainty not explicitly modeled can be found using the quadratic relationship found during the analysis.

Chapter 6: Combination Impact Analysis

6.1 Objectives

The previous chapters of this report focused on the separate effect that individual parameters have on the margins to safety for the MITR. For example, only the thermal hydraulic effect was considered while evaluating the coolant channel gap fabrication tolerances, and the neutronic effect was neglected. This first step provides important insight into which parameters are more impactful on the overall safety of the reactor. However, separate effect analyses alone are not sufficient to quantify the full impact of the fabrication tolerances. Material property parameters, such as enrichment and impurities, act primarily as a source of negative or positive reactivity independent of the effect other parameters have on the core. Other parameters related to the geometry of a fuel element are dependent, and the combined effect should be evaluated. This chapter focuses on the impact these dependent parameters have on the reactor physics and power distribution in LEU Core 1. The first part of this combined analysis is to evaluate the effect of full-core parameter alterations on the fuel cycle length and SDM. The next part of this analysis focused on the thermal hydraulic impact these parameters have at the local level and their effect on the margin to ONB. This combination analysis serves as a preliminary approach to fully understanding the impact of the proposed fabrication tolerances on the core.

6.2 Fuel Specification Combination Impact Methodology

The combination impact analysis consists of varying parameters within the current bounds of the fabrication tolerances. The different alteration approaches are presented for these parameters in the combination effect analysis. The next sections introduce the test matrices for the full-core and local element-level combination analyses. Each of these analyses uses 8 test cases to evaluate various combined parameters.

6.2.1 Combination Impact Parameter Evaluation

The combination impact analysis focuses on three parameters:

- Fuel Mass Loading
- Fuel Plate Thickness
- Coolant Channel Gap Thickness

These parameters are possibly dependent on each other, and their combined effect was necessary to perform. Other parameters, enrichment and impurities, were deemed to be independent and could act purely as positive and negative reactivity to be added to the core.

The first step of the combination impact analysis was to evaluate the combined effects of fuel mass loading and fuel plate thickness. Coolant channel gap thickness is also affected due to variation in fuel plate thickness, but is not altered independently of the fuel plate thickness. This decision was necessary to maintain the outer geometry of the fuel elements. Altering coolant channel gap thickness and fuel plate thickness independently was reserved for the local element analysis. In this case, the effect of changing one coolant channel was spread out over the other coolant channels to ensure the element remains the same size.

One aspect of the combination impact analysis that is different is the process of altering the fuel mass loading (U-10Mo). The separate effect analysis altered the loading by varying the density of the fuel, which kept a consistent amount of moderator. For this combined analysis, the fuel mass loading is changed by altering the thickness of the fuel and keeping a consistent fuel density. The approach for altering the fuel plate thickness is changing the thickness of the cladding in response to the fuel thickness. This approach means that whatever total plate thickness change occurs, accounts for the change in fuel thickness associated with the fuel mass loading alteration. An example of this calculation in an F-type plate is as follows:

1.0% increase in fuel mass loading	→	0.25 mil increase in fuel thickness
3.0 mil decrease in fuel plate thickness	→	3.25 mil decrease in cladding thickness (1.625 on each side) Additional 0.25 mil accounts for the increase due to the fuel mass loading alteration

For this analysis, it is assumed the fuel and cladding have a consistent density for all evaluated cases (Fuel: 17.02 g/cc Cladding: 2.7 g/cc).

6.2.2 Full-Core Combination Impact Test Methodology

The full-core combination impact analysis was similar to other full-core neutronic analyses in that all fuel plates experienced the same alterations. This approach was the main reason why coolant channel gap thickness was not included in the assessment, as it would limit the available test ranges of fuel plate and channel gap thicknesses. This analysis only included values that were currently in the range of tolerances due to the limiting nature of combining some parameters. Table 6-1 includes values to be tested for fuel plate thickness and fuel mass loading.

Table 6-1: Modeled Values for Full-Core Combination Impact Analysis

Fuel Mass Loading (Nominal Element: 968 gU-235)	Plate Thickness (Nominal Fuel Plate: 49.0 mil)
+1.0 %	+3.0 mil (+6.12%)
+0.5%	+1.5 mil (+3.06%)
-0.5%	-1.5 mil (-3.06%)
-1.0%	-3.0 mil (-6.12%)

These values simulated a range amongst the current fabrication tolerances. After choosing the values to be tested, the next step was to determine the necessary combinations. This process was done with the understanding that previous fuel plate thickness and fuel mass loading analyses could represent some of the zero points for the test. This inclusion lessens the number of new evaluations needed for this analysis. Figure 6-1 displays the combinations chosen for this analysis.

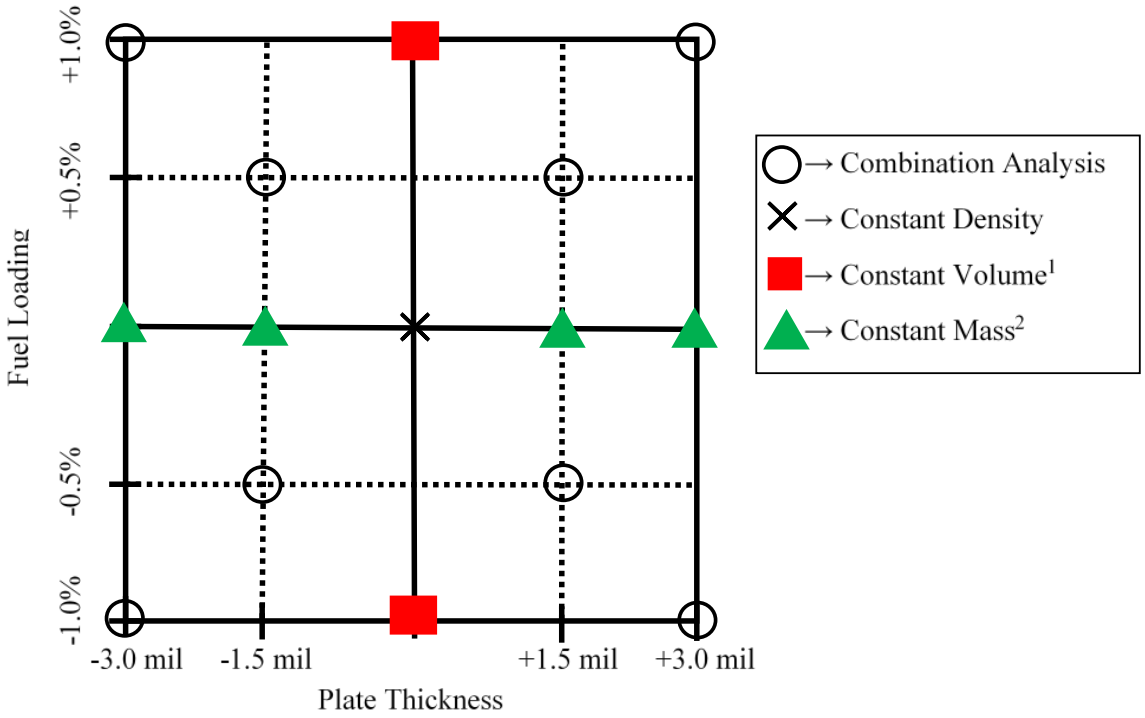

[1]Completed with a different process, altering density of fuel and keeping clad and fuel meat thickness nominal

[2]Completed with a different process, density of clad was not kept constant

Figure 6-1: Full-Core Combination Impact Analysis Test Matrix

As seen in the figure, one aspect of using the previous analyses for the zero points is that there are slight differences in the process of modeling. In the case of the fuel mass loading points, a necessary step is proving that modeling off-nominal loading as a geometrical change is the same as modeling it through a change in density. The zero points created during the fuel plate thickness analysis are also slightly different due to alterations in the density of the cladding to maintain the

same amount of cladding mass. This difference could change the effect that cladding has on the reactor physics. If necessary, additional runs can model zero points in the same fashion as the rest of the analysis. Due to the complicated nature of these models, Table 6-2 lists the thicknesses of fuel and cladding associated with each combination. The table lists these cases in order of expected limiting value. This order was created based on the variations in fuel plate thicknesses and the amount of moderation associated with them. Previous neutronics analyses showed that these changes in the amount of moderation add significantly more negative or positive reactivity as compared to the fuel mass loading. The table includes nominal values of fuel and cladding thickness for comparison.

Table 6-2: Full-Core Combination Impact Analysis Test Matrix

Plate Type	Nominal Fuel Thickness		Nominal Cladding Thickness		Total Pl. Thickness
F	25.0 mil		12.0 mil		49.0 mil
Y	17.0 mil		16.0 mil		49.0 mil
T	13.0 mil		18.0 mil		49.0 mil
Test Case	Fuel Mass Loading		Plate Thickness		Total Pl. Thickness
	Loading	Fuel Thickness (± nom) [mil]	Tot. Pl.Th.	Cladding Th. (± nom) [mil]	
1	+1.0 %	F: 25.25 (+0.25) Y: 17.17 (+0.17) T: 13.13 (+0.13)	-3.0 mil	F: 10.375 (-1.625) Y: 14.415 (-1.585) T: 16.435 (-1.565)	46.0 mil
2	-1.0 %	F: 24.75 (-0.25) Y: 16.83 (-0.17) T: 12.87 (-0.13)	-3.0 mil	F: 10.625 (-1.375) Y: 14.585 (-1.415) T: 16.565 (-1.435)	46.0 mil
3	+0.5 %	F: 25.125 (+0.125) Y: 17.085 (+0.085) T: 13.065 (+0.065)	-1.5 mil	F: 11.1875 (-0.8125) Y: 15.2075 (-0.7925) T: 17.2175 (-0.7825)	47.5 mil
4	-0.5 %	F: 24.875 (-0.125) Y: 16.915 (-0.085) T: 12.935 (-0.065)	-1.5 mil	F: 11.3125 (-0.6875) Y: 15.2925 (-0.7075) T: 17.2825 (-0.7175)	47.5 mil
5	+0.5 %	F: 25.125 (+0.125) Y: 17.085 (+0.085) T: 13.065 (+0.065)	+1.5 mil	F: 12.6875 (+0.6875) Y: 16.7075 (+0.7075) T: 18.7175 (+0.7175)	50.5 mil
6	-0.5 %	F: 24.875 (-0.125) Y: 16.915 (-0.085) T: 12.935 (-0.065)	+1.5 mil	F: 12.8125 (+0.8125) Y: 16.7925 (+0.7925) T: 18.7825 (+0.7825)	50.5 mil
7	+1.0 %	F: 25.25 (+0.25) Y: 17.17 (+0.17) T: 13.13 (+0.13)	+3.0 mil	F: 13.375 (+1.375) Y: 17.415 (+1.415) T: 19.435 (+1.435)	52.0 mil
8	-1.0 %	F: 24.75 (-0.25) Y: 16.83 (-0.17) T: 12.87 (-0.13)	+3.0 mil	F: 13.625 (+1.625) Y: 17.585 (+1.585) T: 19.565 (+1.565)	52.0 mil

6.2.3 Local Combination Impact Test Methodology

After completing the full-core combination impact analysis, the final step is to complete a combination impact analysis of the most limiting element. The local analysis combines the effects of fuel mass loading, fuel plate thickness, and coolant channel gap. Fuel mass loading and fuel plate thickness use the same alteration approach as the full-core analysis, changing the thickness of the fuel and accommodating that change with altering the cladding thickness. However, the fuel mass loading covers a broader range (±3.5%) due to the larger tolerance at a plate level [20]. Similar to the full-core combination analysis, all of the materials within the core maintain a consistent density. The coolant channel gap accommodates changes to the fuel plate and additional changes required by the particular case. Figure 6-2 shows this process with equations. Dotted lines are the original dimensions, whereas solid lines are dimensions after changes.

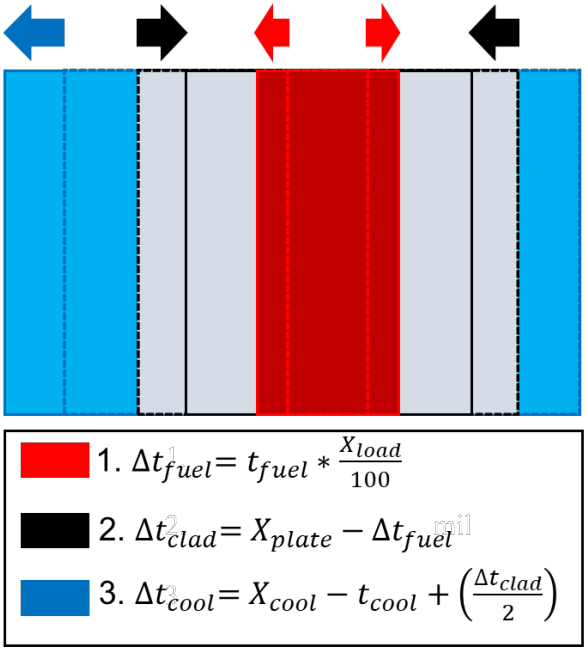

Figure 6-2: Local Combination Impact Analysis Test Matrix

The following table lists the alterations incorporated during this analysis.

Table 6-3: Modeled Values for Local Combination Impact Analysis

Fuel Mass Loading (Nom. F-Plate: 57.74 gU-235)	Coolant Channel Gap (Nom. Ch. 16: 74.6 mil)	Plate Thickness (Nom. Fuel Plate: 49.0 mil)
+3.5 %	79.0 mil	+3.0 mil
-3.5 %	70.0 mil	-3.0 mil

Another aspect of this analysis is maintaining the outer geometry of the fuel element. This aspect involved combining total plate and channel thicknesses and accounting for them in other coolant channels. An example of this would be the case where plate thickness increases by 3.0 mil and

channel 16 is 79.0 mil. This alteration leads to a total increase of 7.4 mil, which necessitates a decrease of 0.39 mil in every other channel.

The proposed test matrix is as follows and ranked in order of expected importance. The table includes nominal thicknesses of fuel, cladding, and coolant channel gap.

Table 6-4: Local Combination Impact Analysis Test Matrix

Plate Type	Nom. Fuel Thickness		Nom. Cladding Thickness		Nom. Coolant Channel Thickness	
F	25.0 mil		12.0 mil		74.6 mil	
Test Case	Fuel Mass Loading		Plate Thickness		Coolant Channel Thickness	
	Load Case	Fuel Thickness (±nom) [mil]	Plate Th. Case	Cladding Th. (±nom) [mil]	Coolant Ch. Th. (±add. Changes)[1] [mil]	Avg. Coolant Ch. Change [mil]
1	+3.5%	25.875 (+0.875)	-3.0 mil	10.0625 (-1.9375)	79.0 (+2.9)	-0.0737
2	+3.5%	25.875 (+0.875)	-3.0 mil	10.0625 (-1.9375)	70.0 (-6.1)	+0.4000
3	-3.5%	24.125 (-0.875)	-3.0 mil	10.9375 (-1.0625)	79.0 (+2.9)	-0.0737
4	-3.5%	24.125 (-0.875)	-3.0 mil	10.9375 (-1.0625)	70.0 (-6.1)	+0.4000
5	+3.5%	25.875 (+0.875)	+3.0 mil	13.0625 (+1.0625)	79.0 (+5.9)	-0.3895
6	+3.5%	25.875 (+0.875)	+3.0 mil	13.0625 (+1.0625)	70.0 (-3.1)	+0.0842
7	-3.5%	24.125 (-0.875)	+3.0 mil	13.9375 (+1.9375)	79.0 (+5.9)	-0.3895
8	-3.5%	24.125 (-0.875)	+3.0 mil	13.9375 (+1.9375)	70.0 (-3.1)	+0.0842

Note 1: These values are changes that account for the fuel plate change. The channel only sees a change of 1.5 mil since the 3.0 mil change is split for both sides of the plate.

6.3 Fuel Specification Combination Impact Results

This section introduces the results of each of the combination impact analyses. The neutronics is presented first to display the full-core effect on fuel cycle length and evaluate the SDM. After, the local analysis results are presented to determine if any of the combined parameters violate the P_{ONB}/ ONB temperature margin criteria.

6.3.1 Full-Core Combination Impact Results

This section discusses the results of the full-core combination impact analysis. The k_{eff} and $\Delta k/k$ of each case are included in Table 6-5. The most significant decrease in reactivity within current bounds is -1.263% $\Delta k/k$, which would lead to a loss of ~84 FPD.

Table 6-5: Full-Core Combination Impact Results

Test Matrix	Alterations		k_{eff}	σ	$\Delta k/k$	FPD
	Fuel Mass Loading	Plate Thickness				
1	+1.0%	-3.0 mil	1.01160	0.00006	+1.224%	+81
2	-1.0%	-3.0 mil	1.01057	0.00006	+1.123%	+74
3	+0.5%	-1.5 mil	1.00562	0.00006	+0.636%	+42
4	-0.5%	-1.5 mil	1.00499	0.00006	+0.574%	+38
5	+0.5%	+1.5 mil	0.99366	0.00006	-0.561%	-37
6	-0.5%	+1.5 mil	0.99306	0.00006	-0.622%	-41
7	+1.0%	+3.0 mil	0.98787	0.00006	-1.151%	-76
8	-1.0%	+3.0 mil	0.98678	0.00006	-1.263%	-84

Looking at these results reveals that the zero points established through the fuel plate thickness separate effects analysis cannot act as the baseline fuel plate thickness points. Additional runs were completed using the rules established by the full-core combination analysis. These include the same thickness alterations while maintaining the cladding density. The results of these runs compared to the fuel plate thickness alterations of the same case are included in Table 6-6. The results from the separate effect fuel plate thickness analysis are labeled as constant mass and include alterations to the cladding density during the thickness changes to maintain cladding mass. The results of the combination analysis are labeled as constant density under the same column and did not change the density of the cladding for any thickness change.

Table 6-6: Updated Baseline Fuel Plate Thickness Results

Fuel Plate Thickness	Constant [Mass/Density]	k_{eff}	σ	Δk_{eff} [1] [pcm]
-3.0 mil	Mass	1.01316	0.00006	+215
	Density	1.01101	0.00006	
-1.5 mil	Mass	1.00630	0.00006	+123
	Density	1.00507	0.00006	
+1.5 mil	Mass	0.99231	0.00006	-96
	Density	0.99327	0.00006	
+3.0 mil	Mass	0.98531	0.00006	-201
	Density	0.98732	0.00006	

Note 1: This value follows Δk_{eff} = Altered - Nominal

The first thing that becomes apparent after viewing these results is that the density of the cladding has a significant effect on core physics when isolated from the amount of moderator. These results show that any increase in cladding density to maintain cladding mass adds positive reactivity to the core, whereas the inverse occurs for any decrease in the cladding density. This effect means the impact of the separate effects fuel plate thickness analysis is more substantial as compared to the same thickness changes in the combination impact analysis. An example is the -3.0 mil case, in which the only difference in alterations is that during the combination analysis, the cladding density was kept consistent. This result shows that the additional cladding density from the fuel plate thickness analyses adds ~200 pcm of positive reactivity. For the opposite case, -200 pcm is added by the lower cladding density. This result was unusual as cladding would typically act as a poison and add negative reactivity. These results prompted an additional run of a nominal core with cladding densities to match the -3.0 mil fuel plate thickness case but with all of the fuel plate thicknesses held at the nominal value of 49.0 mil. The k_{eff} of that case was 1.00154, which is ~+200 pcm added to the nominal case k_{eff} of 0.99923. This result affirms that alteration of the cladding density in the separate effects fuel plate thickness analysis, completed to maintain cladding mass after the thickness changes, have a significant impact on the reactor physics. The impact of this change in cladding density is, however, minimal compared to the effect of the change in amount of moderator. A decrease of 3 mil in plate thickness adds +1178 pcm compared to the +200 pcm impact of keeping the cladding density constant. The amount of moderator will have a much larger impact due to the highly under-moderated core design of MITR.

One possible explanation for this reactivity effect lies in the composition of AA6061, as Al-27 represents 97.5% of the material [23]. The absorption and elastic scattering cross sections of Al-27 are plotted in Figure 6-3, superimposed with the flux of MITR.

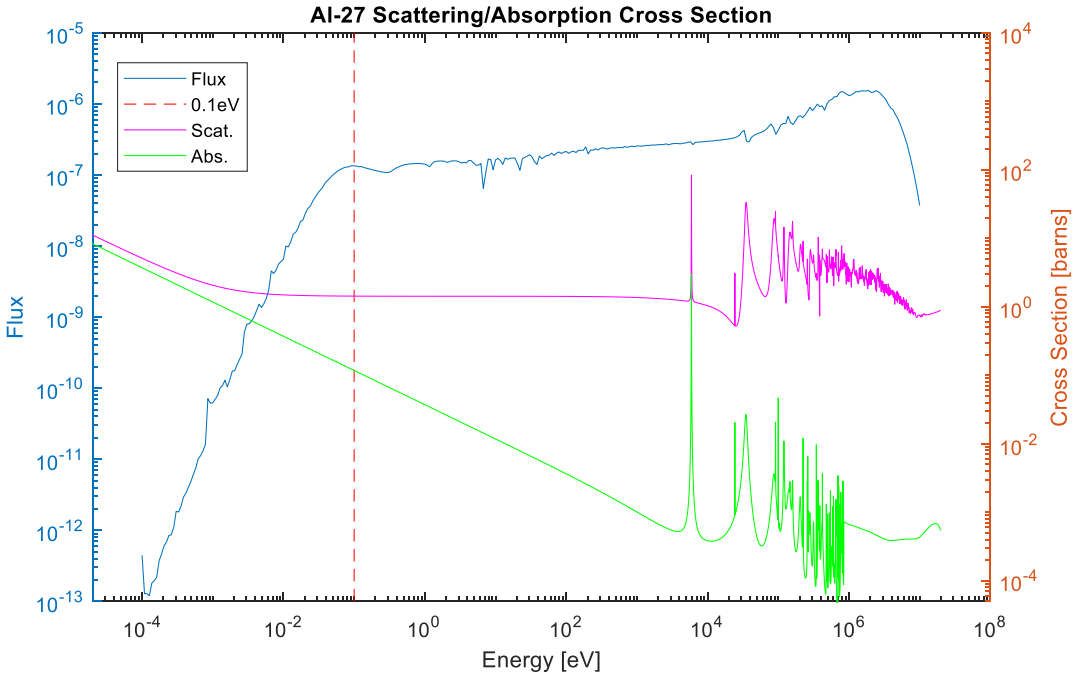

Figure 6-3: Al-27 Elastic Scattering and Absorption Cross Section

This figure shows that at 0.1 eV, the elastic scattering cross section is an order of magnitude higher than the absorption. Due to this, the additional cladding could act as a moderator, even though it is not the primary moderator for the reactor. This effect would lead to more fissions and a higher k_{eff} as a result.

After completing all of the runs, the data was used to create a multivariable function that would have inputs for both percent change in fuel mass loading and percent change in fuel plate thickness. Figure 6-4 displays this function plotted as a surface and includes the function below the figure.

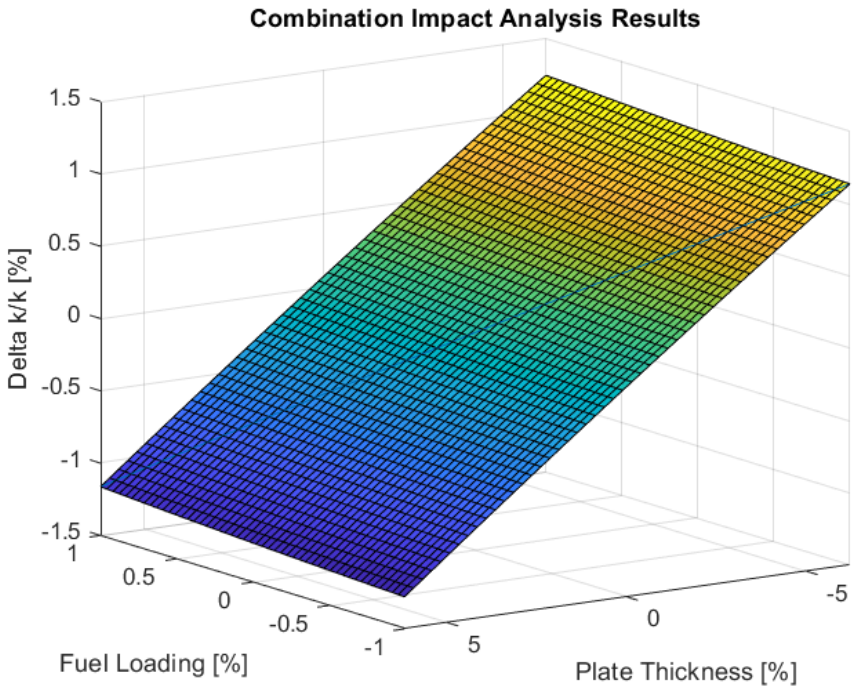

Figure 6-4: Full-Core Combination Impact Analysis Results

$$\Delta k/k_{Combined} = A_1 + B_1(\%load) + B_2(\%load)^2 + C_1(\%plate) + C_2(\%plate)^2 + D_1(\%load)(\%plate) \quad (6\text{-}1)$$

$A_1 = 0.0059$
$B_1 = 0.0548$ $\quad B_2 = 7.5 * 10^{-3}$
$C_1 = -0.1943$ $\quad C_2 = -7.6036 * 10^{-4}$
$D_1 = 4.104 * 10^{-4}$

$$RMSE = 0.0061\% \ \Delta k/k = \sim 0.40 \ FPD$$

This figure shows that the analyzed data (the blue line) fits almost perfectly on the plotted surface. The data also shows that as with the separate effect analyses, moderation has a more significant impact on the core than the amount of fissile material. Equation 6-1 shows the polynomial curve-fit of the results. The quality of this fit was found using the Root Mean Squared Error (RMSE),

which is the average difference between the modeled points and the predicted values. This curve fit has a RMSE of 0.0061% $\Delta k/k$ or 0.40 FPD, which was deemed sufficient for calculation. The coefficient on the first-order fuel mass loading term is similar to the slope found during the separate effect analysis (0.548 versus 0.552). If the baseline fuel plate thickness results from the combined analysis are used to find a slope, this slope is also very similar to the coefficient for that first-order term (0.1943 versus 0.1937). These coefficients are also larger than the other coefficients on the second-order terms. This equation shows that the independent effects of each parameter are larger than the combined effects. Due to this, the slopes of each parameter found for the separate effect analysis are a good approximation of the combined effect on excess reactivity if the off-nominal parameters are given.

Some of the proposed tolerances lead to significant effects on the fuel cycle length. However, these cases, similar to the full-core fuel plate thickness, represent highly conservative cases. This approach means that while this effect can happen within the proposed tolerances, it is unlikely to occur.

The last part of this analysis was to evaluate these cases against the SDM criterion. Again, blades 2 and 3 represent the most limiting blades, and only cases that add positive reactivity were a part of the analysis. Table 6-7 lists the SDM results of the full-core combination impact analysis.

Table 6-7: SDM for Combination Impact Analysis

Case	SDM [% $\Delta k/k$]	
	Blade 2	Blade 3
+1.0% Fuel Mass Loading -3.0 mil Plate Thickness	2.1450	2.1294
-1.0% Fuel Mass Loading -3.0 mil Plate Thickness	2.2599	2.2338
+0.5% Fuel Mass Loading -1.5 mil Plate Thickness	2.8373	2.8246
-0.5% Fuel Mass Loading -1.5 mil Plate Thickness	2.9039	2.8828

This table shows that none of the cases show a violation of the SDM criterion of 1.0% $\Delta k/k$. This realization means that the parameters can have a significant effect on fuel cycle length, but do not take away the margin to criticality.

6.3.2 Local Combination Impact Results

This section introduces the results for the local combination impact analysis. These results are presented similarly to the results associated with the separate effect fuel plate thickness parameter

section. Each of the 8 test cases from the test methodology section was modeled in MCNP with f7 tallies covering the fuel throughout the core. These tallies created STAT7 files for all four stripes from each case. Each of these STAT7 files calculated the lowest P_{ONB} for each case. Figure 6-5 displays the relationship of these values to that of the nominal P_{ONB} of position A-2, 10.2086 MW. The figure displays this power as a black dashed line.

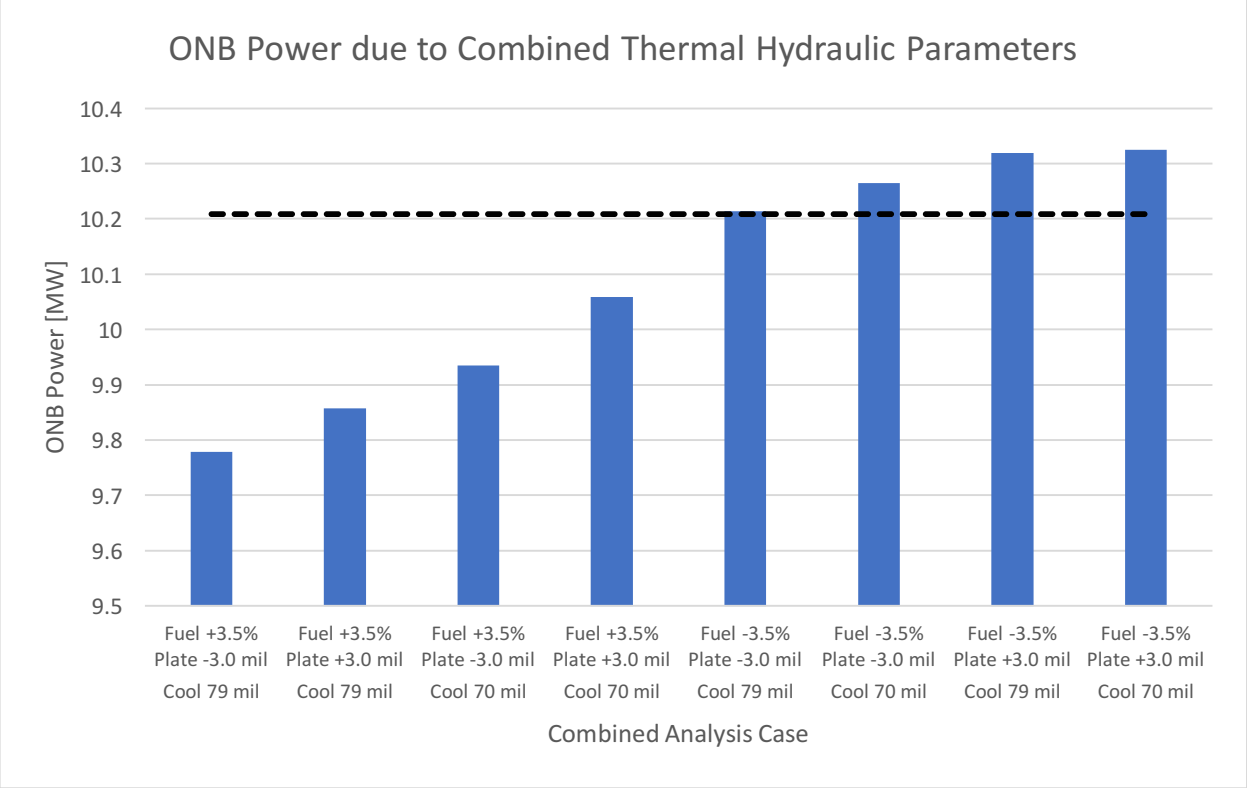

Figure 6-5: P_{ONB} due to Combined Thermal Hydraulic Parameters

These results show that none of the evaluated cases exhibit an P_{ONB} lower than that of the LSSS Power: 8.68 MW. Examining these results further reveals that fuel mass loading is more impactful to the P_{ONB} than any of the other parameters. This realization contradicts what previous analyses observed where the size of the coolant channel was more critical due to the amount of moderation/cooling added or taken away. More substantial fuel mass loading changes presumably caused the resurgence associated with these analyses. The effect on the ONB temperature margin is recorded and shown in Figure 6-6.

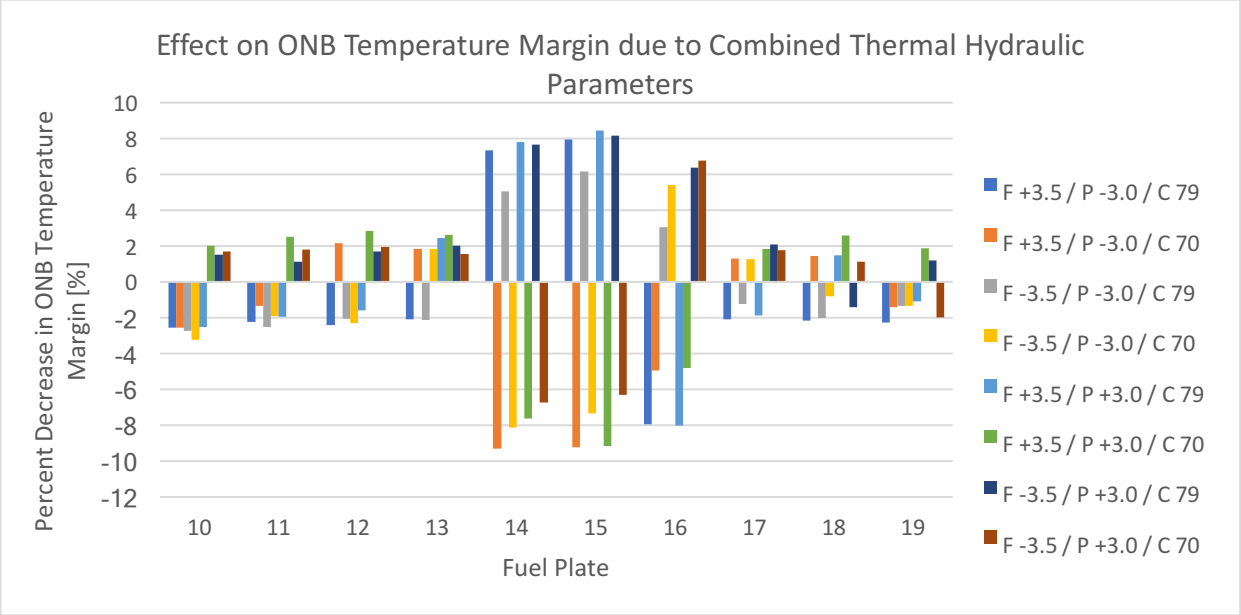

Figure 6-6: Effect on ONB Temperature Margin due to Combined Thermal Hydraulic Parameters

F +3.5 / P -3.0 / C 79	→	Fuel +3.5% / Plate Th. -3.0 mil / Coolant Ch. 79.0 mil
F +3.5 / P +3.0 / C 79	→	Fuel +3.5% / Plate Th. +3.0 mil / Coolant Ch. 79.0 mil
F +3.5 / P -3.0 / C 70	→	Fuel +3.5% / Plate Th. -3.0 mil / Coolant Ch. 70.0 mil
F +3.5 / P +3.0 / C 70	→	Fuel +3.5% / Plate Th. +3.0 mil / Coolant Ch. 70.0 mil
F -3.5 / P -3.0 / C 79	→	Fuel -3.5% / Plate Th. -3.0 mil / Coolant Ch. 79.0 mil
F -3.5 / P -3.0 / C 70	→	Fuel -3.5% / Plate Th. -3.0 mil / Coolant Ch. 70.0 mil
F -3.5 / P +3.0 / C 79	→	Fuel -3.5% / Plate Th. +3.0 mil / Coolant Ch. 79.0 mil
F -3.5 / P +3.0 / C 70	→	Fuel -3.5% / Plate Th. +3.0 mil / Coolant Ch. 70.0 mil

The figure shows that parameters in the local combination analysis affect the ONB temperature margin in different places. An off-nominal channel 16 has the most significant impact on fuel plates 14 and 15, rather than plate 16. These plates surround channel 15, the channel next to the altered channel. This impact occurs as increases in channel 16 assist cooling plate 15, lowering the ONB temperature margin for that plate and the plate next to it. Decreases in channel 16 have the opposite effect and force the adjacent channel to cool more of plate 15. The impact on plate 16 is dependent on the fuel mass loading, similar to the impact observed during the P_{ONB} analysis. None of the evaluated cases experienced a decrease in ONB temperature margin larger than 10%.

6.4 Fuel Specification Combination Impact Conclusions

The combination impact analysis was performed to quantify the effects of several off-nominal parameters, including fuel mass loading, fuel plate thickness, and coolant channel gap thickness within their respective tolerances. The combination impact analysis provided two main results:

- Observing the data showed that the linear effect of the individual parameters was much more dominant than any of the combined effects.
- None of the current parameters when combined within the proposed tolerances, violate the thermal hydraulic criteria on ONB power (P_{ONB}) and ONB temperature margin in the hottest element

The linear effect of these parameters was deemed more dominant due to the comparison of the curve fit coefficients developed during this chapter. The coefficients on the individual first-order parameters were much larger than the coefficient on the combined input. Since these coefficients are so different in magnitude, any alteration has a more significant impact due to the first-order inputs. The strength of the linear effects was further shown comparing the first-order coefficients to the separate effects slopes. These values were very similar, showing the individual linear effect still occurs to the same magnitude when combined with other parameters.

The analysis completed on the thermal hydraulic effects exhibited no violations of the thermal hydraulic criteria. The parameters that heavily influence the power distribution, plate thickness and coolant channel gap, increase the amount of cooling the plate receives. This additional cooling negates the extra moderation, ensuring the reactor maintains proper safety margins.

Chapter 7: Conclusions and Recommendations for Future Work

7.1 Research Overview

The purpose of this assessment was to evaluate the proposed fabrication tolerances of the new MITR LEU fuel system. This work was a crucial step in identifying practical considerations for LEU fabrication. The design parameters included in this assessment were:

- Coolant Channel Gap Thickness
- Enrichment
- Fuel Mass Loading
- Fuel Plate Thickness
- Fuel Homogeneity
- Impurities in Fuel and Cladding/Side Plates

The analysis of these parameters combined multiple levels of the core, ranging from a global effect (full-core) down to a single fuel plate spot. This complicated problem involves both neutronic and thermal hydraulics aspects. The neutronics analyses focused on finding the reactivity effect of the fabrication tolerances. This reactivity effect is then translated to the effect on fuel cycle length or SDM. For the tolerances that focused on more local alterations, thermal hydraulic analyses found the impact of the tolerances on the margin to the thermal hydraulic licensing limit, ONB. These analyses focused on the difference between LSSS power and ONB Power (P_{ONB}), an estimate of the power at which the reactor would have a 3-σ confidence level of not having any instances of ONB. Before reviewing the results, the following values represent the safety criteria of the nominal cores tested:

LEU Fresh Core 1

- SDM: 3.53% $\Delta k/k$
- Position A-2 P_{ONB}: 10.21 MW
- Position C-5 P_{ONB}: 9.66 MW

LEU Equilibrium Core Cycle 13[2]

- Position A-2 P_{ONB}: 9.49 MW

The following sections review conclusions from this research and compare the safety criteria to the above values. This chapter also introduces recommendations for future work.

[2] Neutronic and position C-5 analyses were not completed for LEU Equilibrium Cycle 13, therefore SDM and Position C-5 P_{ONB} of this cycle were not listed for comparison

7.2 Conclusions

Coolant Channel Gap

The first analysis completed was on the effect of coolant channel thickness during an equilibrium cycle. The impact of this parameter was essential to understand due to a combination of the increase in thermal power and the decrease in coolant channel thickness. This analysis focused on the hottest element in the core, position A-2. The results of this analysis include:

- The first F-type plate on either side of the element (plates 4 and 16) would have the most limiting P_{ONB}
- None of the evaluated powers were lower than the LSSS power of 8.68 MW, with the lowest P_{ONB} being 8.95 MW occurring when channel 16 was held at 66.0 mil
- Channels 5, 15, 16, and 17 were the only channels to see a >10% decrease in ONB temperature margin within the proposed tolerances

While the first part of this analysis targeted specific limiting channels, the coolant channel uncertainty analysis showed that the fabrication tolerances could increase >150% while still maintaining sufficient thermal hydraulic margin to LSSS power. These results show that while the new LEU fuel element design has smaller coolant channels, the varying fuel thicknesses in the FYT fuel element design allow for lower power peaking within the element. This flattening out of the lateral power distribution allows for no violations of the thermal hydraulic safety margins at the current fabrication tolerances.

U-235 Enrichment and Fuel Mass Loading

The next analysis completed was on the fresh 22 element core, LEU Core 1. This core was deemed one of the most limiting times in MITR's transition due to the higher average power density and peaking in central positions. This analysis found the effect these tolerances can have on the fuel cycle length. The first of these analyses was on enrichment and fuel mass loading, as these tolerances would have a direct impact on the amount of fissile material in the core. The current tolerance for each parameter is ±1.0%, and the results from these analyses were:

- Enrichment tolerances led to a maximum fuel cycle length decrease of ~7 FPD
- Fuel mass loading tolerances led to a maximum fuel cycle length decrease of ~3 FPD
- Neither tolerance exhibited SDM's that violated the MITR criterion of 1.0% $\Delta k/k$

Enrichment has a more significant effect as fuel mass loading adds U-238 as well, which lowers the resonance escape probability. The fuel mass loading analysis included an additional analysis of the local effects of the broader tolerances at a fuel plate level. This additional analysis focused on the tolerances' impact on the margin to ONB. This analysis was completed for position A-2, the hottest element in the core, and position C-5, the hottest element in the C-ring. The results of this analysis are:

- None of the evaluated cases exhibit an P_{ONB} less than the LSSS power of 8.68 MW
- Current tolerances show that the maximum change in P_{ONB} is ~3% for plate 4 in position A-2 and plate 1 in position C-5
- Neither position exhibited decreases in ONB temperature margin of >10%

These results indicate that the broader tolerances of fuel mass loading at the plate level do not take away the margin to ONB maintained by adherence to the thermal hydraulic criteria. These results do show that position C-5 acts as a more limiting position (lower nominal P_{ONB}) due to peaking caused by the proximity to the heavy water reflector.

Fuel Plate Thickness

After analyzing and finding the minimal effects on the parameters which alter fissile material, the next step was to find the impact of the parameter that alters the amount of moderation, fuel plate thickness. This analysis included two steps, first, altering at the full-core level and then altering at the position A-2 level. The local analysis was completed as well due to the highly conservative nature of a full-core alteration, with all plates at the same off-nominal value. The results of these analyses were:

- Full-core decrease of 3.0 mil in all fuel plates can lead to a decrease of ~92 FPD in fuel cycle length
- Position A-2 decrease of 3.0 mil in all fuel plates can lead to a decrease of ~5 FPD in fuel cycle length
- None of the evaluated cases exhibited SDM's lower than the MITR safety criterion of 1.0% $\Delta k/k$

These results show that neutron moderation has a much more significant effect on the than the amount of fissile material due to reduced fuel plate thickness. A full-core fuel plate thickness alteration shows a significant impact on the fuel cycle length the parameter can have, but the local analysis shows that in a more realistic case, the effect is much smaller and more manageable. In addition to the neutronic analysis, the position A-2 fuel plate thickness was evaluated for the margin to the thermal hydraulic safety limits as well. The results of this analysis showed:

- None of the results violated the LSSS power criterion
- Lowest evaluated power was 9.52 MW when all plates are decreased by 3.0 mil
- Few F-plates exhibited larger than 10% decrease in ONB temperature margin (plates 4, 7, 11, 12, 14, 15, 16, and 17)

These results show that while these cases have larger coolant channels leading to additional moderation, the extra moderator acts as extra cooling as well. This effect negates some of the peaking caused by the additional moderator in the element. This negation allows the thermal hydraulic criteria to be mostly maintained. Some cases require restrictions on the location of the element within the core.

Impurities in Fuel

The last parameter to be studied for its neutronics effect was impurities located in the fuel and cladding/side plates. The results of this assessment were:

- Impurities in the fuel lead to a decrease in fuel cycle length of ~3 FPD
- Impurities in the cladding/side plates lead to a decrease in fuel cycle length of ~33 FPD

The analysis determined that impurities in the fuel have a larger effect due to the higher neutron flux, but the cladding/side plates allow for ~12 times more impurities than the fuel. Due to this, the impurities in the cladding/side plates are more limiting and have a significant effect on the fuel cycle length. Further research is being completed to find a better specification for impurities in the core, and better understand the burnup of impurities. This research will give a better idea of the actual amount of impurities and how long their effect will last in the core.

Fuel Homogeneity

The most local of the analyses completed was on the fuel homogeneity of a single spot on the fuel plate. The proposed tolerances allow for ±10% uncertainty in the fuel homogeneity. STAT7 analyses show that this value could increase ~25% before meeting the LSSS criterion of 8.68 MW.

Table 7-1 provides a summary of the results/findings for each parameter that was evaluated.

Table 7-1: Summary of Evaluation Results for MITR LEU Fabrication Tolerances [20]

Parameter		Nominal Value	Current Tolerance	Comments
Enrichment		19.75 wt%	±0.2 wt%	• Largest negative reactivity for full-core: -0.1103% $^{\Delta k}/_{k}$ (~7 FPD) • SDM = 3.42% $^{\Delta k}/_{k}$ (-0.11% $^{\Delta k}/_{k}$ from nominal)
Fuel Mass Loading	Element[1]	968 gU-235	±9.8 gU-235	• Largest negative reactivity for full-core: -0.0408% $^{\Delta k}/_{k}$ (~3 FPD) • SDM = 3.48% $^{\Delta k}/_{k}$ (-0.05% $^{\Delta k}/_{k}$ from nominal)
	Fuel Plate	F: 57.74 gU-235 Y: 39.26 gU-235 T: 30.02 gU-235	F: ±2.02 gU-235 Y: ±1.37 gU-235 T: ±1.05 gU-235	• Completed for LEU Core 1 • Min. Pos. A-2 Lowest P_{ONB}: 9.69 MW (Pl. 4 @ 18.5 g/cc) • Min. Pos. C-5 Lowest P_{ONB}: 9.05 MW (Pl. 1 @ 18.5 g/cc)
Fuel Plate Thickness		49.0 mil	±3.0 mil	<u>Full-Core Alterations:</u> • Largest negative reactivity for full-core: -1.393% $^{\Delta k}/_{k}$ (~92 FPD) • SDM = 1.90% $^{\Delta k}/_{k}$ (-1.63% $^{\Delta k}/_{k}$ from nominal) <u>Position A-2 Alterations:</u> • Completed for LEU Core 1 • Largest addition of negative reactivity: -0.072% $^{\Delta k}/_{k}$ (~5 FPD) • Pos. A-2 Lowest P_{ONB}: 9.52 MW (Dec. Fuel & Cladding 1.5 mil)
Impurities	Fuel	Traditional: <1200 ppm EBC[2]: <5.0 ppm		• Largest addition of negative reactivity: -0.0490% $^{\Delta k}/_{k}$ (~3 FPD)
	Cladding	EBC[2]: <67.0 ppm[3]		• Largest addition of negative reactivity: -0.4954% $^{\Delta k}/_{k}$ (~33 FPD)
Coolant Channel Gap	Inner Ch.	74.6 mil	70.0-79.0 mil	• Completed for Cycle 13 • Lowest P_{ONB}: 8.95 MW (Ch. 16 @ 66.0 mil)
	End Ch.	65.6 mil	54.0-78.0 mil	
Fuel Homogeneity		±10%		• Completed for Cycle 13 • Can be increased to ±25% before reaching LSSS Power

Note 1: Fuel mass loading was evaluated on a full-core level, but the tolerance is at the element level
Note 2: Equivalent Boron Content (EBC) was calculated for these limits using ASTM EBC Factors
Note 3: 67.0 ppm is calculated using the cladding/side plates impurities limits of 30 ppm, 80 ppm cadmium, 80 ppm lithium

Combination Effect

After completing the separate effect analyses, the final step was a combination analysis on a full-core and element level. The full-core combination impact analysis combined the effects of fuel mass loading and fuel plate thickness.

The results of this analysis for LEU Core 1 showed:

- The maximum decrease in fuel cycle length was ~84 FPD if all fuel elements are fabricated with fuel mass loading decreased by 1.0% and the fuel plate thickness all increased by 3.0 mil
- None of the evaluated cases exhibited SDM's less than 1.0% $\Delta k/k$

This analysis showed that the combined effect of these parameters, given the overall fuel element outer geometry constraint, is smaller than their separate effects. The local analysis, on position A-2, included alterations to the coolant channel gap thickness and showed no violations of the ONB Power (P_{ONB}) or ONB temperature margin criterion. This was due to the parameters that greatly affected the power distribution, fuel plate thickness and coolant channel gap, also increasing the cooling to those plates. In this way, fuel mass loading became the more limiting parameter at the local level.

7.3 Recommendations for Future Work

7.3.1 Recommendation 1: Initial Fresh Core Loading

The primary analysis of this research was on the impact of parameters during LEU Core 1, the all-fresh 22 LEU fuel element core that will serve as the first cycle of the conversion, unless, as is noted in this assessment, a mixed HEU-LEU core transition is found acceptable. This analysis was an essential aspect of the research due to the more substantial impact of fabrication tolerances during this cycle. This loading period is different from other loading periods as a typical loading period sees the addition of three or four new elements. This difference in impact is evident when looking at the neutronics effects of the full-core fuel plate thickness and position A-2 fuel plate thickness analyses. Those results showed that the local element had a ~20 times lower effect than the full-core analysis, even in the hottest position in the core. To account for the more significant possible swings in reactivity at the initial loading, it is recommended to increase confidence in the fuel element fabrication and quality control of the fuel plate thicknesses of the elements. This step would focus primarily on the geometry of the elements to ensure the change in the amount of moderator is not too different from the completed analyses. Fuel plate thickness was deemed to have the most significant impact on the core physics and is necessary to properly control this parameter at the initial loading and future loading. Performing these extra checks enables the reactor to operate at expected power and be safe from significant impacts to fuel cycle length or SDM.

7.3.2 Recommendation 2: Impurities in Cladding/Side Plates

The other tolerance that sits in violation of the imposed rules/criteria is the impurities within the cladding and side plates. The proposed tolerances allow a maximum of:

- 30 ppm of Boron
- 80 ppm of Cadmium
- 80 ppm of Lithium

These impurities lead to 67 ppm of EBC, which analyses show can cause a decrease of ~33 FPD in fuel cycle length. The solution to this effect is two-fold, the first of which is research into the burnup of these impurities. This research can show that the impurities might not have the impact previously suggested. If this research proves the currently expected effect does occur, then there is necessary work needed to understand the amount of impurities better and thus to lower the specification. To accomplish this, it is recommended for NRL to receive the materials assays of the incoming fuel elements so that it may better understand the amount of impurities in the core and test those values. The fuel certification report can include this materials assay.

7.3.3 Recommendation 3: Reactor Specific EBC Factors

One aspect of this research observed to be outdated was the use of ASTM EBC factors. These values were originally for use within a PWR, where the spectrum leans more thermal than that of MITR. Due to this, the ratios created between natural boron and other impurities rely on only using the thermal cross section to compare their reaction rates. This focus is limiting for reactors, such as MITR, that have a harder spectrum with higher amounts of fission at the 0.1-0.2 eV range. Part of the analysis completed during the LEU Core 1 section was to create reactor-specific EBC factors that would account for the spectrum of MITR. It is recommended these factors should be used for further analyses as they better model the actual effects of these impurities within the reactor. Initial results have shown that these EBC factors significantly better estimate the effect of directly modeled impurities for MITR. It is also recommended that reactor-specific EBC factors are assessed for other reactors that currently use the ASTM EBC factors.

7.3.4 Recommendation 4: Expanded Local Analyses

Much of the necessary work for this analysis has been completed, and these analyses have shown sufficient margin to the thermal hydraulic safety limits. However, some of the local analyses could be expanded to better model the local thermal hydraulic effects throughout the core. This expansion would include two steps: testing other fuel positions and evaluating existing position analyses to be more thorough. The first of these steps would involve extending analyses such as the coolant channel gap thickness/uncertainty analyses to position C-5, which proved to have the

lowest nominal P_{ONB} of the positions studied. This step could further expand to analyze each of the 24 positions in the core. This analysis would better prove that the existence of peaking around the core would not cause violations of the thermal hydraulic criteria. The local combination analysis could expand to other positions, specifically position C-5. The test matrix would need reworking to fit other positions where the most limiting plate was not an F-type plate but would be an essential aspect of understanding the effects of peaking in the other fuel positions.

While it would be necessary to extend these analyses to further positions, the other step of this recommendation would be to expand these analyses within the current fuel positions. One possible way to accomplish this would be to analyze the effects of multiple channels being at minimal values and adjusting the rest of the channels to still fit within the position. In addition to the extension of the coolant channel gap analysis, another recommendation would be to expand the local combination analysis to analyze other plates and channels within the positions, rather than just the most limiting plates. Incorporating these two steps would give a better understanding of the impact fabrication tolerances have on the local thermal hydraulic safety margins throughout the core.

Appendix A: HEU Fuel Element ICR Analysis

As part of MITR fuel element fabrication requirements, BWXT completes measurements and inspections to determine that a fuel element meets all fabrication specifications. If any of the specifications fall outside of the fabrication tolerance, this is reported in an INL Change Request (ICR), which NRL staff review and decide whether a fuel element will be accepted or rejected. One of the fuel fabrication parameters in an ICR that may have a significant impact on fuel performance is a coolant channel being outside the specified fabrication tolerance range. The specified nominal coolant gap for the MITR HEU fuel element is 78±4.0 mil [24].

This appendix summarizes analyses performed to quantify the impact of the off-nominal coolant channel gap on MIT operation safety margin. The Onset of Nucleate Boiling (ONB) is adopted as the Limiting Safety System Settings (LSSS) of the MITR, hence the change in ONB temperature margin is adopted in the assessment to quantify the impact [7].

ICR Test Methodology

MITR fuel elements are manufactured by BWXT and follow specifications identified in Drawing R3F-201-4 "MIT Reactor MITR-2: Fuel Element Assembly". **Error! Reference source not found.** displays the relevant specifications for this assessment.

Table A-1: Nominal Channel Specifications for MITR Fuel Element [24] [25]

Nominal Thickness for full Channel	78.00 mil
Tolerance for Full Channel	±4.00 mil[1]

Note 1: This range is given in TRTR-3, where it references drawing no. R3F-201-4

In addition to specifications given in the drawings, additional research has been done to calculate the range of channel thicknesses received by MITR. Keng-Yen Chiang completed this additional research in 2012, using data from all previous elements, finding the channel thicknesses fall within ±5.4 mil of the nominal thickness at a 3-sigma confidence level (99%) [26].

A variety of thicknesses were evaluated for each channel at LSSS to quantify the effect of off-nominal channels. Table A-2 shows the inputs for LSSS used in this assessment.

Table A-2: LSSS conditions for MITR

Power	7.40 MW
Coolant Outlet Temperature	60 °C
Mass Flow Rate	1800 gpm (111.7 kg/s)

The off-nominal thicknesses evaluated in this assessment were 70, 71, 72, 73, 73.5, 82.5, 83, 84, 85, 86 mil, with a 1.33 mil standard deviation. These thicknesses include the largest off-nominal channel seen in recent ICR's, a 70 mil channel (ICR-J57-0011 in 2014).

STAT7 Results

The STAT7 code modeled how the off-nominal channel would affect the mass flow rate and thus the cooling provided to the channel. Using these changes, STAT7 produced the temperatures of ONB as well as the surface temperatures for the cladding on each side of the fuel plate to find the ONB temperature margin shown in equation A-1. The percent change of this value was calculated using equation A-2.

$$\Delta T_{ONB} = T_{clad,ONB} - T_{co} \tag{A-1}$$

$$Percent\ Change = \frac{\Delta T_{ONB,ICR} - \Delta T_{ONB,nom}}{\Delta T_{ONB,nom}} * 100\% \tag{A-2}$$

This value represents the percent change in ONB on each surface of the channel. Rather than use an average, the values represented are for the top axial node of each surface, as this is the most vulnerable axial node to this change in all evaluations. **Error! Reference source not found.** displays the percent change in ONB for each channel.

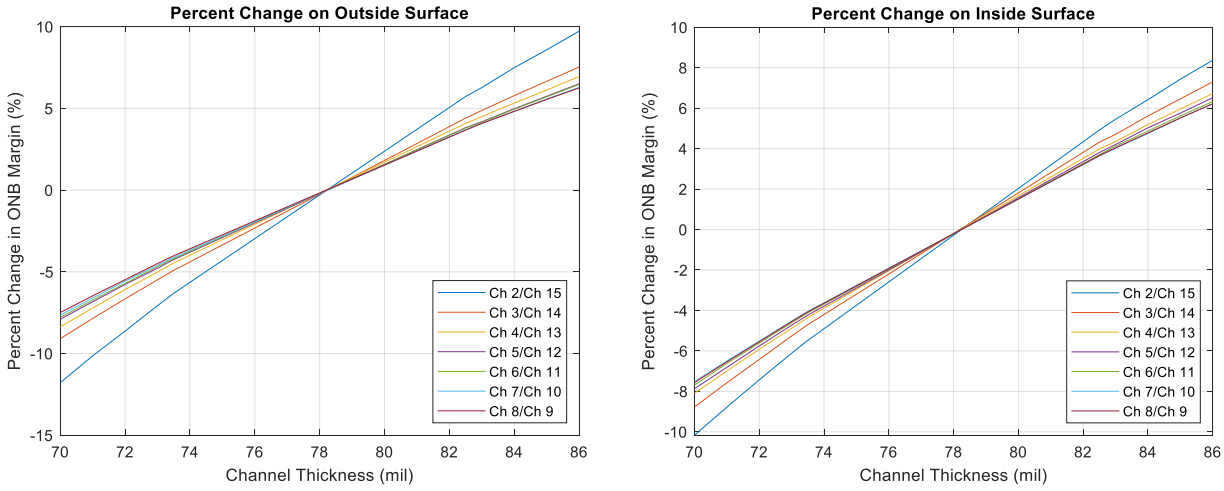

Figure A-1: Percent change in ONB Temperature Margin on the (left) outer surface of the channel and (right) inner surface of the channel

These changes follow the expected changes coming from the percent change in mass flow rate associated with each alteration. The figure shows a channel smaller than nominal is more concerning than a larger channel due to a smaller channel decreasing the ONB temperature margin. The outer channel is most limiting because the neutron flux is highest there, causing the outer plates of the element to operate hotter than other interior plates. Figure A-2 shows a zoomed-in view of the smaller than nominal channels evaluated.

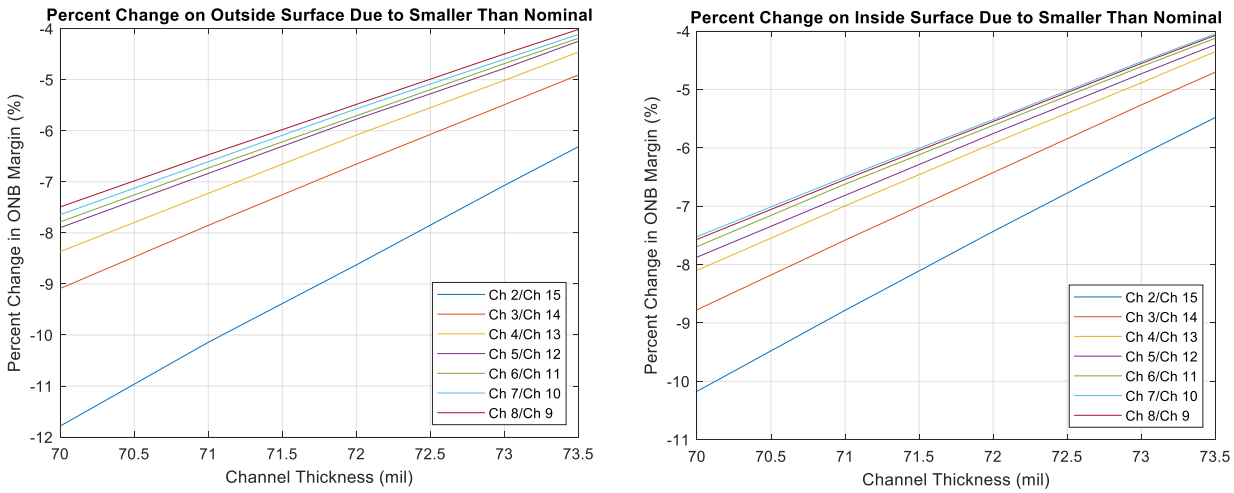

Figure A-2: Percent change in ONB Temperature Margin for smaller than nominal changes (70-73.5 mil) on (left) outer surface and (right) inner surface

These plots show to limit the ONB temperature margin reduction by less than 10%, an off-nominal channel cannot be less than 71 mil in the outermost channel (Ch 2/15). These STAT7 runs are at a 3-sigma confidence level at 99.865% [16].

Verification Method

The analysis completed in this assessment was verified using an analytically derived equation to obtain the ratio of mass flow rates of the nominal versus off-nominal case. This relationship uses the ratio of nominal hydraulic diameter compared to the off-nominal diameter. The derivation of this expression starts with equation A-3, the pressure drop, and the Blasius correlation for the friction factor.

$$\Delta P = f\frac{L}{D_h}\frac{\dot{m}^2}{A^2\rho} \tag{A-3}$$

$$f = 0.316Re^{-0.25} = 0.316\left(\frac{\dot{m}D_h}{\mu A}\right)^{-0.25} \tag{A-4}$$

Plugging in the correlation for the friction factor, using A and simplifying gives the following equation

$$\Delta P = 0.316\mu^{0.25}\frac{L}{{D_h}^{1.25}}\frac{\dot{m}^{1.75}}{A^{1.75}\rho} \tag{A-5}$$

Setting the nominal and ICR pressure drops equal give the following expression, further simplified assuming negligible changes in viscosity and density.

$$0.316\mu^{0.25}\frac{L}{{D_{h_{nom}}}^{1.25}}\frac{{\dot{m}_{nom}}^{1.75}}{{A_{nom}}^{1.75}\rho} = 0.316\mu^{0.25}\frac{L}{{D_{h_{ICR}}}^{1.25}}\frac{{\dot{m}_{ICR}}^{1.75}}{{A_{ICR}}^{1.75}\rho} \tag{A-6}$$

$$\frac{{\dot{m}_{nom}}^{1.75}}{{D_{h_{nom}}}^{1.25}{A_{nom}}^{1.75}} = \frac{{\dot{m}_{ICR}}^{1.75}}{{D_{h_{ICR}}}^{1.25}{A_{ICR}}^{1.75}} \tag{A-7}$$

This expression can be further simplified using the definitions of the area and hydraulic diameter

$$A = L * t \tag{A-8}$$

$$D_h = \frac{4L * t}{2(L + t)} \approx 2t, \text{if } t \ll L \tag{A-9}$$

Equation A-10 shows the final expression used in the verification analysis after applying these definitions.

$$\frac{\dot{m}_{ICR}}{\dot{m}_{nom}} = (\frac{t_{ICR}}{t_{nom}})^{\frac{12}{7}} \tag{A-10}$$

This equation was derived using the friction factor equation from the final manual for STAT7 and assuming the pressure drop over the core was consistent while the derivation can be found in Chiang's thesis [26] [16].

Table A-3 gives a summary of this verification analysis.

Table A-3: ICR Verification Calculations

Channel Thickness (mil)	Mass Flow Rate Ratio Calculated using Equation A-10	Mass Flow Rate Ratio Calculated using STAT7
70	0.8307	0.8589
71	0.8511	0.8760
72	0.8931	0.8935
73	0.8718	0.9109
73.5	0.9031	0.9199
82.5	1.1009	1.0830
83	1.1124	1.0919
84	1.1355	1.1106
85	1.1587	1.1293
86	1.1822	1.1484

Conclusions

The assessment found that a reduction in the coolant channel gap results in a decrease in channel flow rate and ONB temperature margin. The assessment shows that significant departures from nominal values in the full outer channels, <71 mil, is predicted to cause the ONB temperature margin to decrease by 10%. Therefore, it is recommended that a fuel element with coolant channel gap <71 mil not be accepted for insertion, unless comprehensive neutronic and thermal hydraulic analyses show that ONB temperature margin for all fuel plates in the fuel element will not be reduced by more than 10% throughout each fuel cycle.

Appendix B: MITR LEU Fuel and Cladding Impurities Breakdown

Composition and Impurities of U-10Mo Fuel

The fuel used for the MITR LEU Conversion is U-10Mo. This section introduces the breakdown of U-10Mo fuel and then introduces the impurities limits associated with the fuel. **Error! Reference source not found.** displays this fuel breakdown. The fuel consists of 10 wt% Molybdenum.

Table B-1: LEU U-10Mo Fuel Breakdown [20] [27]

Isotope	Symbol	Units	U or Mo Composition	Total Composition
Uranium 235	U-235	wt%	19.75±0.2	17.775
Uranium 238	U-238	wt%	79.53±0.2	71.577
Uranium 232	U-232	negligible (≤0.002 ppm or 2E-9 wt%)		
Uranium 234	U-234	wt%	≤0.260	≤0.234
Uranium 236	U-236	wt%	≤0.460	≤0.414
Total Uranium		wt%		90
Molybdenum 92	Mo-92	wt%	14.15	1.415
Molybdenum 94	Mo-94	wt%	9.03	0.903
Molybdenum 95	Mo-95	wt%	15.73	1.573
Molybdenum 96	Mo-96	wt%	16.67	1.667
Molybdenum 97	Mo-97	wt%	9.66	0.966
Molybdenum 98	Mo-98	wt%	24.69	2.469
Molybdenum 100	Mo-100	wt%	10.07	1.007
Total Molybdenum		wt%		10

SPC-1635 also gives the breakdown for what impurities are allowed for in the U-10Mo fuel. The specification does not give isotopic breakdowns for each element, so they are assumed to be natural isotopic composition. The specification limits total impurities to be ≤ 1200 ppm, while if all of the individual impurities are allowed to be at their maximum, the total would be 2506 ppm [20]. This appendix includes a total isotopic breakdown of each natural isotopic composition.

Table B-2: LEU U-Mo Fuel Impurities [20]

Impurity	Symbol	Concentration Limit $[\frac{\mu g}{gU-Mo}]$
Aluminum	Al	≤ 150
Beryllium	Be	≤ 1.0
Boron	B	≤ 2.0
Cadmium	Cd	≤ 1.0
Calcium	Ca	≤ 100.0
Carbon	C	≤ 800.0
Chromium	Cr	≤ 50.0
Cobalt	Co	≤ 5.0
Copper	Cu	≤ 50.0
Dysprosium	Dy	≤ 5.0
Erbium	Er	≤ 100.0
Europium	Eu	≤ 2.0
Gadolinium	Gd	≤ 1.0
Iron	Fe	≤ 250.0
Lead	Pb	≤ 5.0
Lithium	Li	≤ 3.0
Magnesium	Mg	≤ 50.0
Manganese	Mn	≤ 24.0
Nickel	Ni	≤ 100.0
Phosphorus	P	≤ 50.0
Samarium	Sm	≤ 2.0
Silicon	Si	≤ 250.0
Sodium	Na	≤ 25.0
Tin	Sn	≤ 100.0
Tungsten	W	≤ 100.0
Vanadium	V	≤ 30.0
Zirconium	Zr	≤ 250.0
Total Impurities		≤ 1200

The HEU fuel currently in use does not contain similar amounts of impurities as the LEU fuel will. The specification for the HEU fuel (TRTR-3) document did not account for any impurities within the fuel [28].

The zirconium interlayer allows for 1000 ppm of oxygen, but this is not accounted for due to the negligible absorption effects of oxygen; it has an EBC Factor of 1.68E-7 [20].

Composition and Impurities in AA6061 Cladding

The cladding used in the MITR LEU Conversion is AA6061 with T6 heat tempering [20]. ASTM B209M gives the composition of this cladding. This specification does not give isotopic breakdowns for each element, so it is assumed to be natural isotopic composition again. For the elements that have a range, it is assumed the value is in the middle. Table B-3 gives this AA6061 breakdown. Values highlighted in yellow are not included in the MCNP models in this assessment. These values are not included in the MCNP model as studies were completed to show these isotopes were not present in the AA6061 used in the HPRRs.

Table B-3: AA6061 Specification [23]

Element	Atomic Total Composition (Set Value)	Weight Total Composition
Aluminum	96.530	94.910
Silicon	0.4-0.8 (0.6)	0.614
Iron	0.7	1.425
Copper	0.15-0.4 (0.275)	0.637
Manganese	0.15	0.300
Magnesium	0.8-1.2 (1.0)	0.886
Chromium	0.04-0.35 (0.195)	0.370
Zinc	0.250	0.596
Titanium	0.15	0.26
Other Elements	0.15	N/A[1]

[1]This is written as N/A due to no knowledge of what element and no knowledge of mass

The impurities content allowed for in the cladding, side plates, and nozzles are specified in section 5.2 of ANL/RTR/TM-18/2 "Information for the Specification of Low Enriched Uranium Fuel Elements for the MITR" [21]. Table B-4 shows these impurities limits.

Table B-4: AA6061 Impurities [21]

Impurity	Symbol	Concentration Limit $[\frac{\mu g}{g AA6061}]$
Boron	B	≤ 30
Cadmium	Cd	≤ 80
Lithium	Li	≤ 80
Total Impurities		≤ 190

The current LEU specification allows for more impurities than the HEU specification. According to TRTR-3, the side plates and nozzle pieces have a maximum of 30 ppm of boron [28]. This amount is similar to the LEU cladding as each allows for 30 ppm of boron, but the TRTR-3 does not mention cadmium or lithium as allowable impurities [28]. If the impurities allowed for by the

LEU cladding are weighted with EBC Factors, it is approximately 67 ppm of boron, which is more than two times the proposed specification for the HEU cladding.

AA6061 Cladding Isotopic Composition

Zinc is highlighted as it is not included in the MCNP file. Values in parentheses from Table B-3 are used for calculations.

Table B-5: Cladding Isotopic Breakdown

Element	Isotope	Cladding Isotopic Composition [at%]
Aluminum	Al-27	96.530
Chromium	Cr-50	0.008
	Cr-52	0.163
	Cr-53	0.019
	Cr-54	0.005
Copper	Cu-63	0.190
	Cu-65	0.085
Iron	Fe-54	0.041
	Fe-56	0.642
	Fe-57	0.015
	Fe-58	0.002
Magnesium	Mg-24	0.790
	Mg-25	0.100
	Mg-26	0.110
Manganese	Mn-55	0.150
Silicon	Si-28	0.553
	Si-29	0.028
	Si-30	0.019
Titanium	Ti-46	0.012
	Ti-47	0.011
	Ti-48	0.111
	Ti-49	0.008
	Ti-50	0.008
Zinc	Zn-64	0.123
	Zn-66	0.06925
	Zn-67	0.01
	Zn-68	0.04625
	Zn-70	0.0015

Naturally Occurring Isotopic Compositions

This appendix includes the natural isotopic compositions for elements contained within the fuel, cladding, and impurities in both.

Table B-6: Natural Concentrations of Elements included in Fuel, Cladding, and Impurities for MITR LEU Conversion

Element	Isotope	Natural Isotopic Composition [at%]
Aluminum	Al-27	100
Beryllium	Be-9	100
Boron	B-10	20
	B-11	80
Cadmium	Cd-106	1.25
	Cd-108	0.89
	Cd-110	12.49
	Cd-111	12.80
	Cd-112	24.13
	Cd-113	12.22
	Cd-114	28.73
	Cd-116	7.49
Calcium	Ca-40	96.94
	Ca-42	0.65
	Ca-43	0.14
	Ca-44	2.09
	Ca-46	0.004
	Ca-48	0.19
Carbon	C-12	98.90
	C-13	1.10
Chromium	Cr-50	4.35
	Cr-52	83.79
	Cr-53	9.50
	Cr-54	2.37
Cobalt	Co-59	100
Copper	Cu-63	69.15
	Cu-65	30.85
Dysprosium	Dy-156	0.06
	Dy-158	0.1
	Dy-160	2.34
	Dy-161	18.91
	Dy-162	25.51
	Dy-163	24.9
	Dy-164	28.18

Element	Isotope	Natural Isotopic Composition [at%]
Erbium	Er-162	0.139
	Er-164	1.601
	Er-166	33.503
	Er-167	22.869
	Er-168	26.978
	Er-170	14.910
Europium	Eu-151	47.81
	Eu-153	52.19
Gadolinium	Gd-152	0.2
	Gd-154	2.18
	Gd-155	14.8
	Gd-156	20.47
	Gd-157	15.65
	Gd-158	24.84
	Gd-160	21.86
Iron	Fe-54	5.85
	Fe-56	91.75
	Fe-57	2.12
	Fe-58	0.28
Lead	Pb-204	1.4
	Pb-206	24.1
	Pb-207	22.1
	Pb-208	52.4
Lithium	Li-6	7.59
	Li-7	92.41
Magnesium	Mg-24	79
	Mg-25	10
	Mg-26	11
Manganese	Mn-55	100
Nickel	Ni-58	68.077
	Ni-60	26.223
	Ni-61	1.140
	Ni-62	3.635
	Ni-64	0.926
Phosphorus	P-31	100
Samarium	Sm-144	3.07
	Sm-147	14.99
	Sm-148	11.24
	Sm-149	13.82
	Sm-150	7.38
	Sm-152	26.75
	Sm-154	22.75

Element	Isotope	Natural Isotopic Composition [at%]
Silicon	Si-28	92.2
	Si-29	4.7
	Si-30	3.1
Sodium	Na-23	100
Tin	Sn-112	0.97
	Sn-114	0.66
	Sn-115	0.34
	Sn-116	14.54
	Sn-117	7.8
	Sn-118	24.22
	Sn-119	8.59
	Sn-120	32.58
	Sn-122	4.63
	Sn-124	5.79
Titanium	Ti-46	8.25
	Ti-47	7.44
	Ti-48	73.72
	Ti-49	5.41
	Ti-50	5.18
Tungsten	W-180	0.12
	W-182	26.50
	W-183	14.31
	W-184	30.64
	W-186	28.43
Vanadium	V-50	0.25
	V-51	99.75
Zinc	Zn-64	49.2
	Zn-66	27.7
	Zn-67	4.0
	Zn-68	18.5
	Zn-70	0.6
Zirconium	Zr-90	51.45
	Zr-91	11.22
	Zr-92	17.15
	Zr-94	17.38
	Zr-96	2.80

References

[1] National Nuclear Security Administration, "Nonproliferation," [Online]. Available: https://www.energy.gov/nnsa/missions/nonproliferation. [Accessed 2020].

[2] Research and Test Reactors Department, "RERTR: "Reduced Enrichment for Research and Test Reactors," Argonne National Laboratory, 18 May 2020. [Online]. Available: https://www.rertr.anl.gov/index.html. [Accessed 18 May 2020].

[3] E. H. Wilson, A. Bergeron, J. A. Stillman, T. A. Heltemes, D. Jaluvka and L. Jamison, "U.S. High Performance Research Reactor Conversion Program: An Overview on Element Design," Argonne National Laboratory, Argonne, 2017.

[4] D. Carpenter, G. Kohse and L. Hu, "MITR User's Guide, Rev. 3," Masssachusetts Insititute of Technology, Cambridge, 2012.

[5] K. Sun, A. Dave, L. Hu, E. Wilson, D. Jaluvka, S. Pham and T. Heltemes, "Transitional Core Planning and Safety Analyses in Support of MITR LEU Fuel Conversion," July 2018.

[6] A. J. Dave, K. Sun and L. W. Hu, "Thermal-hydraulic analyses of MIT Reactor LEU Transition Cycles," MIT Nuclear Reactor Laboratory, Cambridge, 2018.

[7] Massachusetts Institute of Technology Reactor Laboratory, "Safety Analysis Report for the MIT Research Reactor," Nuclear Regulatory Committee, Cambridge, 2011.

[8] K. Sun, L.W. Hu, E. H. Wilson, A. Bergeron and T. A. Heltemes, "Low Enriched Uranium (LEU) Conversion Preliminary Safety Analysis Report for the MIT Research Reactor (MITR)," Massachusetts Institute of Technology, Cambridge, 2018.

[9] "Certification Report Massachusetts Institute of Technology Research Reactor Fuel Element No. MIT-411," BWXT, Lynchburg, 2016.

[10] D. K. Morrell, L. V. Wages, E. L. Shaber, E. S. Lau, A. J. Vinnola and G. N. Fillmore, "Specification TRTR-3 MIT Reactor Fuel Elements Revision 2," Lockheed Martin Idaho Technologies, Idaho Falls, 1999.

[11] A. Bergeron, E. H. Wilson, G. Yesilyurt, F. E. Dunn, J. G. Stevens, L. W. Hu and T. H. Newton Jr, "Low Enriched Uranium Core Design for the Massachusetts Institute of Technology Reactor (MITR) with Un-finned 12 mil-thickn Clad UMo Monolithic Fuel," ANL/GTRI/TM-13/15, Argonne National Laboratory, November 2013.

[12] K. Sun, A. Dave, L. Hu, E. Wilson, T. Heltemes, S. H. Pham and D. Jaluvka, "Transitional Cores and Fuel Cycle Analyses in support of MIT Reactor Low Enriched Uranium Fuel Conversion".

[13] L. Hu, K. Sun, A. Dave, E. Block and J. Foster, "MITR Startup Plan for Initial LEU fueled Core," Nuclear Reactor Laboratory, Massachusetts Institute of Technology, Cambridge, 2019.

[14] NRC, "U.S. NRC Glossary," [Online]. Available: https://www.nrc.gov/reading-rm/basic-ref/glossary/shutdown-margin.html. [Accessed 2020].

[15] X-5 Monte Carlo Team, i, "MCNP - Version 5, Vol. I: Overview and Theory", LA-UR-03-1987," 2003. [Online].

[16] F. E. Dunn, L. W. Hu and E. Wilson, "The STAT7 Code for Statistical Propagation of Uncertainties in Steady-State Thermal Hydraulics Analysis of Plate-Fueled Reactors," Argonne National Laboratory, Argonne, 2016.

[17] S. H. Pham, "Verification and Validation of the STAT7 Code - ANL/RTR/TM-18/1," Argonne National Laboratory, 2018.

[18] *Standard Practice for Determining Equivalent Boron Contents of Nuclear Materials (C1233),* West Conshohocken, PA: ASTM International, 2015.

[19] D. A. Brown, M. B. Chadwick, R. Capote, A. C. Kahler, A. Trkov, M. W. Herman and et al., "ENDF/B-VIII.0: The 8th Major release of the nuclear reaction data library with CIELO-project cross sections, new standards and thermal scattering data," *Nucl. Data Sheets,* vol. 148, no. 1, 2018.

[20] Idaho National Laboratory, *Specification for Low Enriched Uranium Monolithic Fuel Plates (SPC-1635),* Idaho Falls, 2016.

[21] J. White, D. Jaluvka, J. Stillman, R. Kmak and E. Wilson, *Information for the Specification of Low Enriched Uranium Fuel Elements for the Massachusetts Institute of Technology Reactor (ANL/RTR/TM-18/2),* Argonne National Laboratory, 2018.

[22] MATLAB, "polyval and polyfit," *MATLAB Help Documentation,* 2019.

[23] *Standard Specification for Aluminum and Aluminum-Alloy Sheet and Plate (B209M-14),* West Conshohocken, PA: ASTM International, 2014.

[24] D. K. Morrell, G. N. FIllmore, L. V. Wages, E. L. Shaber, E. S. Lau and A. J. Vinnola, "Specification TRTR-3 MIT Reactor Fuel Elements Revision 2," Lockheed Martin Idaho Technologies, Idaho Falls, 1999.

[25] Krasnick and Barnett, "MIT Reactor MITR-2: Fuel Element Assembly," Massachusetts Institute of Technology Reactor, Cambridge, 1998.

[26] K. Chiang, "Thermal Hydraulic Limits Analysis for the MIT Research Reactor Low Enrichment Uranium Core Conversion Using Statistical Propagation of Parametric Uncertainties," Massachusetts Institute of Technology, Cambridge, 2012.

[27] E. H. Wilson et al., "Comparison and Validation of HEU and LEU Modeling Results to HEU Experimental Benchmark Data for the Massachusetts Institute of Technology MITR Reactor," Argonne National Laboratory, December 2010.

[28] D. Morrell, G. Fillmore, L. Wages, E. Shaber and E. Lau, *Specification for MIT Research Reactor Fuel Elements (TRTR-3),* Lockheed Martin Idaho Technologies Company, 1997.

[29] A. J. Bieniawski, "An overview of the global threat reduction initiative accelerating threat reduction," in *International Topical Meeting on Research Reactor Fuel Management*, Vienna, 2009.